UNIVERSITÀ DEGLI STUDI DI MILANO

Graduate School of Animal Health and Production:
Science, Technology and Biotechnologies

Department of Veterinary Science and Public Health (DIVET)

PhD Course in Biotechnologies Applied to Veterinary and
Animal Husbandry Sciences
(Cycle XXVI)

Doctoral Thesis

The role of Numb in stem cell homeostasis and breast tumorigenesis

VET/03-VET/05

Marco COAZZOLI
Nr. R09059

Tutors: Prof. Giorgio POLI and Prof. Salvatore PECE
Supervisor: Dott.ssa Daniela TOSONI
Coordinator: Prof. Fulvio GANDOLFI

Academic Year 2013

TABLE OF CONTENTS

ABSTRACT

In this thesis I report my investigations on the role of Numb, a known cell fate determinant in regulating Stem Cell homeostasis and in the pathogenesis of human and mouse breast cancer. I have investigated the characterization of the biological and molecular features of Numb KO murine breast model in comparison with Numb deficient human breast cells model. I exploited an *in vitro* system (the mammosphere assay) to propagate and enrich breast SCs, in combination with a cell membrane labeling system (PKH-assay) to purify SCs.

The absence of Numb in both murine and human models helped to clarify the role of this "fate determinant" starting from the SC first mitotic division *in vitro* up to the *in vivo* tumorigenesis and related Numb reconstitution consequences.

Through the comparison of the self-renewal properties of normal and cancer SCs, both in terms of proliferative cell fate and Numb partitioning, and the study of the molecular mechanisms underlying abnormal growth properties, functional attenuation and pharmacological restoration of signaling pathways in mammary CSCs, I have attempted to answer the open questions regarding the role of SCs in cancer development and maintenance, focusing the attention on a first possible direct evidence for cancer SC targeted therapy.

INTRODUCTION

Mammary gland structure and development

The mammary gland has an apparently simple cytoarchitecture, a structure like that could be difficult to reconcile with the diversity of breast cancer phenotypes (Stingl and Caldas, 2007). This has led to the hypothesis that, despite its morphological simplicity, this structure is functionally complex and molecularly heterogeneous (Stingl and Caldas, 2007).

The mammary gland is composed by two different cellular compartments: the epithelium which surrounded by an external layer of myoepithelial cells, and the stroma, also called the mammary fat pad, that is mainly composed of adipocytes, but also of other cell types, as well as fibroblasts, haematopoietic cells, blood vessel and neurons.

The epithelium is a branched ductal system and a lobulo-alveolar compartment where rare resident multipotent mammary stem cells (MSCs) rule the development of the gland during embryogenesis, and its modifications in postnatal life (Williams and Daniel, 1983).

The ducts branch into decreasingly smaller ductules that constitute the terminal ductal lobular units (TDLUs) also known as terminal end buds (TEBs, Fig. 1a,c black arrows, Fig. 2a), which are composed in turn of alveoli. Ducts and alveoli present a central lumen that opens to the body surface through the nipple.

Mammary epithelial cells represent the fundamental functional unit of the gland. The cellular epithelial architecture is composed of a bilayer of luminal cells surrounding the inner lumen and an external layer of myoepithelial and basal cells (Daniel & Smith, 1999)

The luminal epithelial cells of the alveoli undergo functional differentiation in pregnancy and produce milk. Basal and myoepithelial cells, whose contraction facilitates the milk release, surround both ducts and alveoli. The extensive system of ducts and alveoli is embedded by fibroblasts and adipocytes that compose the stroma of the mammary gland. (Hennighausen and Robinson, 2001, 2005; Smalley and Ashworth, 2003) This "second" population grew its importance since the concept of "mammary fat pad" has been assumed. This structure has been no more considered as an inert supporting matrix. Indeed the mammary fat pad is a site of hormone action with stromal estrogen receptor (ER), a site of growth factor synthesis and a source of lipid as well (Hovey et al., 1999).

The mammary gland develops in defined stages that are connected to sexual development and reproduction. These are embryonic, prepubertal, pubertal, pregnancy, lactation, and involution (Fig. 1). Epithelial and stroma cells derived embryologically from ectoderm and mesoderm, respectively. Embryonically, mammary gland development begins as an epithelial bud in the ventral surface of the fetus, that penetrates the mesenchyme and form a rudimental ductal system

connected to the body surface trough the nipple. The number and location of glands vary among different classes of mammals.

In mice, five pairs of glands develop along a ventral line, whereas only one pair develops in the thoracic region in humans (see Materials and Methods Fig. 3 “Diagram of Mammary Tissue”). During puberty the ducts grow and branch further so that, in the mature animal, the entire fat pad is filled with a complete ductal system. The alveolar compartment expands and matures during pregnancy, and then, during lactation, secretes milk. Lactation is followed by involution, a stage during which alveoli undergo apoptosis and remodeling to restore a simple ductal structure. Alveolar expansion and maturation, lactation and involution initiates with a new pregnancy (Hennighausen and Robinson et al., 2001, 2005; Smalley and Ashworth, 2003).

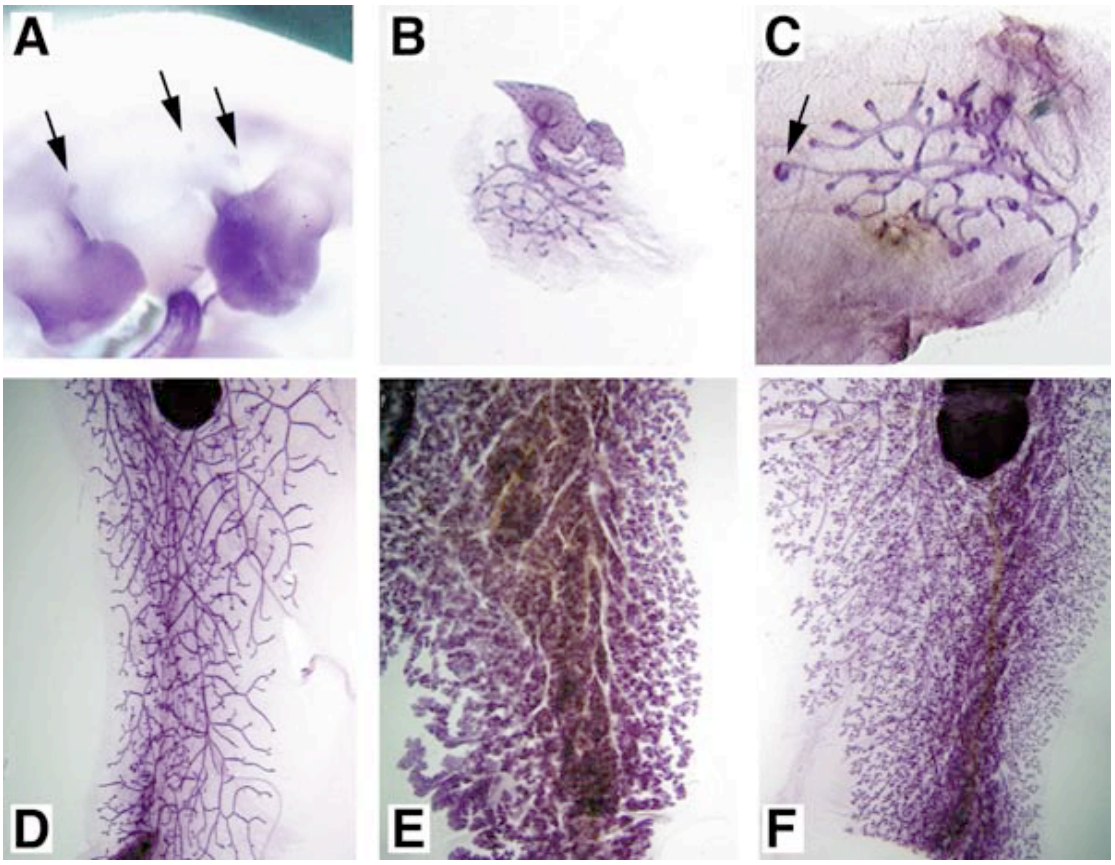

Figure 1
Stages of mouse mammary gland development
Whole mount images of mouse mammary gland during its development. (A) Epithelial bud in the fetus (Arrows). (B-D) Ductal tree in newborn (B), 3 week-old (C) and adult (D) animal (arrow in C
indicate a TEB). (E) Alveolar development during pregnancy. (F) Alveolar involution. Modified from Hennighausen and Robinson, 2001.

SCs AND BREAST DEVELOPMENT

It has been proposed that the cells forming the epithelial compartment of the mammary gland are derived from mammary SCs, which have the capacity to self-renew and give rise to progenitor cells, which are destined for either a basal or a luminal fate. The presence of SCs should be the basis of the profound capacity for

alveolar renewal in each subsequent pregnancy. It is generally thought that, in the mammary gland of pubertal mice, SCs reside in the TEBs, the structures at the end of the ducts that constitute their growing units. TEBs are composed of a mass of body cells surrounded by a layer of cap cells. Cap Cells are the putative SCs; they generate the outer side of the TEB and will differentiate in the myoepithelial, basal or luminal cells. The ductal lumen forms because of apoptosis occurring in the mass of developing body and luminal cells. TEBs disappear at the end of the puberty, when the mammary gland reached its full development (Smalley and Ashworth, 2003).

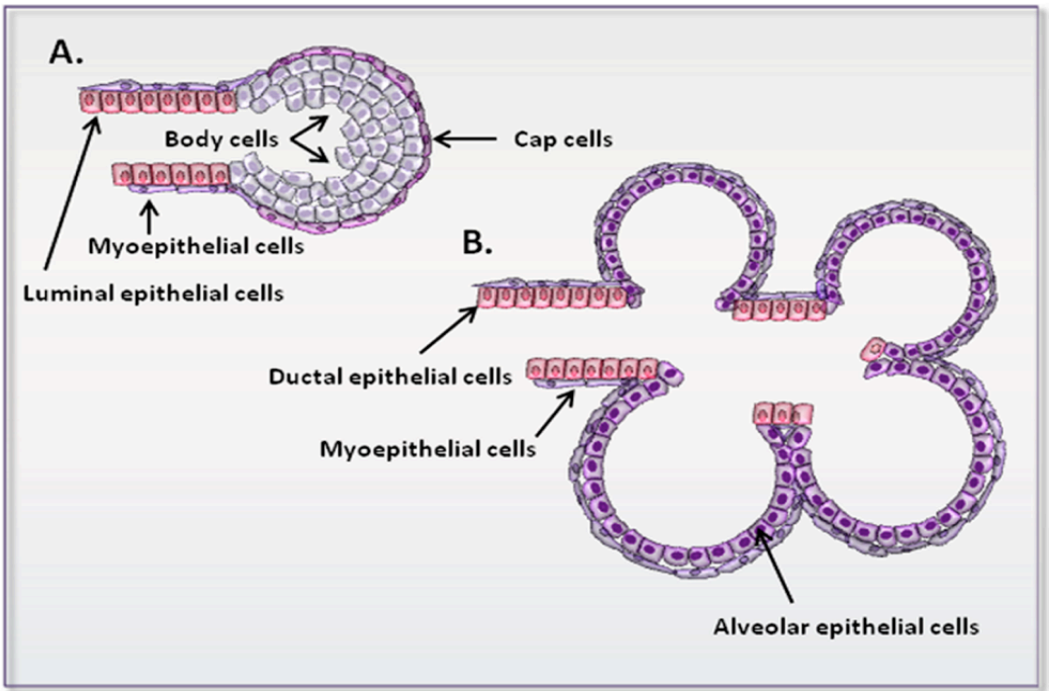

Figure 2
Structure of mammary epithelium on different stages of differentiation.
(A) Prepubertal and pubertal mammary gland. Ducts terminate with highly proliferative terminal end buds (TEBs).
(B) Extensive ductal branching during pregnancy. Formation of alveolar structures required for milk production.
(Gajewska et al., 2013)

Human breast cancer

Breast cancer is one of the most common cancers and a major cause of death despite the significant advances in the comprehension of its pathogenesis, diagnosis and treatment over the last decades (Ferlay et al., 2010).

The heterogeneity of breast cancer complicates the clinical management of patients and represents a major problem in the prediction of prognosis and response to therapy. The molecular understanding of both inter- and intra-tumor heterogeneity has until recently been poor. Inter-tumor heterogeneity has long been recognized by histo-pathologists who, based on their microscopic observations, were able to identify and classify 17 different histological subtypes of breast cancer with different clinical behavior (Tavassoli et al., 1999). Beyond gross histological differences among tumors, pathologists have also been able to develop a grading system based on the level of differentiation, number of mitoses and nuclear pleomorphism, to classify tumors into different grades with different clinical behavior. For example, according to The Gleason System (Gleason, Mellinger 2002) tumors are classified on the base of their level of differentiation and grade of complexity, scoring from a G1 to a G3 class where a G1 represents a well differentiated, less aggressive type of tumor while a G3 is a poorly differentiated kind, and more aggressive associated with a bad prognosis.

Pece et al. recently demonstrated that G3 tumors differ from G1 class on the base of their SC content (Pece et al., 2010) arguing a possible critical involvement of SCs in

the determination of the molecular and pathological differences pathogenesis among breast tumors. According to these evidences, and to the "SC theory of cancer" (see later) SCs plays are the major interest of my research study.

The Stem Cell Theory of Cancer

SCs are a long-lived cell population responsible for tissue formation, homeostasis and repair. They are defined by their ability to perpetuate themselves through self-renewal and to generate mature cells of a particular tissue through differentiation. Since SCs have been identified in several tissues like blood, breast, colon, lung, liver and brain, it seems reasonable to propose that every tissue is maintained by tissue-specific SCs. An attractive hypothesis proposes that SCs or their direct progenies, due to their extended life span, are the ideal target of cell transformation, and that cancers are thus supported by transformed SCs, which retain the same self-renewing and differentiating properties of their normal counterparts (Reya et al., 2001; Shipitsin and Polyak, 2008). The first demonstration of the existence of a rare population of cancer-initiating cells came from studies performed in 1994, by the John Dick group in Toronto (Lapidot et al., 1994). Their experiments led to the formal demonstration that, within a tumor, only specific cell subsets were able to generate a new tumor upon transplantation. Since the transplanted tumors showed the same cell heterogeneity of the original one and could be further transplanted to obtain tertiary tumors, these experiments also demonstrated that tumor-initiating

cells possess the ability to self-renew and differentiate. Thus, these rare cells share the same features of normal SCs and for this reason they are referred to as Cancer SCs (Campbell and Polyak, 2007; Visvader and Lindeman, 2008). The first report of cancer SCs in human breast cancer samples came in 2003 when Al-Hajj showed how cancer SCs highly enriched samples were able to generate breast carcinoma upon transplantation into the mammary tissue of NOD-SCID mice (Al-Hajj et al., 2003).

Based on these findings, the Cancer Stem Cell Hypothesis implicates that a particular subset of tumorigenic cells with stem cell-like properties drives tumor initiation, progression and relapse.

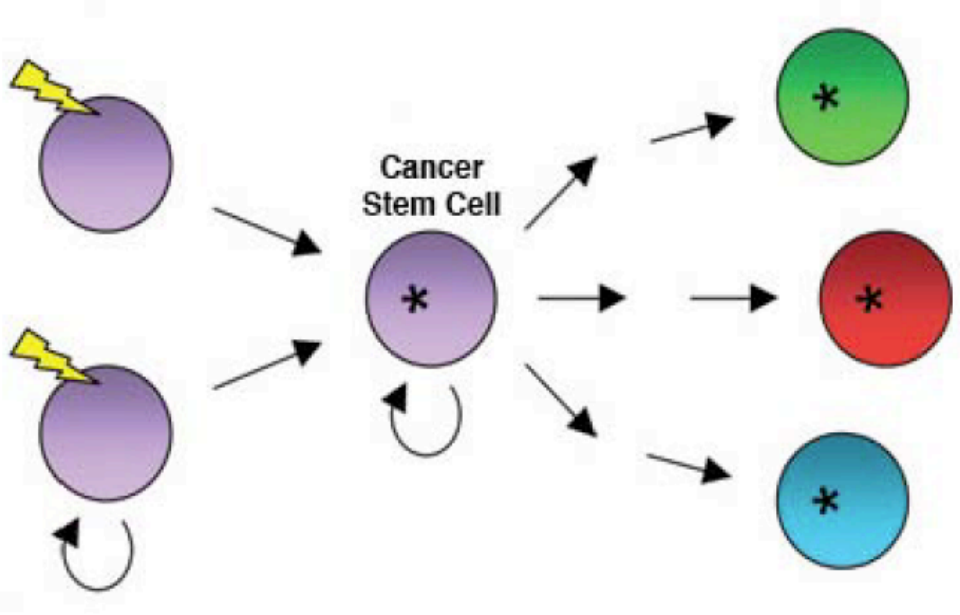

Figure 3
Cancer stem cell hypothesis
Cancer-causing mutations are likely to occur in normal adult stem or progenitor cells. These cells give rise to "Cancer Stem Cells" that can self-renew and differentiate to produce all the other cells of the tumor.
Modified from Campbell and Polyak, 2007.

Cancer Stem Cells

The concept of tumor has deeply changed throughout the years. At the beginning tumors were traditionally regarded as biologically homogenous populations of cells with high proliferating activity. Than with the assumption of "Cancer Stem Cells" concept, the tumor has been approached as an aberrant organ initiated by a tumorigenic cancer cell that acquired the capacity for not-ended proliferation through accumulated mutations. One critical limitation to the validation of this concept is our poor understanding of the biological and molecular differences between SC and CSCs. It is still unknown whether CSCs, as compared to SCs, have different growth potential, life span, drug sensitivity and, more importantly, which are the relevant underlying molecular pathways. Well is known that this subpopulation of tumorigenic cells have SC properties and they are thought to drive and sustain growth and metastasis of spontaneously occurring tumors (Clarke and Fuller, 2006; Zhang and Rosen, 2006).

CSCs have been defined on the basis of their ability to seed tumors in animal hosts, to self renew and to spawn differentiated offspring (Clarke et al., 2006). Accordingly, the representation of CSCs within a population of cancer cells can be measured by the number of cells that are required, at limiting dilutions, to seed new tumors. (Gupta et al., 2009)

SCs, CSCs and Non-CSCs

There are several analogies between normal stem cells and tumorigenic cells, most notably as normal adult SCs, CSCs have the ability to generate more SCs ('self-renewal') and to differentiate (Reya et al., 2001).

Both of them have extensive proliferative potential and the ability to give rise respectively to new normal and abnormal outgrowth; both tumors and normal tissues are composed of heterogeneous combinations of cells, with different phenotypic characteristics and different proliferative potentials (Fidler et al., 1977 Nowell et al., 1986). Since CSCs are endowed as SCs with proliferative potential, but lack in control on it, they can lead to the production of any cancer cell type, accounting for tumor heterogeneity.

According to the cancer clonal origin concept (Fearon et al., 1987), CSCs give rise to phenotypically diverse progeny composed of cells with indefinite proliferative potential, but also non-CSCs, which are not able to self-renew and cannot differentiate to produce other tumor cell types. Non-CSCs are phenotypically heterogeneous cells that exhibit various degrees of differentiation, their presence in the tumor is an attempt of "process of organogenesis", that is however aberrant and poorly regulated (Reya et al., 2001).

CSCs are supposed to arise from normal stem or progenitor cells and are thought to persist as a small fraction of the total cells in the tumor; tumor progression is a result

of the expansion of these cells. According to this model, tumors can be considered as aberrant, hierarchically organized tissues, with cancer SCs responsible for their phenotypical and functional properties and their proliferation potential (Campbell and Polyak, 2007;Visvader and Lindeman, 2008).

Weinberg underlines the possibility for CSCs to differentiate into non-CSCs, but also the reverse process must now also be considered. There is a possibility of a bidirectional interconvertibility, a dynamic equilibrium between CSCs and non-CSCs within tumors, this equilibrium may be shifted in one or another direction by contextual cues within the tumor microenvironment. Non-CSCs upon these conditions may become reprogrammed into CSCs via a process called Epithelial to Mesenchymal Transition (EMT), this shift could raise CSCs number up within the tumor (Santisteban et al., 2009).

Several recent reports have suggested that some 25% of the cancer cells within certain tumors have the properties of CSCs (Kelly et al., 2007; Quintana et al., 2008) so CSCs are not a so rare subpopulation within tumors.

The ratio between CSCs and non-CSCs is a critical issue in the tumor evolution. This proportion differs on the basis of the stage of malignant progression reached by a tumor (Harris et al., 2008; Chiou et al., 2008), it is no accident the tumor malignancy is evaluated on the degree of differentiation manifested by the cancer cells within a tumor (Gupta et al., 2009).

This assumption further charges CSCs responsibility in tumor development. A plausible corollary is that the selective ablation of CSCs should lead to the ''sterilization'' of the tumor and to its cure (Cicalese et al., 2009).

Alternatively CSCs can be eliminated by inducing their differentiation. Histone deacetylase (HDAC) inhibitors may have therapeutic value as "differentiation – inducing" agents driving the differentiation of mesenchymal-like cancer cells and CSCs, which could trigger apoptotic responses or chemosensitize (Singh et al., 2010).

MOLECULAR PATHOGENESIS OF BREAST CANCER

Breast carcinogenesis involves a series of progressive changes that accumulate in the stepwise acquisition, by breast epithelial cells, of the so-called "hallmarks of cancer": i.e., genome instability, sustained proliferative signaling, evasion of growth suppressors, resistance to cell death, replicative immortality, induction of angiogenesis, activation of invasion and metastasis, reprogramming of energy metabolism, and evasion of immune destruction (Hanahan & Weinberg 2011). These acquired abilities, which drive and sustain cancer growth and metastasis, reflect the accumulation of genetic changes that are mainly categorized in two classes: 1) loss of function of tumor suppressor genes and 2) gain of function of oncogenes. The antagonistic mechanisms between oncogenes and oncosuppressors indeed finely

rules the multiple events controlling the entry in mitosis and the correct operation of this complex pathway is responsible for the cell homeostasis even when it is lost.

An oncogene is a mutated and/or overexpressed gene (defined proto-oncogene in its wild-type form) that alone, or in collaboration with other changes, promotes cellular transformation, growth and invasion. In contrast, a tumor suppressor gene normally counteracts cell growth or other processes that may increase invasive and metastatic potential and whose loss of function promotes malignancy. In addition to protein-coding genes, in the last decade the importance of non-coding RNAs and their involvement in tumorigenesis has been documented, together with their ability to work as oncogenes or tumor suppressor genes (Croce et al., 2008).

The factors acting in tumorigenesis

The most frequently activated and best characterized oncogenes in breast cancer include v-erb-b2 erythroblastic leukemia viral oncogene homolog 2 (ERBB2), phosphatidylinositol-4,5-bisphosphate 3-kinase, catalytic subunit alpha (PI3KCA), v-myc avian myelocytomatosis viral oncogene homolog (MYC), and cyclin D1 (CCND1). In contrast, the tumor suppressor protein p53 gene (TP53), the breast cancer susceptibility genes 1 and 2 (BRCA1 and BRCA2), the phosphatase and tensin homolog gene (PTEN), the E-cadherin gene (CDH1), the retinoblastoma gene (RB1) and members of the cyclin-dependent kinase inhibitor (CKI) family represent the

most frequently altered tumor suppressor genes in breast cancer. Undoubtedly, many more oncogenes and tumor suppressor genes contribute to breast carcinogenesis. Given the heterogeneity of breast cancers, a better understanding of the genetic lesions that drive tumorigenesis in the mammary gland, will lead to improvements in the clinical management of breast cancer patients.

The role of p53 Tumor Suppressor and the pathogenesis of cancer

The gene TP53 is located on 17p13.1, it has been studied for the last 30 years. The encoded protein p53 is a tumor suppressor and is considered as one of the most important molecules in human cancer since it is the most frequently mutated tumor suppressor in human tumors (Levine et al., 1997). More than 50% of all cancer cases carry TP53 mutations. This frequency is slightly lower in breast cancer with 15 – 34% of cases harboring TP53 mutations (Hartmann et al., 1997).

p53 has been defined as the "guardian of the genome" (Lane et al., 1992). The protein p53 acts primarily as a transcription factor, inducing the expression of genes involved cell cycle checkpoint activation, DNA repair, cell migration, cell metabolism, cellular senescence, apoptosis and autophagy in response to cellular stresses displaying hence a potent anti-proliferative and pro-apoptotic functions (Vogelstein et al., 2000).

When normal cells are damaged by ionizing radiation or mutagens, p53 is activated by phosphorylation to maintain cellular homeostasis and accumulates in the nucleus where it binds as a tetramer to specific sequences to activate transcription of these genes. One of the target genes induced by p53 is p21, an inhibitor of cyclin-dependent kinases (CDKs) that causes cell cycle arrest. GADD45, another p53 target gene, is in charge of repairing damaged DNA. When repair is successful p53 is degraded by the action of the ubiquitin-ligase MDM2 and the cell cycle restarts. When GADD45 cannot repair the genome because of excessive DNA damage, p53 trans-activates the pro-apoptotic gene BAX, which induces apoptosis (Levine et al., 1997).

p53 dysfunction/inactivation allows cells to survive DNA damaging insults, which may result in the accumulation of activating mutations in proto-oncogenes or inactivating mutations in tumor suppressor genes and, consequently, to malignant transformation.

The p53-MDM2 axis

About 50% of all tumors analyzed display mutation or loss of p53, this data puts in evidence the key role of p53 in tumorigenesis as tumor suppressor (Levine et al., 1994).

When the cell undergoes a stress condition, p53 is activated and rule either a G1 arrest in cell cycle or apoptosis. When the cell is in physiological condition, p53 is always synthetized but even rapidly degraded to maintain its basal activity controlled. Several mechanisms participate to both stabilize and activate p53. Its fate is decided by the direct competition between acetylation and ubiquitination for the same residues (Ito et al., 2002; Li et al., 2002). The major sites for p53 ubiquitination are located at its C terminus, and acetylation of these residues during times of cell stress serves to block protein degradation and stabilize p53 (Brooks et al., 2006)

The MDM2 oncoprotein plays a central role in that regulatory process (Fakharzadeh et al., 1993). The p53-MDM2 interaction domain has been co-crystallized revealing that the N-terminal region of MDM2 forms a deep hydrophobic cleft in which three p53 amino-acid residues, Phe19, Trp23 and Leu26, deeply insert into (Kussie et al., 1996).

MDM2 protein level and its RNA as well fall after DNA damage, caused for example by UV irradiation. In these conditions Mdm2 itself can be acetylated (Wang X et al., 2004) on residues within the RING domain. In this way Mdm2 becomes inactivated and leads to an increase in p53 transcriptional activity (Brooks et al., 2006; Lane et al., 1992).

Vice versa, after DNA repair, to downsize p53 activity, MDM2 levels increase: as consequence MDM2 binds p53 in the nucleus and carries it in the cytoplasm where

p53 is degraded in the proteasome (Shirangi et al., 2002; Xirodimas et al., 2001; Bottger et al., 1997). These two proteins thus form an autoregulatory feedback loop in which p53 positively regulates MDM2 levels and MDM2 negatively regulates p53 levels and activity, while in unstressed cells, both p53 and MDM2 are kept at very low levels (Wu et al., 1993).

In several p53-mutated tumors, p53 is overexpressed, but MDM2 is not. That happens because these tumors loose this feedback and p53 is not regulated by MDM2 anymore (Brooks et al., 2006).

Furthermore in some wild-type p53 tumors, the Mdm2 gene overexpression can block p53 function and promote the tumor growth independently of p53 (Chen et al., 1996).

MDM2 can be so considered as a p53 real controller mediating p53 degradation in unstressed cells and controlling p53 levels and activities during the stress response (Shirangi et al., 2002). Mediating p53 ubiquitination, MDM2 facilitates the termination of the stressed cellular state and thus maintains low steady-state levels of p53 in unstressed normal cells. (Brooks et al., 2006)

The p53-binding site on MDM2 has a key role for the functional consequence of the interaction between the two proteins. The very same amino acids in p53 that contact MDM2 are required indeed for p53 to activate transcription (Lin et al., 1994)

MDM2 can so block p53 ability to act as a transcription factor, by competing with the transcriptional machinery for p53 interaction. In addition, there are several indications that MDM2 itself may play a role in cell cycle progression or tumorigenesis independent of its ability to inhibit the tumor suppressor functions of p53 (Ganguli et al., 2003).

By the way MDM2 is not the only factor influencing p53 homeostasis, there is a third partner, Numb indeed, interacting with both of them. As recently demonstrated by Colaluca, Numb, the protein that I'm studing in my thesis, by binding the p53-MDM2 complex can influence p53 homeostasis (Colaluca et al., 2008) since in presence of Numb, p53 is preserved by ubiquitination executed by MDM2; this condition is lost upon Numb deficiency bringing to an early decrease of p53 levels. These evidences support previous data edited by Pece, where G3 tumors, notably the most difficult to treat, resulted enriched in SC content (Pece et al., 2004) and nevertheless emerged to be Numb lacking in a conspicuous percentage of cases (Pece et al., 2004; Colaluca et al., 2008).

This scenario strongly focuses the attention on Numb not only in relationship with the p53-MDM2 axis, but also with the cell fate itself. Intrigued by these evidences we decided to study the role of Numb in SC compartment homeostasis and its loss as possible crucial event in the tumorigenesis.

Contribution of the NUMB–HDM2–p53 axis to breast cancer

Colaluca has recently shown how the cell-fate determinant Numb can influence the tumor suppressor protein p53 homeostasis. Loss of Numb in breast cancers would result, therefore, in both the activation of the potential oncogene Notch and the diminution of tumor suppression by p53 (Carter et al., 2008).

The evidence of an axis between MDM2 and p53, but also between p53 and Numb suggests the existence *in vivo* of multiple binary complexes (NUMB–HDM2, NUMB–p53 and HDM2–p53), or of a tricomplex NUMB–HDM2–p53 (Colaluca et al., 2008). In physiological conditions, Numb preserves p53 protein levels and its activity, and regulate p53-dependent phenotypes.

The simultaneous presence of NUMB–HDM2–p53 together prevents the ubiquitination and degradation of p53. The real mechanism through which Numb preserves p53 is still unknown; Numb may simply intercalate between p53 and MDM2 or rather inhibit the conformational change that involve the p53–MDM2 complex after their interaction. This last event in particular is indeed critical for ubiquitination of p53.(Momand et al., 1992; Haupt et al., 1997; Kubbutat et al., 1997; Carter et al.,2008).

The recent identification of Numb as a protein controlling p53 levels and activity (Colaluca et al., 2008) leads obviously to the possibility that Numb can regulate cancer development.

Many evidences show how Numb is often loss in breast cancers, indeed one third of all breast tumors are Numb-deficient; the lack of Numb causes decreased p53 levels and both these events correlate with aggressive disease and poor prognosis chemoresistance (Westhoff et al., 2009).

Colaluca demonstrated that Numb overexpression increases p53 stability and activity showing that Numb levels are relevant to the p53-mediated cellular responses, in particular in breast tumors where the loss of Numb expression is frequently detected. Thereby Numb might be relevant to SC homeostasis because of its influence on p53, than a p53/Numb signaling axis might function as a tumor suppressor pathway in mammary SCs: in support of that the reduction in p53 levels was caused by loss of Numb, throughout MDM2, while forced re-expression of Numb or silencing of MDM2 restored normal p53. On the other hand the loss of Numb expression could contribute hence to malignant transformation by reducing p53 activity, Thereby p53/Numb axis has to be considered as an additional mechanism with possible involvement in tumorigenesis in breast cancer in which mutations of p53 are relatively infrequent if compared with the entire panel of tumors displaying p53 mutations (Pharoah et al., 1999). Accordingly, restoring Numb expression or p53 levels in Numb-deficient tumors should constitute an effective SC-targeted therapy.

The Numb-Notch axis

The first evidences of Numb relevance in SC fate came from studies carried in *Drosophila*. In this model, Numb is membrane associated and during mitosis it symmetrically segregates influencing Notch repartition and function (Cayouette & Raff 2002). The effects of Numb loss were previously studied indeed focusing the attentions on the Numb-Notch axis. (Pece et al., 2004)

Notch is a plasma membrane receptor; it binds to a family of transmembrane ligands, resulting in cleavage of the receptor, translocation of the intracellular domain to the nucleus and activation of a number of target genes. Its function is involved in the control of cell fate specification and in the maintenance of the balance between proliferation and differentiation in development and homeostasis in many cell lineages (Artavanis-Tsakonas et al., 1999; Mumm and Kopan, 2000), and alterations in Notch signaling have been implicated in tumorigenesis (Robbins et al., 1992; Gallahan et al., 1996; Capobianco et al., 1997).

Numb inhibits Notch through its N-terminal phosphotyrosine-binding domain (PTB) (Guo et al. 1996) in a sort of biological antagonism influencing cell development and homeostasis. Nevertheless Numb prevents the translocation of activated Notch to the nucleus inducing its ubiquitination and meanwhile controlling Notch intracellular domain degradation (McGill & McGlade 2003).

Numb-mediated control on Notch is relevant to the normal mammary parenchyma

and its subversion contributes to human mammary carcinogenesis. This signaling is lost in some 50% of human mammary carcinomas, due to specific Numb ubiquitination and proteasomal degradation. When Numb is lost, in Numb-negative tumors, increased Notch signaling is observed, but it reverts to basal levels after enforced expression of Numb. The pharmacological inhibition of Notch has been proposed as possible approach to suppress Numb-negative tumors growth (Pece et al., 2004).

Mode of division of normal SCs

All SCs can generate identical copies of themselves but also give rise to more differentiated progeny by undergoing both symmetrical and asymmetrical divisions.

An asymmetric cell division is defined as any division that gives two sister cells that have different fates, differences in size, morphology, gene expression pattern, or the number of subsequent cell divisions undergone by the two daughter cells (Horvitz and Herskowitz, 1992). On the other hand, a hallmark of symmetric SC division is the increase in the number of SCs.

The two cells generated by asymmetric divisions differ markedly in their proliferative potential: the SC remains quiescent or slowly proliferates (''self-renewal''), whereas the progenitor cell undergoes multiple rounds of divisions before entering a postmitotic fully differentiated state. This mechanism ensures the production of large

numbers of differentiated progeny, while maintaining a relatively small pool of long-lived SCs (Morrison and Kimble, 2006). Mammalian adult SCs, which are supposed to divide asymmetrically under steady-state conditions (Januschke and Gonzalez, 2008; Morrison and Kimble, 2006), retain the capacity to divide symmetrically expanding in number through rounds of symmetric self-renewing divisions, whereby each SC produces two new cells with identical SC fate and proliferation potential; in this way it is possible to refill the SC pools depleted by injury or disease (Morrison and Kimble, 2006).

Intrinsic mechanism vs extrinsic mechanism

Cells undergoing asymmetric divisions use apical-basal or planar polarity of the surrounding tissue to set up an axis of polarity, this axis is used to orient the mitotic spindle and to polarize the distribution of specific protein determinants, responsible in the cell fate (intrinsic mechanism). Classic examples of asymmetric divisions that are controlled by an intrinsic mechanism are provided by the *C.elegans* zygote (Morrison and Kimble, 2006) and the *Drosophila* larval neural SCs (Neuroblasts) (Januschke and Gonzalez, 2008).

Alternatively, according to the "stem niche" concept (extrinsic mechanism), the SC maintains the potential to self-renew because of the asymmetric placement of daughter cells in relation to stem cell niche external micro-environment. Only the

daughter cell that remains close to the niche has access to the extrinsic signals necessary for maintaining SC identity and the daughter cell placed away from the niche is exposed to signals that induce differentiation (Li and Xie, 2005).

The intrinsic mechanism

Asymmetric SC division can be obtained through regulated assembly of cell polarity which brings to asymmetric partitioning of cell components that determine cell fate; these "fate determinants" are inherited by only one of the two daughter cells throughout controlled segregation ruled by proteins like Par-3, Par-6, atypical PKC (aPKC) (Betschinger and Knoblich, 2004; Suzuki and Ohno, 2006; Goldstein and Macara, 2007). Asymmetric localization of PAR-aPKC complex at the apical cortex initiates the asymmetric partition of cell fate determinants while the regulated mitotic spindle orientation ensures their segregation through the cell polarity complex to one daughter; among the "fate determinants", Numb plays a critical role. For example in undifferentiated neural progenitors, during the development of the mouse cortex, Numb asymmetrically accumulates to precursors destined for neurogenesis (Shen et al., 2002). Numb is also asymmetrically distributed to progeny of cultured satellite muscle cells, where it promotes myogenic differentiation of one daughter cell (Conboy and Rando, 2002; Shinin et al., 2006). Thus, asymmetric segregation of Numb may be a mechanism that control asymmetric division.

Interestingly, both mammalian basal epidermal progenitors (Lechler and Fuchs, 2005) and cortical ventricular zone neural progenitors (Chenn and McConnell, 1995) seem to exploit the "intrinsic mechanism" to regulate the orientation of mitotic spindles which relies on the cortical localization of the PAR–aPKC complex (Lechler and Fuchs, 2005), a mechanism that also controls the asymmetric division of *Drosophila* and *C. elegans* SCs (Morrison and Kimble, 2006).

Recent studies stress the importance of these "fate determinants" even for their influence on factors like p53 (Colaluca et al., 2008), all along considered among the major controllers in mitosis (Innocente et al., 1999) and in asymmetric divisions as well (Cicalese et al., 2009).

Numb, polarity, SC division and cancer

Polarity is defined as a structural and/or functional asymmetry (Casanova et al., 2007). Cells like epithelial cells and neurons are intrinsically polarized in situ, whereas others become polarized transiently in response to external cues, for example, migrating cells, lymphocytes and phagocytes. Cell polarity is involved also in the cell fate determination throughout the asymmetric cell division, in which fate determinants become differentially distributed between daughter cells (reviewed by Suzuki & Ohno, 2006; Betschinger & Knoblich, 2004). Recently research groups focused their attention on Numb because of its involvement in SC asymmetric cell

division driven by evidences on Numb critical role emerged in *Drosophila* and vertebrates.

Numb in Drosophila developmental model system

The previous studies conducted in *Drosophila* put in evidence a complex pattern of functions played Numb. (Uemura et al., 1989). Numb is an evolutionary conserved membrane associated protein (Verdi et al., 1996). Its link with the membrane is guaranteed by the phosphotyrosine binding domain (PTB) (Li et al., 1998) and by several N-terminal positively charged amino acids that might interact with membrane phospholipids. During interphase, Numb is distributed uniformly around the plasma membrane. The membrane association before their asymmetric localization may be an example of "reduction of dimensionality", through which a protein gets a two-dimensional distribution in the plasma membrane rather than a three-dimensional diffusion in the cytoplasm. Through this mechanism the protein is quickly available to delocalize in the following mitotic phase (Jan et al., 1998).

Role of Numb in SC division

Since the firsts studies in *Drosophila*, results have put in evidence how Numb is involved in SC fate determination mechanisms such as the asymmetric mitotic

division with crucial consequences in the following daughter cells development. Indeed the asymmetrical partitioning of Numb during cell division of the sensory organ precursor (SOP) gives rise differentially to sensory neurons and other supporting cells of the external sense organ in the *Drosophila* peripheral nervous system (Rhyu et al., 1994). On the other hand, defects of Numb can affect the asymmetric division than increasing SC number; this evolves in tissue overgrowth bringing to brains growth to enormous size and eventually death. Loss of Numb function resulted in SCs offspring aberrant differentiating in the SOP, leading to the production of support cells without sensory neurons. Moreover Numb mutations typically lead to an overproliferation of neuroblasts during larval stages (Caussinus and Gonzalez 2005).

These findings established in *Drosophila* a causal relationship among loss of polarity, loss of Numb, symmetric division in the neuroblast and tumorigenesis in the mutant neuronal tissue. Thus, asymmetric division might function as a mechanism of tumor suppression in the *Drosophila* neuroblast, and impaired fate specification during SC division might be one of the initial events that drive these cells into malignancy. Moreover impairment in asymmetric cell division and tumorigenesis occurring after Numb loss strongly argue a role of Numb as “fate determinant” but also as tumor suppressor (Pece et al., 2004; Caussinus and Gonzalez 2005; Bello et al., 2006;

Betschinger et al., 2006; Lee et al., 2006; Wang et al.,2009; Wang et al.,2007; Gonzalez et al., 2007; Castellanos et al., 2008)

It is unclear whether there is also a direct causal relationship between loss of SC polarity and/or asymmetric divisions and tumor initiation even in mammals but the genes that control asymmetric cell divisions in *Drosophila* have an evolutionarily conserved role in the regulation of cell polarity and in tumor suppression, suggesting that polarity loss may contribute causally to cancer in mammals (Gonzalez et al., 2007; Januschke and Gonzalez, 2008).

During mitosis, Numb concentrates in the plasma membrane area overlying only one of the two spindle poles so acquiring a polarized distribution. Thereby Numb segregates into one of the two daughter cells during cytokinesis (Rhyu et al., 1994). Numb unequal segregation during the asymmetric cell divisions (intrinsic mechanism) is directed by the conserved Partition Defective Complex (Par) (Ohno et al., 2001; Suzuki and Ohno 2006) containing Par3, Par6 and by atypical protein kinase C (aPKC) (Henrique and Schweisguth, 2003; Macara et al., 2004). Three classes of Par proteins can be distinguished: the serine/ threonine kinase PAR-1 (Guo and Kemphues 1995) and the RING finger protein PAR-2 (Boyd et al. 1996) accumulate on the posterior cell cortex ruling the epithelial apical-basal polarity, whereas the anterior cell cortex is occupied by the PSD95/Dlg/ZO1 (PDZ) domain proteins PAR-3, PAR-6 and aPKC.

In mammals Numb binds to membranes through its N terminus, this plasma membrane affinity is regulated by Numb phosphorylation status (Knoblich et al. 1997) which is dynamically regulated by G protein coupled receptors and by direct activation of PKC. Both mammalian and *Drosophila* Numb interact with, and are substrates for aPKC throughout phosphorylation on specific serine residues. Numb indeed has a region containing at least 12 serines between amino acids 218 and 366. These residues are putative PKC phosphorylation sites. The phosphorylation on these residues neutralizes the charges and prevents membrane localization of Numb (Smith et al., 2007) (Dho et al., 2006).

Through this mechanism, PKC regulates Numb movement between the cell cortex and the cytosol in mammalian cells (Dho et al., 2006). When this pathway is activated, Numb localizes to the basolateral membrane and is excluded from the apical domain, which accumulates aPKC. Numb phosphorylation by aPKC serves as a conserved mechanism to regulate its polarized distribution during asymmetric cell divisions (Smith et al., 2007 Wirtz-Peitz et al. 2008).

Mode of division in CSCs

As previously demonstrated (Reya et al., 2001), there are several analogies between SCs cells and CSCs, but the responsible for CSCs tumorigenic potential could be found reasonably among their differences.

WT mammary SCs undergo limited rounds of mitotic division rapidly losing self-renewal potential in culture, before entering a post-mitotic fully differentiated state (progenitors cells) (Daniel et al., 1968). CSCs are nearly immortal and their potential be serially transplanted is virtually unlimited. CSCs by dividing asymmetrically, guarantee the self-renewal division; this strategy allows CSCs number retain and differentiation but leaving them unable to expand in number. Therefore, in order to expand their pool, CSCs must perform both asymmetric and symmetric divisions; the latter generates two new daughters with the same CSC fate (Morrison and Kimble, 2006).

By dividing symmetrically and asymmetrically they can increase their number producing only identical CSC daughters in some divisions and only identical differentiated daughters in others. This combined strategy brings to a differentiated progeny, hence CSCs maintain tumor cell heterogeneity and lead to the continuous expansion of the tumor mass. The mechanism responsible in this switch is still unclear but studies on $p53^{null}$ CSCs advanced a hypothesis on the role of p53 in CSC mitotic division (Gatza et al., 2008).

CSCs and p53

According to the first studies on the role of p53 in SC division, it has been reported that p53 imposes an asymmetric proliferative fate on daughter cells both in mouse

embryo fibroblasts and in one mammary epithelial cell line (Rambhatla et al., 2001) while the loss of p53 was found to increase self-renewal of neural SC in a sphere-forming assay arguing a switch from an asymmetric to a symmetric phenotype (Meletis et al., 2006; Piltti et al., 2006). In support of this, $p53^{null}$ CSCs are near immortal in culture due to not ended self-renewal and undergo symmetric self-renewing divisions; in the $p53^{null}$ mammary gland, CSC number is increased and they expand progressively, thus indicating that $p53^{null}$ SCs divide symmetrically also *in vivo*. On the other hand an increased WT p53 activity (p53+/m mice) has decreased regenerative capabilities upon serial transplantation, suggesting early stem cell exhaustion (Gatza et al., 2008).

p53 loss in CSCs: symmetric trend of division

The loss of p53 in levels and activity, because of its overt reported role of "guardian of genome" (Lane et al., 1992), has plausibly consequences on SC proper mechanisms as the asymmetric division.

Cicalese recently reported evidences of p53 involvement in the positive regulation of asymmetric vs. symmetric division in CSC murine model (Cicalese et al., 2009) proofing how the frequency of symmetric self-renewing divisions in CSCs is increased due to attenuated p53-signaling. Colaluca furthermore showed that the cell fate determinant Numb mediates the increase in p53 levels and activity, and the

regulation of p53-dependent phenotypes, through the formation of a Numb-p53-HDM2 ternary complex (Colaluca et al., 2008). These observations imply that p53, together with other tumor suppressors like Numb, could play a pivotal role in the regulation of SC self-renewal in the mammary gland by imposing an asymmetric mode thus self-renewing divisions.

p53 loss in CSCs: a possible solution

All together the previous finding suggest the possibility that p53 carries out its tumor suppression function by regulating self-renewal division. The deregulation of the machinery that controls and ensures the correct balance between symmetric and asymmetric SC division may lead to alteration of tissue homeostasis, increase of the SC pool and, finally, cancer.

According to that, since p53 is a potent suppressor of mammary transformation, an inhibition of SC symmetric divisions by p53 restoration could lead to tumor suppression in the mammary epithelium. The direct answer to this hypothesis comes from *in vitro* pharmacological approach where Nutlin, rescuing p53 activity, leads to rapid exhaustion of cultured mammospheres converting the prevailing mode of division of ErbB2 tumor SCs from symmetric to asymmetric and reduces tumor growth (Cicalese et al., 2009).

p53 targeted therapy: Nutlin

Because of its involvement in p53 homeostasis and in SC fate determination, MDM2 could be a target for cancer therapeutic intervention (Freeman et al., 2000). Indeed once freed from MDM2, p53 rapidly accumulates in the nuclei of cancer cells, activates p53 target genes and the p53 pathway, resulting in cell-cycle arrest and apoptosis.

MDM2 can down-regulate p53 only if the p53-MDM2 complex takes place. Therefore, inhibition of MDM2-p53 binding is a possible strategy for p53 stabilization and activation (Vassilev et al., 2007).

This result can be obtained by the use of a small molecule inhibitor, for example Nutlin, a cis-imidazoline compound (Tovar et al., 2006).

As other MDM2 inhibitors, Nutlin can block the p53-MDM2 complex formation. Crystal-structure studies demonstrated that Nutlin binds to a MDM2 hydrophobic cleft provided with crucial amino acid residues for p53-MDM2 coupling. Nutlin remarkably mimics their molecular interactions and by binding MDM2, it can dismiss p53 from this interaction, in that way, Nutlin preserves p53 levels and activity bringing to cell cycle arrest and suppresses tumor growth *in vivo* (Vassilev et al., 2004) (Bottger et al., 1997b; Blaydes et al., 1997 Brown et al., 2009).

The "cancer stem cell-targeting therapy"

The major issue in cancer therapy is the explanation of tumor relapse after chemotherapy or irradiation treatment. Current therapies, in fact, have been developed to target the bulk of the tumor mass, so far the only approach successful to reduce tumors. Unfortunately, it seems that both normal and CSCs are more resistant to chemotherapy than their differentiated progenies. This fact may be due to an increased expression of anti-apoptotic proteins, such as those of the BCL-2 family (Al-Hajj et al., 2003; Reya et al., 2001), or of transporting proteins, such as MDR1 and ABC transporters (Jordan et al., 2006). Due to their ability to remain quiescent, SCs are relatively resistant to cytostatic drugs, which act mainly on dividing cells (Gil et al., 2008; Reya et al., 2001; Visvader and Lindeman, 2008), therefore, despite dramatic responses on the tumor mass, these therapies could affect only the differentiated progenies of CSCs since the rare CSCs are not targeted. In contrast, CSC-targeted therapies that foresee the selective ablation of the rare CSCs, may represent an attractive method to eradicate the whole tumor mass (Fig. 4). Despite several studies supporting this strategy, (Guzman et al., 2005; Yilmaz et al., 2006; Piccirillo et al., 2006) there is only little experimental evidence that the selective ablation of CSCs would lead to the killing of the entire tumor mass without affecting normal SCs and their differentiated offspring (Jordan et al., 2006; Tan et al., 2006; Visvader and Lindeman, 2008).

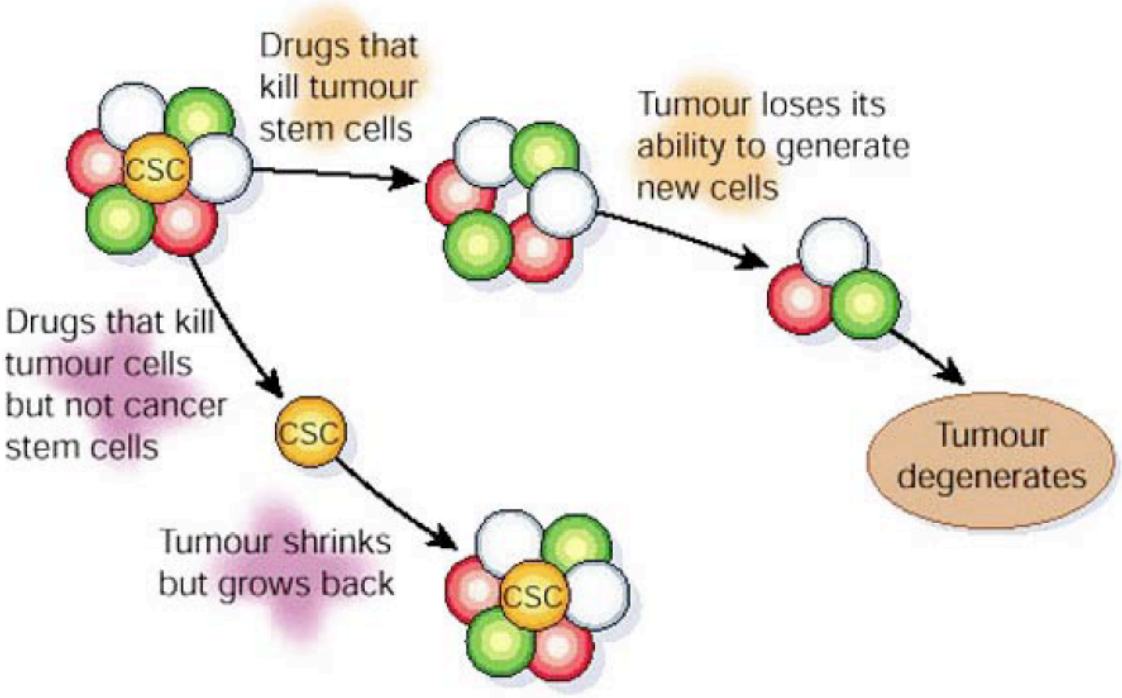

Figure 4
Cancer SC-targeted therapy
Conventional therapies may shrink tumors by killing mainly differentiated SC progenies. Cancer SCs, less sensitive to these therapies, could remain viable and re-establish the tumor. By contrast, therapies specifically targeting cancer SCs could arrest tumor maintenance or growth.
Modified from Reya et al., 2001.

In this thesis I report my investigations on the characterization of the biological and molecular features of Numb KO murine breast model in comparison with Numb deficient human breast cells model. I exploited an *in vitro* system (the mammosphere assay) to propagate and enrich breast SCs, in combination with a cell membrane labeling system (PKH-assay) to purify SCs.

The absence of Numb in both murine and human models helped to clarify the role of this “fate determinant” starting from the SC first mitotic division *in vitro* up to the *in vivo* tumorigenesis and related Numb reconstitution consequences.

Through the comparison of the self-renewal properties of normal and cancer SCs, both in terms of proliferative cell fate and Numb partitioning, and the study of the molecular mechanisms underlying abnormal growth properties, functional attenuation and pharmacological restoration of signaling pathways in mammary CSCs, I have attempted answer the open questions regarding the role of SCs in cancer development and maintenance, focusing the attention on a first possible direct evidence for cancer SC targeted therapy.

RESULTS

Numb is asymmetrically distributed at SC mitosis and partitions into the "stem" daughter cell.

According to the first studies carried on *Drosophila*, focused on Numb partition dynamics during stem cells (SCs) mitosis, Numb acquires a polarized distribution, it concentrates in the plasma membrane area overlying only one of the two spindle poles, than segregates into one of the two daughter cells (Rhyu et al., 1994). This asymmetrical distribution in *Drosophila* triggered the interest on Numb and enhanced the study of several scientific groups.

Recently our scientific group demonstrated that during mouse and human mammary SCs (MSCs) cytokinesis, Numb is partitioned unequally, segregating into one of the two daughter cells (Cicalese et al., 2009; Pece et al., 2010). In the current work, we exploited the PKH26 dye-based methodology (Cicalese et al., 2009; Pece et al., 2010) to verify whether Numb segregates into the daughter cell that retains the SC identity (the "stem" daughter cell) or into the one that assumes a progenitor fate (the "progenitor").

Five weeks old mice mammary glands were surgically explanted, reduced mechanically and digested as described in Materials and Methods (Tissue collection and digestion). Epithelial cells were purified from the bulk mammary cell population, seeded in SC selective medium (MESCM) and let grow in non-adherent condition. SCs are relatively quiescent and survive in anchorage independent conditions

withstanding *anoikis*, an apoptotic process due to anchorage detachment. In these conditions a single SC proliferates in suspension as a floating spherical clonal structure since the innate shape reachable in non-adherent condition by dividing cells is the sphere; this culture method selects for the SC growth and for the formation of the so called mammosphere (MS).

A single WT MS is structured by ~300 progenitor cells and contains only one SC, (Cicalese et al., 2009), thereby SCs compose a small fraction of the entire dissociated bulk mammary epithelial cell population. SCs were purified from this first generation of MSs throughout the use of PKH26 (see Materials and Methods "Isolation of primary SCs from mouse breast"). PKH26 is a lipophilic dye and it was used to stain the bulk mammary population before undergoing the selective culture method. PKH26 stains all the cells, SCs included. This dye will be half-retained by the SC from the first mitotic division, while progressively diluted by the counterpart of progenitors cells (PC) undergoing several following rounds of mitosis until reaching the number liable for MS size.

To track the SCs, aware of their quiescent or slowly dividing state, the employment of a lentiviral infection was chosen. A single cell population from dissociated MSs was stained with PKH-488, the green fluorescent analog of red PKH26, and lentivirally transduced with Numb-DsRed; the first rounds of mitotic division were monitored by time-lapse (TL) video-microscopy. Exploiting PKH-488 we were able to identify the

SC as the cell retaining the higher amount of lipophilic dye after the very first mitotic division and during the following ones; in the mean while the DsRed signal carried by Numb allowed us to track Numb distribution. Our aim was to see whether Numb was equally divided between the two daughter cells or rather retained by one of them. The TL identified the PKH^{pos} SC as the Numb-retaining cell (Fig. 1). Together with the identification of the Numb retaining daughter cell, TL analysis helper us to study the SC first mitotic division discriminating between symmetric and asymmetric mode.

The mode of SC division was established by two criteria

- an initial asymmetric division of the SC, followed by symmetric divisions of the progenitor, led to a typical 1-2-3-5 progression in the cell number; conversely a symmetric division of the SC led to a 1-2-4 pattern;
- retrospectively the "stem" daughter cell was identified as the cell that remained quiescent and therefore retained the PKH-488 dye (Cicalese et al., 2009; Pece et al., 2010), while the progenitor divided further to yield a limited progeny; this pattern was clearly identifiable only when an initial asymmetric division had occurred, since a fully symmetric pattern of SC division led to progressive dilution of the dye.

We found that, predominantly, MSCs divided asymmetrically and that Numb partitioned in the cell retaining the PKH dye, thereby the "stem" daughter cell (Fig. 2).

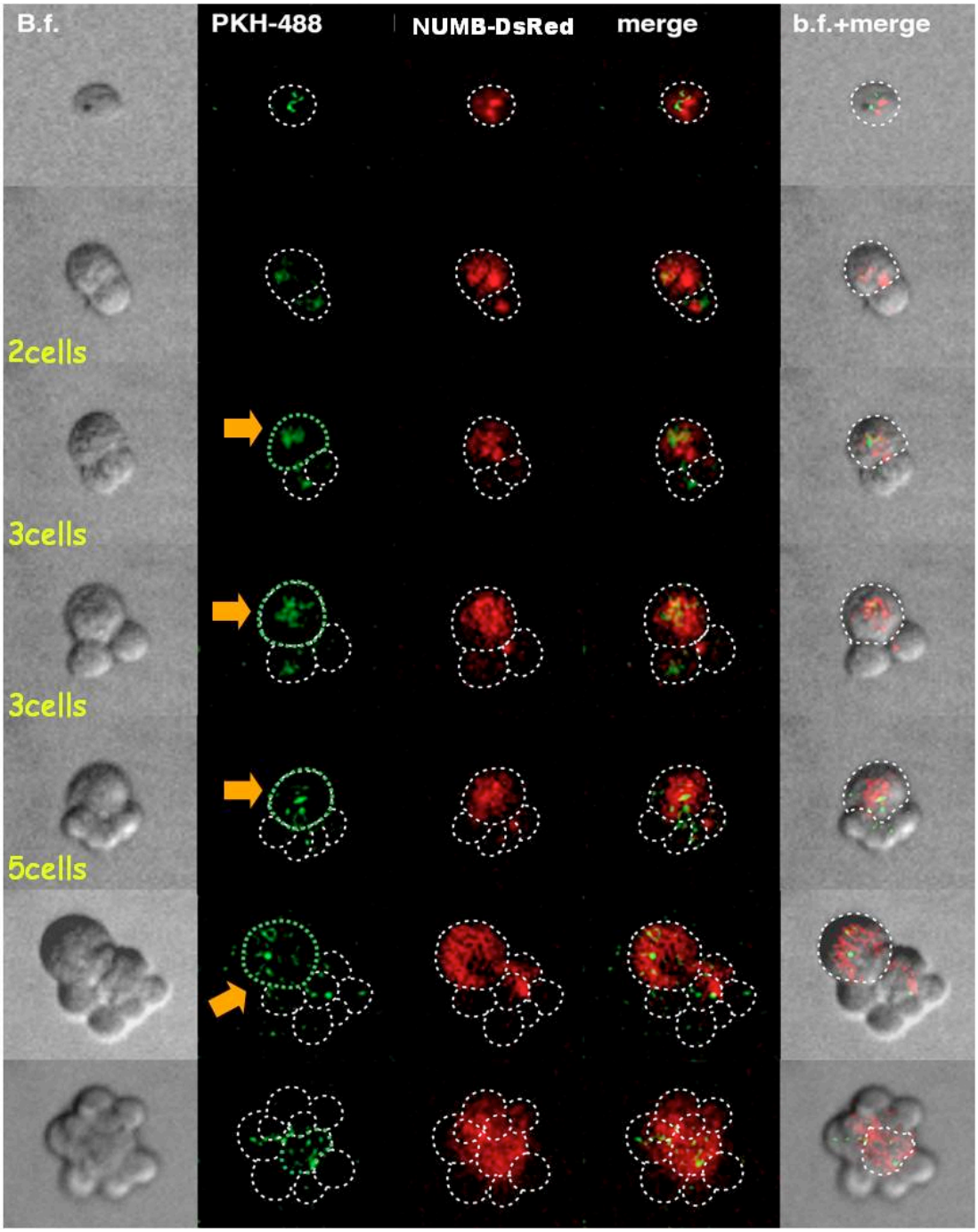

Figure 1
Time Lapse analysis. Numb partition in SC first mitotic division
Mouse MECs were labeled with PKH 448 and pLVX puro Numb DsRed. Quiescent/slowly dividing SCs fraction retained PKH dye during the first divisions (green). 488 nm green light tracks SCs (yellow arrows) in the forming MS. 660 nm red light: Numb DsRed Merge panel is presented both in fluorescence and bright field (b.f+merge)

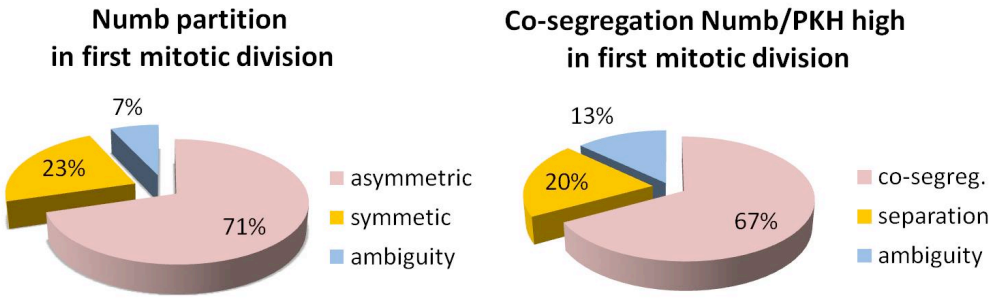

Figure 2
TL statistical analysis.
Numb partition in first mitotic division. Cake graph on the left summarizes the percentage of asymmetric vs. symmetric events on total number of 56 observations.
The graph on the right estimates the percentage of co-segregations Numb/PKH$^{high\ pos}$ cells on total 32 mitotic divisions observed.

Numb KO and Numb KD: loss of Numb causes replicative symmetry in MSCs

Once identified the Numb-retaining daughter cell as stem cell, we investigated the consequences of Numb ablation in MSCs. To perform this study we exploited both the *in vitro* and the *in vivo* approach.

The *in vivo* implications of Numb loss were studied throughout the Numb KO engineered mouse model that was obtained using the CRE-loxP recombinase system (Wang Y et al., 1996).

Within the normal mammary gland, the SCs are located within the epithelial basal compartment. These cells express both luminal (citokeratin CK8, CK18) and

basal/myo-epithelial markers (cytokeratin CK5, CK6, CK14) (Howard et al., 2000; Petersen et al., 2010)

The use of the CK5 promoter let us to specifically knock down Numb in the stem cell compartment. CK5 transcription is regulated by its CK5 promoter that is active in breast and in several epithelial tissues, including the basal cell layer of the epidermis, hair follicles, oral epithelium, vagina, stomach, esophagus, bladder, and thymus (Ramirez et al., 1994; Stingl et al., 2006; Pece et al., 2010). To obtain the Numb KO mouse model we crossed Cre-loxP conditional Numb-KO mice (Zilian et al., 2001 Wilson et al., 2007) with CK5-Cre mice (Ramirez et al., 2004) (see Materials and Methods "The Cre/loxP recombination system in transgenic mice").

Aim of the work

The aim of the project is to study the role of Numb and the consequences of its loss in breast stem compartment. To reach this goal we developed the murine Numb KO model exploiting the Cre/loxP recombination system. The Numb KO mouse lacks in Numb in all the tissues in which K5 is active and among these, the breast is included. In support to this strategy and to validate the results coming from Numb KO mouse model we could count on Numb KD *in vitro* model using ShRNA (short hairpin) silencing technique in WT murine breast primary cells.

Numb Knocking Out: efficacy of murine model

To verify whether Numb KO murine model displayed correctly Numb loss in breast and in stem cell compartment, biochemical analysis (Western Blot) was carried on the primary mammary epithelial cells (MECs) obtained from breast digestion of Numb KO mice breast and related spawned MSs.

Numb KO mice breast confirm a markedly reduced Numb level both in MECs and MSs, thereby we step forward analyzing first of all the possible *in vivo* phonotypical effects of Numb loss and than, through *in vitro* assays, we tested Numb KO MECs sphere forming efficiency (SFE) and related MS propagation.

Numb KO in vivo read out

Numb KO mice breast did not display evident morphological changes to a first necroscopical analysis. We thereby decided to perform a whole mount analysis on the entire fat pad. This approach consist in a low magnification screening to get information about possible gross alterations of the major structures composing the breast fat pad. This histological technique permits to focus the attention on number and dimension of primary and secondary ducts, rate of branching and acini size. Whole mount analysis was performed using Carmine Alum technique (see Materials and Methods “Mammary gland Whole Mount staining with Carmine Alum”), and it was accompanied by classical histological investigation with hematoxilin/eosin (H/e)

staining for a higher magnification analysis that put in evidence enlarged and hyperbranched ducts (Fig. 3c,d; Fig. 4b) together with hyperplastic (Fig. 4c; Fig. 5b, c), dysplastic and preneoplastic lesions, such as hyperplastic alveolar nodules (HANs) (Medina et al., 1976, 1996; Cardiff, et al., 2000).

This is the most extensively characterized lesion and it is similar to the differentiated alveolar cells normally found in pregnant mammary gland of lactating mice. HANs were originally identified as persistent focal areas of alveolar hyperplasia in non-pregnant mice.

These morphological evidences strongly argue a fundamental role of Numb in breast tumorigenesis, emerging from the analysis of phenotype obtained throughout its loss in murine Numb KO model.

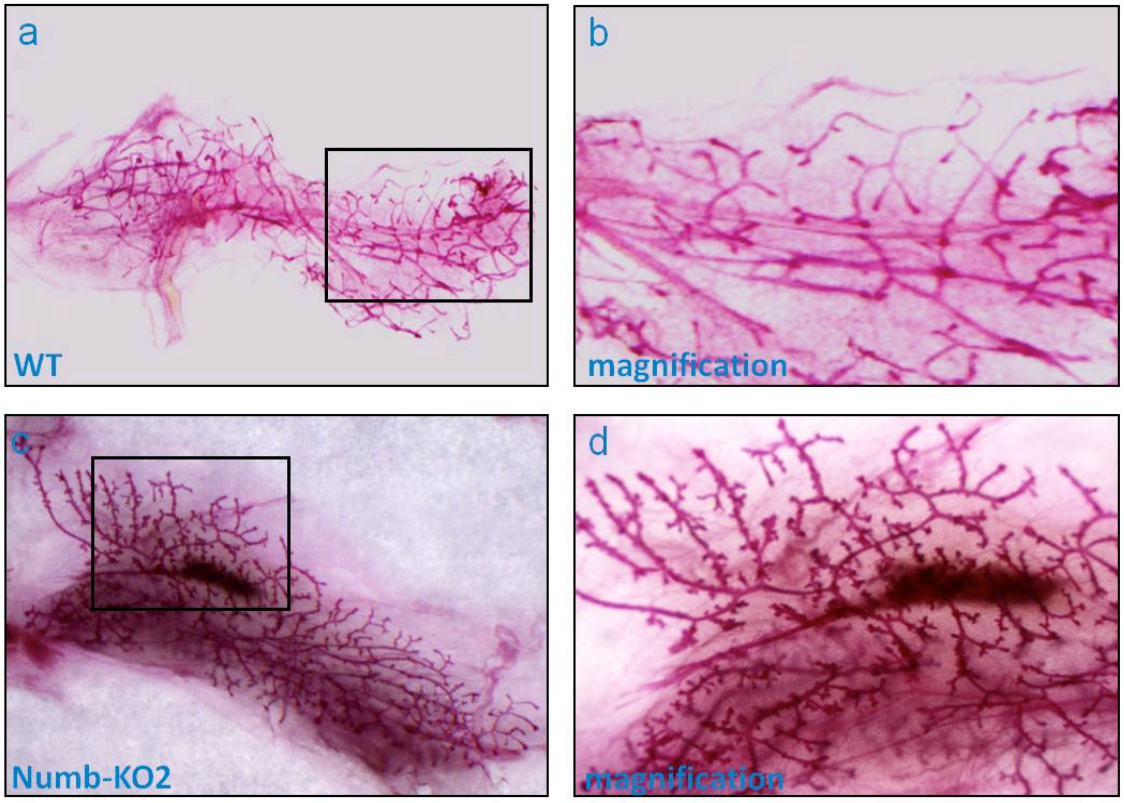

Figure 3
Numb KO mouse model: macroscopic breast analysis.
Carmine Alum staining was used on whole mount inguinal breasts to investigate the ductal architecture.
(a) WT control breast phenotype, magnification in figure b.
(c) Numb KO2 breast phenotype, magnification in figure d.

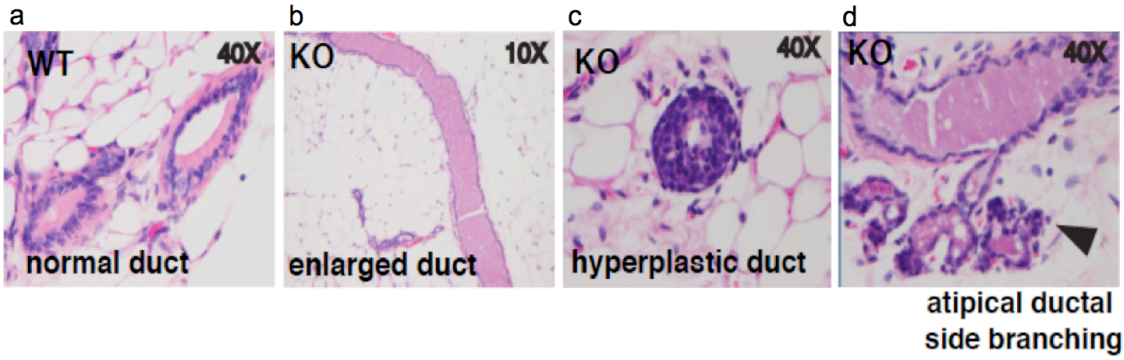

Figure 4
H/e microscopic breast analysis on FFPE: Comparison between WT and Numb KO mouse breast:
(a) Typical bilayered asset of WT epithelial duct with correctly sized lumen.
(b) Possible Numb KO phenotype: enlarged duct with filled lumen delimitated by stretched epithelium.
(c) Possible Numb KO phenotype: Hyperplastic Duct, loss of epithelial architecture, reduced/absent lumen
(d) Ductal hyperbranching (black arrow): Numb KO breast displays increased number of secondary ducts exiting from primary ducts side.

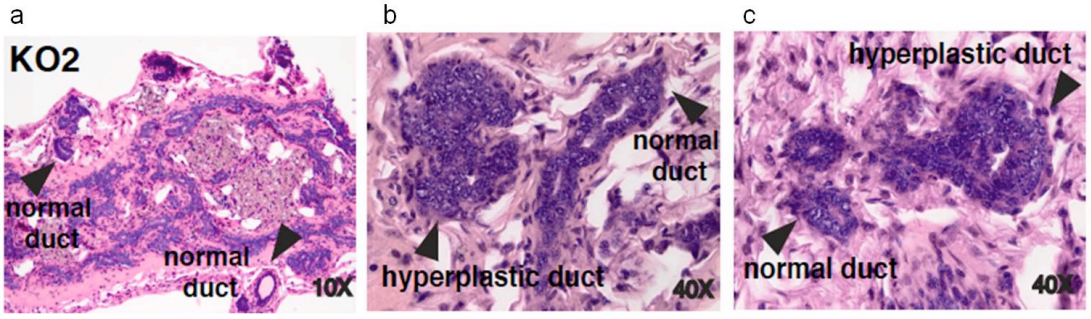

Figure 5
Numb KO mouse model: microscopic breast analysis.
H/e analysis of FFPE Numb KO2 breast. In evidence the presence of both normal and hyperplastic ducts in the same sample (black arrows). Representative images are shown.

Numb KO in vitro read out

Biochemical analysis (Western Blot – WB) carried on that primary mammary epithelial cells (MECs) obtained from breast digestion of Numb KO mice breast displayed markedly reduced Numb levels (Fig. 6a,b). According to previous studies (Colaluca et

al., 2008; Pece et al., 2004), Numb plays a crucial role in two major pathways. Numb has been demonstrated to inhibit Notch function preventing its translocation to the nucleus inducing its ubiquitination and meanwhile controlling Notch intracellular domain degradation (McGill & McGlade 2003; Pece et al., 2004). Recently Numb has been entrusted with the role of p53 regulator, participating in the formation of the Numb-p53-MDM2 tricomplex, which is responsible for the regulation on p53 ubiquitinilation and than the control of p53 homeostasis (Colaluca et al., 2008). Therefore a possible approach was identified in the biochemical analysis of the molecular partners interacting with p53 and Notch in order to verify whether the loss of Numb brought to changes in their activity. QPCR analysis reports how the loss of Numb causes decreased p53 levels respect to WT counterpart and congruent alterations of positively regulated (mdm2, p21) and negatively-regulated (nanog) p53 targets (Fig. 6c). Furthermore Notch activity is enhanced, proofed by increased transcription of the Notch targets, hey1 and hey2 (Fig. 6c). A similar alteration at the level of p53 and Notch pathways has been seen in the Numb KD MSs (Fig. 6c).

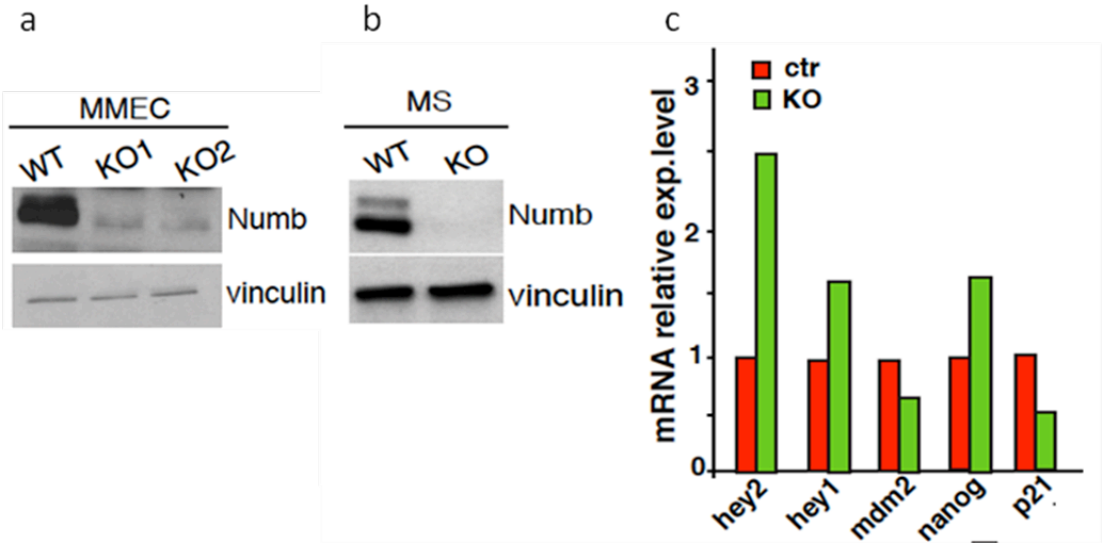

Figure 6
Analysis of the efficiency of conditional Numb Knocking Out in mouse MECs and related spawned MSs.
(a, b) Immunoblot analysis of Numb expression in total cell lysates (30µg) of MEC and related spawned MSs Both Numb KO1 and KO2 lines were considered in MMECs analysis. Numb levels were detected with Ab#21 monoclonal antibody. Vinculin was detected as a protein loading control.
(c) QPCR analysis of Numb targeted factors mRNA relative expression. Hey1, hey2 and nanog levels were considered as readout of Notch signaling, p21 and MDM2 levels for p53 activity. Immunoblots are representative of 2 experimental repeats.

Numb KO cells in vitro propagation: the Mammosphere assay

Since p53 is largely considered one of the major tumor suppressors controlling cell cycle and cell homeostasis (Lane et al., 1992), often involved in different tissues tumorigeneris. The Cancer Stem Cells (CSCs) theory (Clarke et al., 2006) identifies in CSCs expansion the responsible for tumorigeneris as well as for tumor relapse; following this hypothesis, we decided to investigate on a possible SC compartment expansion in Numb KO model, where, as previously said, the loss of Numb brings to a decreased p53 activity.

To verify whether the loss of Numb levels and activity by knocking out had caused an expansion of the SC compartment we performed the *in vitro* Mammosphere assay (see Material and Methods: Mammosphere assay and SFE). This experiment consists in a precise retroactive study of SCs number relying on the sphere number found after a determined period of MECs culture. The combination of SCs culture medium (MESCM see Material and Methods) and the lack of adhesion, let only the SCs proliferate spawning floating spheroid colonies, identified as mammospheres (MSs) and their final number is indicative of the SCs number included in the early bulk population. The final number of spheres divided for the starting number of cell seeded (multiplied for 100) scores the Sphere Forming Efficiency index.

Thereby the sphere size can be easily calculated by disaggregating the MSs to a single cell suspension; the number of cells obtained divided for starting MSs number gives a value to MSs size.

This assay allows us to estimate the starting number of SCs in a sample, their self-renewing potential and nevertheless to notice a possible SC number increase upon serial propagation *in vitro*. This last step consists in a prolonged culture assay throughout consecutive passages. MSs were mechanically desaggregated and seeded in single cell suspension to let the next generation MSs grow. Indeed once the SC is released from its PCs envelope that inhibited SCs mitosis, the SC can divide again spawning another sphere; that process can be repeated up to 3/4 times in WT sample

until the self-renewing extinguishment. On the other hand, in tumor samples, as previously demonstrated (Cicalese et al., 2009; Pece et al., 2010), CSCs grow in number throughout the generations *in vitro* bringing to an increase in SFE index and MSs size. In that case the self-renewing potential is unlimited and the sphere propagation can be carried on for a not ended number of generations.

To quantify the starting SC number in out samples we exploited the Fluorescence-activated cell sorting (FACS) analysis. Bulk MEC population obtained from digestion of WT and Numb KO breasts were counted, stained with PKH26 and seeded in 5/6 days selective SC culture (absence of adhesion in MESCM). PKH26 is a lipophilic dye that is half-retained by the SC thereby resulting PKH^{HIGH} stained from the first mitotic division, while progressively diluted by the counterpart of progenitors cells (PC) undergoing several following rounds of mitosis (thereby PKH^{LOW} and PKH^{NEG}). FACS discriminates and collects PKH^{HIGH} SCs hence purified from the mammary epithelial buck population (see Materials and Methods "Isolation of primary SCs from mouse breast").

We tested both MECs and derived MSs, obtained from individual Numb-KO mice and WT mice. Numb-KO MECs contained ~3-4-fold more SCs than WT ones, with a SC frequency of ~1:8,000 in Numb-KO, and ~1:30,000 in WT cells (Tosoni Unpublished preliminary data).

Throughout *in vitro* analysis we observed that the 1st generation WT MSs were approximately ~100µm sized and contained ~300 cells/MS, with a SFE of ~0.3%, in agreement with the assumption of the correlation between the number of SCs and spawned MSs proposed in previous reports (Cicalese et al., 2009). On the other hand, MSs originated from Numb-KO MECs were ~2-fold larger (~500-600 cells/MS) and showed a ~2-3-fold higher SFE.

The bigger size of these MSs and the higher SFE index of their constituting cells argue a higher amount of SCs inside them: we estimated a frequency of ~4-5 SCs per MS. We observed moreover that MSs derived *in vitro* from Numb-KO MECs had a SCs frequency of ~1:150/200 (Tosoni Unpublished preliminary data).

Upon serial propagation *in vitro*, WT-MSs progressively lost self-renewal ability, consistent with previous reports in mouse and human (Cicalese et al., 2009; Pece et al., 2010). Conversely, the number of Numb-KO MS increased over time, with a constant ~2-3-fold expansion rate. In agreement with the correspondence between the starting SC number and the spawned MS (Cicalese et al., 2009; Pece et al., 2010), the observed increase of MS number through the consecutive passages *in vitro* argues a SC compartment expansion in Numb KO model. The step responsible of this event is the SC first mitosis, when the SC should divide in 1 SC and 1 progenitor following an asymmetric mode (see "Mode of division in SCs"). If a symmetric division occurs, the SC divides in 2 SC amplifying the resulting SC pool.

Throughout the time-lapse (TL) video-microscopy approach, we were able to demonstrate how Numb-KO SCs divided predominantly in a symmetric fashion (90%, Fig. 12b), and with a faster division rate compared to WT cells. The entire set of observations was replicated using an alternative strategy, the functional ablation (*in vitro* Numb KD) of Numb in WT-MECs (Fig. 7, Fig. 8).

Numb Knocking Down *in vitro*

Similar results were obtained from *in vitro* Numb KD. WT MECs were infected with the lentiviral construct pLKO Sh Numb exploiting the ShRNA (short hairpin) silencing technique (see Materials and Methods). Among several constructs, pLKO #39 was chosen for its efficacy witnessed by biochemical analysis (WB Fig. 7a). Therefore a possible approach was identified in the biochemical analysis of the molecular partners interacting with p53 and Notch in order to verify whether the loss of Numb brought to changes in their activity. WB analysis and QPCR report how the loss of Numb causes decreased p53 levels (Fig. 7b) respect to WT counterpart and congruent alterations of positively regulated (mdm2, p21) (Fig. 7b,c) and negatively-regulated (nanog) p53 targets (Fig. 7c).

Furthermore Notch activity is enhanced, proofed by increased transcription of the Notch targets, hey1 and hey2 (Fig. 7c). A similar alteration at the level of p53 and Notch pathways has been seen in the Numb KD MSs.

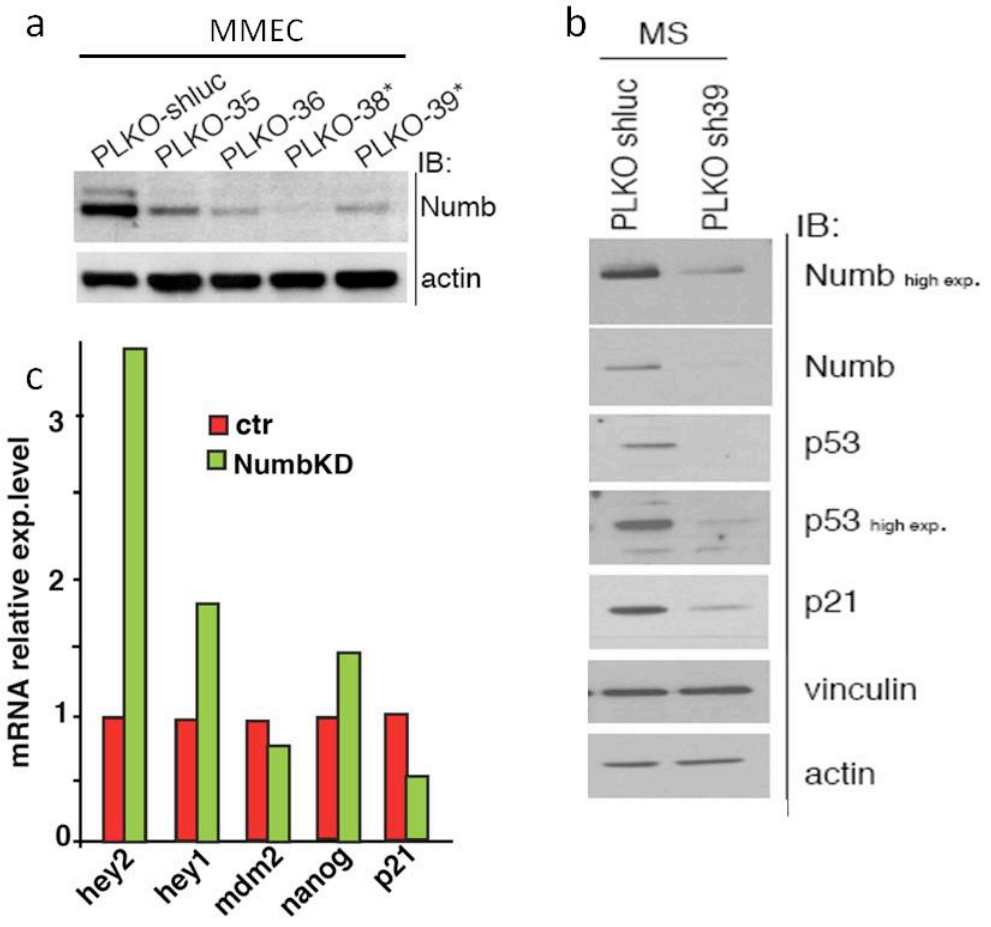

Figure 7

Analysis of the efficiency of ShRNA technique Numb Knocking Down in mouse WT MECs and related spawned MSs.

(a) Immunoblot analysis of Numb expression in total cell lysates (30µg) of MMECs after infection with PLKO Sh35,36,38,39. PLKO Sh39 was chosen and PLKO-ShLuc was used as negative control.

(b) Immunoblot analysis of Numb expression in total cell lysates (30µg) of MSs spawn by PLKO Sh39 infected MMECs. Both short and long (high exp.) exposure images of Numb and p53 immunoblots are reported. Numb levels were detected with Ab#21 monoclonal antibody. Vinculin was detected as a protein loading control.

(c) QPCR analysis of Numb targeted factors mRNA relative expression. Hey1, hey2 and nanog levels were considered as readout of Notch signaling, p21 and MDM2 levels for p53 activity. Immunoblots are representative of 2 experimental repeats.

The entire panel of Numb KO *in vitro* experiment previously exposed was performed using Numb KD cells. According to results coming from mammosphere assay, Numb KD MSs displayed a bigger size compared to WT (Fig. 8b,d). After having performed an *in vitro* serial propagation we noticed an increasing estimated SFE for these cells throughout the consecutive passages, likewise in Numb KO cells (Fig. 8 lower table). These data argues a higher amount of SCs inside Numb KD MSs suggesting a possible switch from an asymmetric to a symmetric mode of division consequent to Numb knocking down. These evidences suggested that Numb silencing is a suitable alternative model to reproduce the results obtained from the Numb KO mouse model.

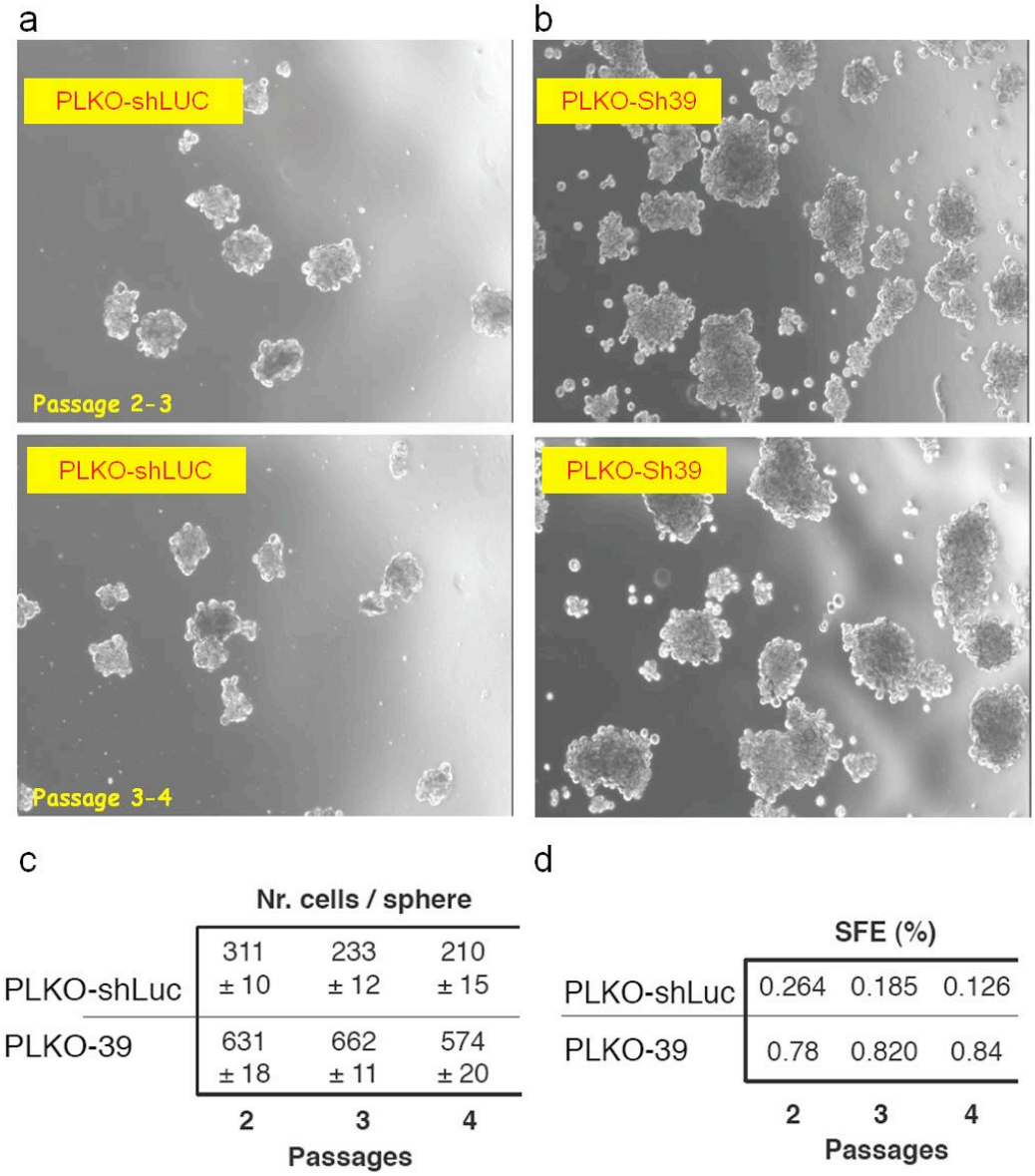

Figure 8

Effects of Numb ablation on SCs organotypic outgrowths in culture suspension and SFE.
SFE assay was performed on FVB cells collected from first generation sphere mechanical desaggregated and repeated for the next 2-4 passages.
(a) Control cells were infected with PLKO-ShLuc.
(b) Numb KD was assessed through PLKO Sh39 infection
(c) Spawned spheres were counted and collected each passage, than desaggregated in single cells, of which number was considered to calculate sphere size and next passage SFE (d)

Aberrant mammary morphogenesis and tumor initiation by loss of Numb

According to previous studies (Hennighausen and Robinson et al., 2001, 2005; Smalley and Ashworth, 2003), the SC is the only responsible for tissue organogenesis. This means that SCs, when inserted in a permissive context, can spawn the entire complex structure of the surrounding environment. In our case, SC showed the ability to spawn MSs *in vitro* as an attempt of morphogenesis. To investigate whether SC were able to re-constitute the epithelial tissue structure, we transplanted Numb KO bulk MECs and to quantify the SC number, MECs transplantation was performed at limiting dilution to score the mammary repopulating unit (MRU) index or the cancer initiating cell (CIC) number. These indexes are denotive of SC number in the starting bulk MEC population transplanted. A range of cell dilution, from 10^5 to 10 cells was chosen for the injection in 5 weeks NOD SCID mice inguinal breast, closed to nipple area where the endogenous epithelium is concentrated and the remaining fat pad was cleared to give space to cell outgrowth.

The so obtained outgrowths were analyzed through histological assay in order to quantify the epithelial structures.

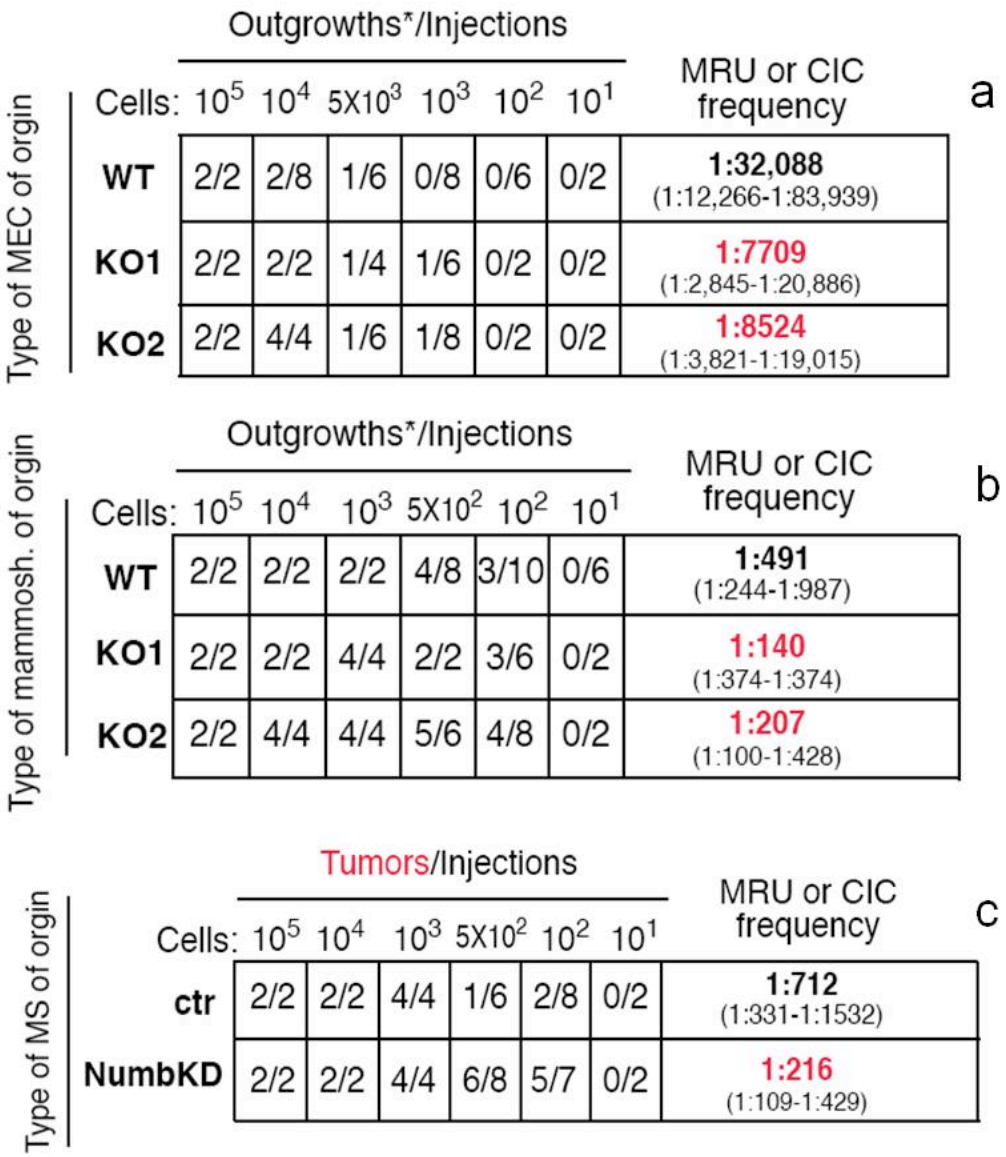

Figure 9

***in vivo* Numb KO and Numb KD cell transplantation assay. MRU and CIC frequency.**

(a) Numb KO1 and KO2 MECs lines were transplanted at limiting dilution in cleared fat pad mice. A range of cell dilution, from 10^5 to 10 cells, was chosen and the mammary repopulating unit (MRU) index or the cancer initiating cell (CIC) number were calculated on the base of the eventual outgrowth obtained.

(b) MSs spawned by Numb KO1 and KO2 MECs were desaggregated and the obtained cells transplanted at the same previous limiting dilution. MRU and CIC frequency were calculated.

(c) Cells obtained from Numb KD MSs desaggregation were transplanted at the same range of dilution. MRU and CIC frequency were calculated

Macroscopically, the outgrowths generated by WT-MEC and WT-MS cells were indistinguishable from the normal mammary gland but after a deeper histological analysis, in 7 of 10 cases, the reconstituted mammary tissue generated by Numb-KO cells displayed a number of gross morphological alterations. Primarily these outgrowths displayed hyper-branched and enlarged ducts alongside areas of ductal hyperplasia and severe dysplasia together with preneoplastic lesions such as HANs (Medina et al. 1976) and areas of frank malignancy. In a fraction of cases (3 of 10), the outgrowths generated by Numb-KO cells were overtly neoplastic; the cells obtained from breast digestions of two cases among these were identified as KO1 and KO2 and chosen to carry on the following experiments in relation to the shown tumorigenic skills.

The selected KO1 and KO2 were transplanted the day after the digestion: cells were multiple injected at limiting dilution in order to score their mammary repopulating unit (MRU) frequency as readout of their cancer initiating cells (CIC) content.

Both KO1 and KO2 MECs gave outgrowths with a higher frequency arguing a higher SCs fraction if compared to WT MECs; the loss of Numb could be the responsible of the SCs (or even CSCs) increase in these Numb KO MECs (Fig. 9a,b).

The entire set of observations, obtained with Numb-KO MECs, could be replicated with the xenotransplantation of MSs spawn by both Numb KO and Numb KD MECs (Fig. 9c).

The tumorigenic skill of our Numb KO model was even confirmed even by 3D culture assay. Indeed, Numb-KO MECs seeded on 3D-organogenic Matrigel assay, generate outgrowths displaying features of faulty morphogenesis, with disorganised, filled and hyperproliferative structures, as opposed to the typical bilayered and hollowed acinar/lobulo-alveolar structures generated by WT-MECs (Fig. 10).

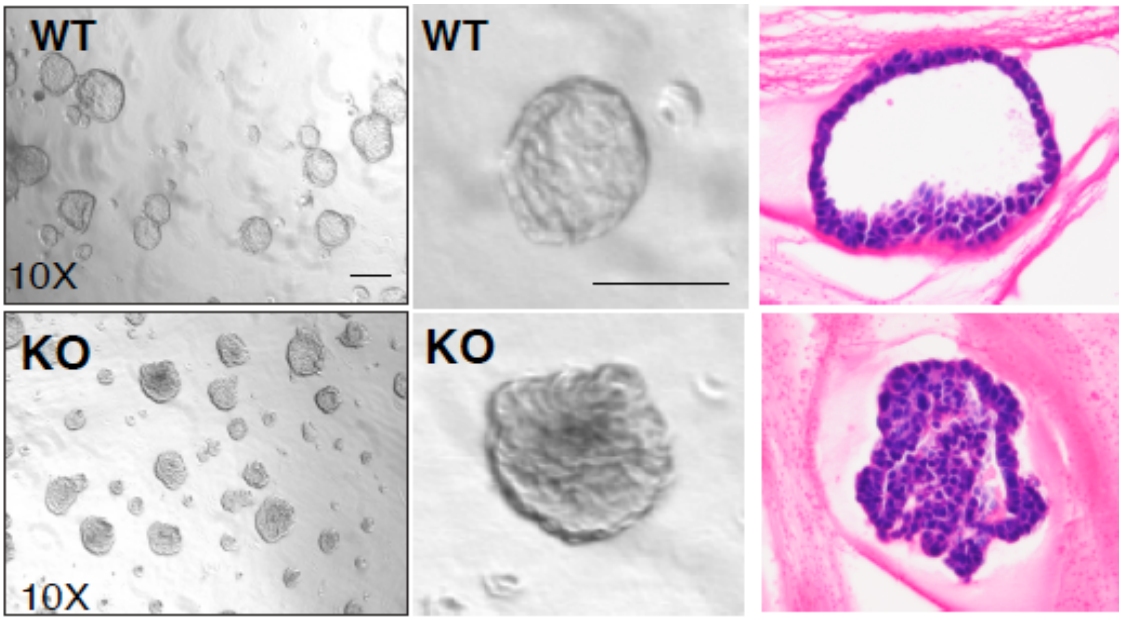

Figure 10
3-D Matrigel assay; differences between WT and Numb KO acinis.
Morphological analysis of overlay seeded WT and Numb KO cells spawned spheres on matrigel support
Left: Bright field and related magnification of WT vs KO MSs.
Right: Histological (H/e) analysis; confrontation between lumen dimension and epithelial structures

As previously demonstrated, Numb unequally partitionates during MSC division segregating into the "stem" daughter cell, ruling the asymmetric fate determination of the SC itself.

The subversion of this mechanism, through the loss of Numb expression, switches SC division from asymmetric to symmetric, causing the expansion of the SC compartment and contributing to the acquisition of a malignant phenotype observable *in vitro*, in MSs expansion (Fig. 8), *in vivo*, in breast outgrowth (Fig 3,4,5) and in matrigel assay organogenesis (Fig. 10).

NUMB RESCUE *IN VITRO* AND *IN VIVO*

To verify whether Numb restore could revert the malignant phenotype displayed by Numb KO MECs and MSs, we infected the Numb KO lines with the pLVX lentiviral vector carrying the Numb gene, tagged with DsRed fluorescent protein (Fig 11 right). In addition to *in vivo* Numb tracking, the use of pLVX-Numb-DsRed ensures the overexpression of Numb protein; in our context, in Numb KO cells, we tried to rescue Numb physiological levels and function. Afterwards we evaluated possible changes in MSs size and MECs SFE *in vivo* upon pLVX-Numb-DsRed infection.

Reconstituted Numb-KO MECs displayed successful Numb and also p53 rescue in terms of protein levels. Moreover, p21 level, which was decreased as consequence of p53 fall in Numb KO model, was restored. (WB Fig. 11 left)

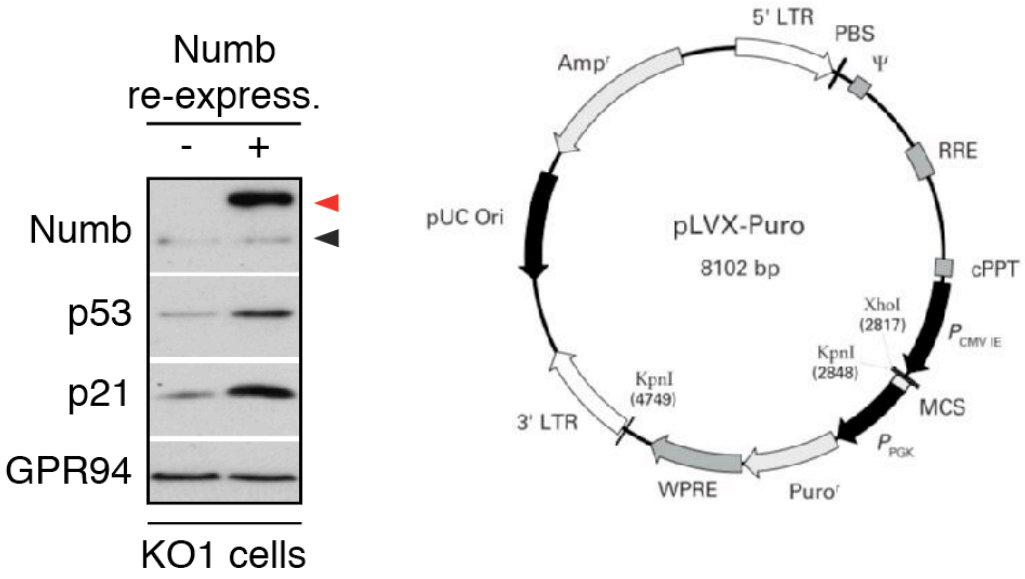

Figure 11
Left: Immunoblot. Numb rescued cells upon lentiviral infection
Right: pLVX-puro lentiviral plasmid carries the fusion protein Numb-DsRed.
Numb was re-expressed in Numb KO cells.
pLVX EV infection (-), pLVX puro NumbDsRed infection (+).
Total cell lysates (30µg) from Numb KO (-) and Numb re-expressed Numb KO (+) were immunoblotted with Ab#21 monoclonal antibody. Anti p53 (Cell Signaling) Anti p21 (Santa Cruz Biotechnology) were used. GRP94 was detected as a protein loading control. Numb levels in Numb re-expressed cells are indicated by red arrow, endogenous Numb levels by black arrow.

Effects of Numb rescue can be observed also in Time-Lapse analysis. Numb KO Stem Cells perform predominantly symmetric first mitotic divisions; Numb overexpression inverts this trend: after infection indeed the majority of observed mitosis showed an asymmetric mode of division (Fig. 12b). Evidences of Numb rescue came from *in vitro* analysis of Numb KO MSs grown from pLVX-Numb-DsRed infected MECs. These

MECs used to spawn spheres with a ~2-fold decrease SFE if compared with Numb KO MECs. These Numb rescued MSs moreover displayed a ~60% smaller size (Fig. 12a).

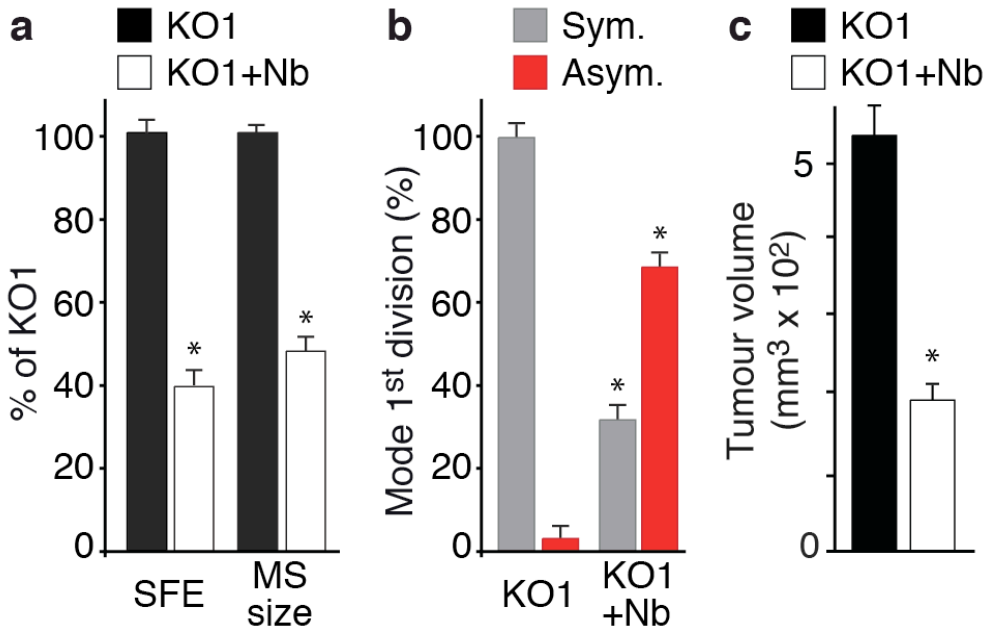

Figure 12

in vitro **effects of Numb rescue on Numb KO1 cells upon pLVX Numb DsRed lentiviral infection.**

(a) Bar graph represents the SFE and MSs size in Numb KO (KO1 -black column) cells and the same parameters after Numb recue (KO1+Nb -white column).

KO1 cells were compared with KO1+Nb cells exploiting TL analysis to get eventual changes in 1st mitotic division after Numb rescue. Bar graph "b" reports the ratio between symmetric (grey column) and asymmetric (red column) events both in KO1 and KO1+Nb cells.

Numb re-expressed (pLVX NumbDsRed infected) Numb KO cells were injected in one side breast, pLVX-EV infected Numb KO cells were injected as control in the other side breast and let both the tumor masses develop.

in vivo **effects are reported in figure "c". Bar graph displays the differences between the tumor volumes reached by Numb KO (KO1) control cells (black column) and Numb rescued Numb KO cells (KO1+Nb) (white column).**

We investigated also the possible effects of Numb rescue *in vivo*. pLVX-Numb-DsRed infected MECs were transplanted in NOD SCID mice. The tumors raised were ~2-fold smaller in size compared to mock-infected controls (Fig 12c).

To exclude the possibility that the smaller size of the tumors was due to increased apoptosis or decreased proliferation, we demonstrated by IHC analysis performing an anti-KI67 staining that the proliferation was not affected. Moreover Numb reconstituted tumors did not show a higher number of Caspase-3 activated cells, thereby arguing that these cells do not undergo apoptosis (Fig. 13).

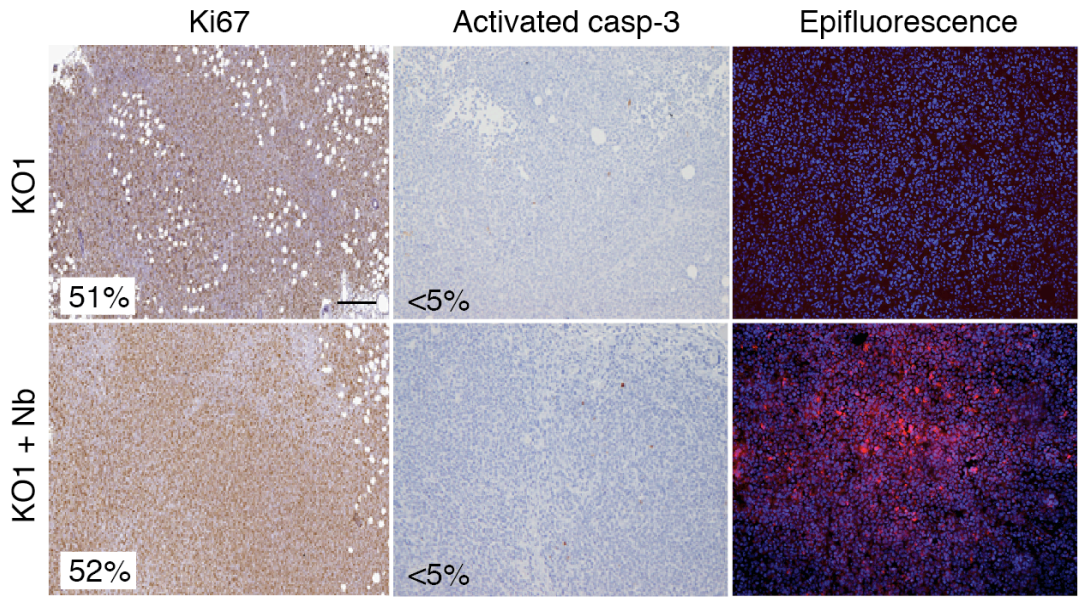

Figure 13
IHC on tumors derived from Numb KO (KO1) and Numb re-expressed Numb KO (KO1+Nb) FFPE sections were stained for KI67 (Thermo Scientific #9106) to score the proliferation index. Consecutive sections were stained for Activated Caspase (Cleaved Caspase 3, Asp175 Cell Signaling #9661) to quantify the number of apoptotic events.
Sections were scanned with Aperio ScanScope XT and DAB signal was quantified and analyzed with Spectrum Version 11.0.0.72 (Aperio Technologies)
OCT Frozen sections were DAPI stained and observed in red fluorescent light (560nm). Numb DsRed fluorescent fusion protein was detected.

According to published data (Cicalese et al. 2009), the tumor suppressor p53 controls the SC fate ruling the ratio of symmetric vs. asymmetric divisions. According to what has been previously shown about the role of Numb in stabilizing p53 protein (Colaluca et al 2008), here we show that Numb is required to maintain the correct p53 levels in the SC compartment to ensure the proper ration asymmetric vs. symmetric divisions. Loss of Numb causes a decrease in p53 levels and activity, and the consequence is a switch towards symmetric SC divisions. Thereby, Numb may function by modulating p53 activity in the MSC compartment.

p53 rescue: Nutlin-3 *in vitro*

Evidences that the Numb-p53 axis might have a role in the control of the MSCs number by imposing an asymmetric mode of division came from experiments of Numb protein levels rescue and p53 restoration. In particular, Numb control of p53 homeostasis seems to have a crucial role in tumorigenesis; the issue is that we clarified this mechanism by imposing a SC directed approach throughout a lentiviral infection, not suitable in clinic strategies.

Since our aim, as research group committed in experimental oncology, is to carry in clinical area our knowhow on molecular dynamics involved in breast tumorigenesis, it becomes necessary to develop a pharmacological approach suitable to interfere with

the mechanisms responsible for breast tumorigenesis. Thereby we considered as a possible direct strategy to hit p53-MDM2 axis.

The p53-MDM2 autoregulatory feedback loop governs p53 amounts (Wu et al., 1993). MDM2 is an ubiquitin ligase responsible for p53 ubiquitin-dependent proteolytic degradation. Overexpression of MDM2 in human cancer, e.g., gene amplification of MDM2, targets p53 and interrupts the p53 network. (see "The p53-MDM2 axis"). We used Nutlin-3, a cis-imidazoline compound. (Tovar et al. 2006) to inhibit p53-MDM2 complex formation. Nutlin-3 as other MDM2 inhibitors, can block the p53-MDM2 complex formation. This mechanism is proofed by crystal-structure studies demonstrating that Nutlin-3 binds to a MDM2 hydrophobic cleft provided with crucial amino acid residues for p53-MDM2 coupling (Kussie et al., 1996). Nutlin-3 remarkably mimics p53 in its molecular interactions with its ubiquitin ligase MDM2 (Fig. 14 right). By binding MDM2, Nutlin-3 can dismiss p53 preventing its ubiquitin-dependent proteolytic degradation. In this way, Nutlin-3 preserves p53 levels and activity bringing to cell cycle arrest and suppresses tumor growth *in vivo* (Vassilev et al., 2004). The entire set of *in vitro* Nutlin-3 treatments was performed applying 10μM final concentration for 24 and 48 hours. Nutlin-3 treatment was performed both in cell suspension for biochemical analysis and in Methylcellulose-based medium (MethoCult™ Stemcell Technologies) for TL experiments. Since Nutlin-

3 powder was resuspended in DMSO (according to product datasheet) all the control samples were treated with an equal volume of DMSO.

Given that Numb-KO MSCs had overall lower p53 level and activity because of the lack of Numb, as previously demonstrated by Numb *in vitro* rescue in Numb KO cells upon pLVX-Numb-DsRed infection, we treated Numb KO cells from dissociated MSs to Nutlin-3 to test whether the restoration of p53 activity could restore the asymmetric mode of division and prevent the expansion of the SC compartment. Biochemical analysis (WB) confirmed p53 levels restoration after Nutlin-3 treatment; even p53 activity is restored as shown by p21 level, susceptible to p53 positive regulation (Fig.14 left).

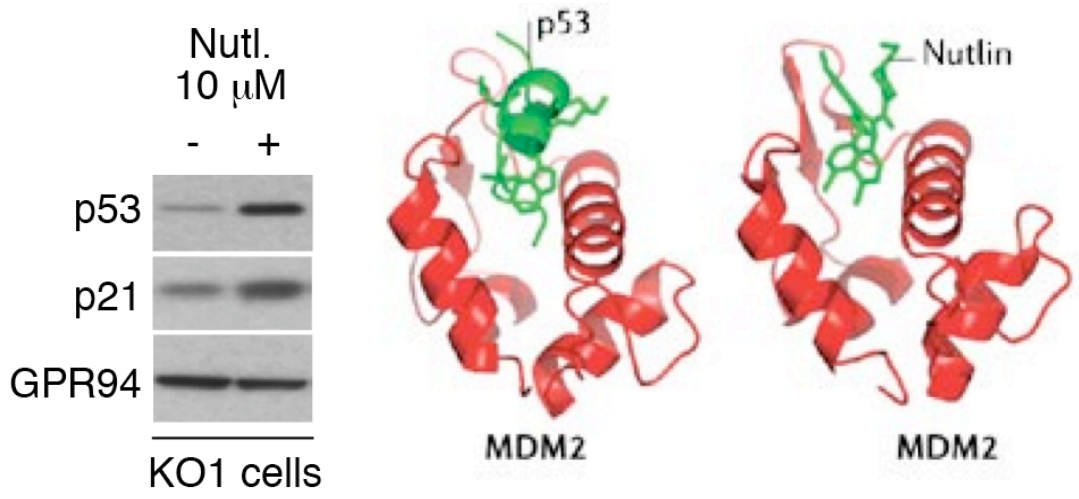

Figure 14
Left: Immunoblot. p53 rescue via Nutlin-3 *in vitro* treatment.
Numb KO (KO1) cells were treated with 10 μM Nutlin-3 for 24h Total cell lysates (30μg) from DMSO treated KO1 (-) as control and Nutlin-3 treated KO1 (+) were immunoblotted with Anti p53 (Cell Signaling) Anti p21 (Santa Cruz Biotechnology). GRP94 was detected as a protein loading control.
Right: Nutlin-3 fills MDM2 pocket avoiding MDM2-p53 binding.
Figure adapted from Nalepa et al, 2006

The mammosphere assay performed on Nutlin-3 treated Numb KO cells put in evidence a drug dependent SFE reduction accompanied by a significant decrease in MS average size (Fig. 15a), whereas, consistent with previous reports (Cicalese et al., 2009), no effect was observed on the growth of control MSs.

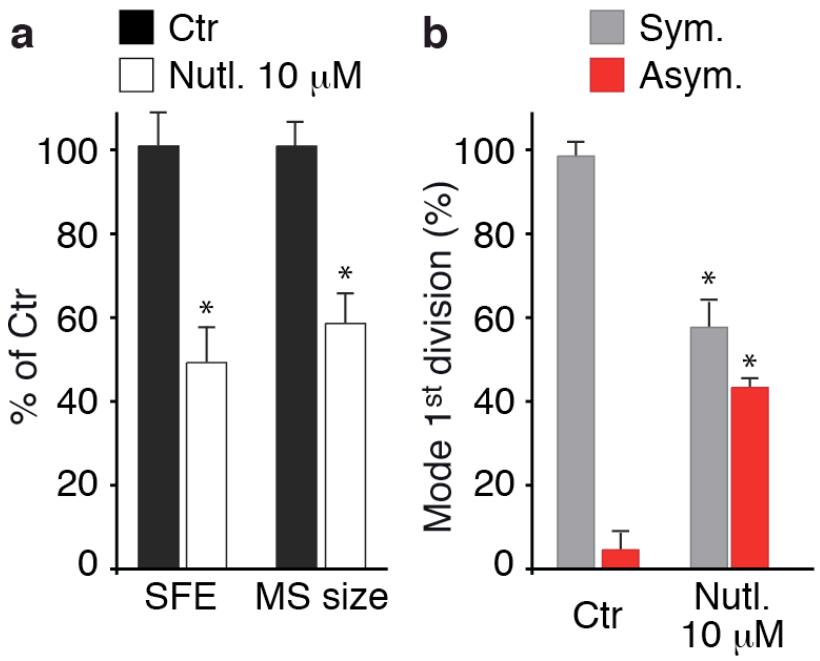

Figure 15
***in vitro* effects of p53 rescue via 10 μM Nutlin-3 treatment on Numb KO cells**
(a) Bar graph represents the SFE and MS size in DMSO treated (control) Numb KO cells (KO1 -black column); the same parameters where considered after 24 hours 10 μM Nutlin-3 treatment (Nutl 10 μM -white column) and p53 rescue validation (Western Blot Fig. 13 left). Control KO1 cells were compared with Nutlin-3 treated KO1 cells exploiting TL analysis to get eventual changes in 1st mitotic division after p53 rescue. Bar graph "b" reports the ratio between symmetric (grey column) and asymmetric (red column) events both in control KO1 and Nutlin-3 treated KO1 cells.

TL analysis was performed to verify whether Nutlin-3 treatment also had skewed the mode of first mitotic division. Numb KO cells use to divide in symmetric mode in almost the totality of mitosis observed. That involves an increase in SC compartment since the first mitosis produces two SC, doubling their number throughout the serial propagation *in vitro*. Nutlin-3 treatment induced Numb KO cells to switch their mode

of division, from a complete symmetric fashion to an almost equal distribution of symmetric and asymmetric events (Fig. 15b).

This last data in particular focus the attention on a possible Nutlin-3 dependent reduction in SC compartment that would lead to decrease in Numb KO cells tumorigenic potential. This hypothesis pushed us to perform the next set of *in vivo* experiments.

Loss of Numb-induced tumorigenesis is p53-dependent

According to the results obtained by mammosphere assay performed on Numb KO cells undergone to Nutlin-3 *in vitro* treatment, likewise SFE and MSs size reduction and nevertheless evident switch in SCs first mitotic division mode, we reasoned that deregulation of p53 function, as a consequence of the absence of Numb, might be the mechanism responsible for the tumorigenic properties of Numb-KO model and these properties may be related to Numb KO SC content.

In fact we previously verified that the tumorigenicity of these cells was Numb-dependent; by restoring Numb expression (pLVX Numb-DsRed infection) we obtained an increase of p53 levels and function accompanied by SFE reduction and sizeable switch from symmetric to asymmetric division. Given that Numb KO cells displayed sensibility to Nutlin-3 *in vitro* treatment, proofed even in these context by increased p53 levels and function, SFE reduction increase in asymmetric division events, we

considered the possibility that tumors grown from Nutlin-3 *in vitro* treated cells should be sensitive to Nutlin-3 mediated p53 restoration

To test this hypothesis, we selected a Numb-KO MEC primary line that grew as tumors (identified as KO1) in the mammary fat pad transplantation assay. Numb KO MECs were Nutlin-3 *in vitro* treated in order to revert the tumorigenic phenotype of KO1 line, and than transplanted in NOD SCID mice.

Nutlin-3 treatment resulted in tumors that were half the size of control tumors (Fig. 15-2).

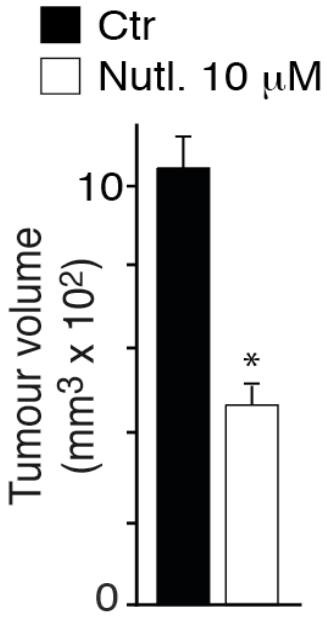

Figure 15-2
***in vivo* effects of *in vitro* Nutlin-3 treatment on KO1 cells**
***in vitro* Nutlin-3 treated KO1 cells were injected in one side breast, DMSO treated KO1 cells were injected as control in the other side breast and let both the tumor masses develop. Bar graph displays the differences between the tumor volumes reached by KO1 control cells (black column) and Nutlin-3 treated KO1 cells (white column).**

To study the effects of Nutlin-3 *in vivo* treatment on Numb KO MECs, we transplanted untreated KO1 cells and allowed tumors to reach a palpable size of ~0.5 cm in diameter prior Nutlin-3 *in vivo* treatment (Fig.16a dashed red line).

Nutlin3 was administered intraperitoneally every 3 days for 12 days (4 treatments) using a dose of 20 mg/kg). At the end of the treatment, tumors in Nutlin3-treated mice had continued to expand at the same rate as tumors in mock-treated mice (Fig.16a) reaching the same size. This result identifies the SC compartment as Nutlin-3 specific target. Indeed by injecting the drug in the palpable tumor lesion, no evident changes in tumor volume can be seen because the tumor size growth is dependent on progenitors proliferation. Once the first mitotic division has taken place and the first progenitor cell spawn, the SC can even be treated with Nutlin-3 and new SC divisions prevented, but the progenitor, that is not sensitive to Nutlin-3, will undergo to successive mitosis and lead the tumor growth.

To verify this hypothesis, we performed mammosphere assay on MECs obtained from tumors derived from *in vivo* Nutlin3-treated animals, these samples displayed a decreased SFE, if compared to mock-treated animals (Fig.16c). A significant difference became apparent even upon re-transplantation, indeed the second generation tumors that were obtained from MECs derived from Nutlin-3 *in vivo* treated mice displayed decreased growth rate, indeed they were ~2-fold smaller respect to tumors from mock-treated animals (Fig. 16b).

The Numb KO – Nutlin-3 treated tumors generated in the following transplantation assay were smaller compared to control counterpart as a consequence of the *in vivo* Nutlin-3 treatment, which reduced the number of SCs.

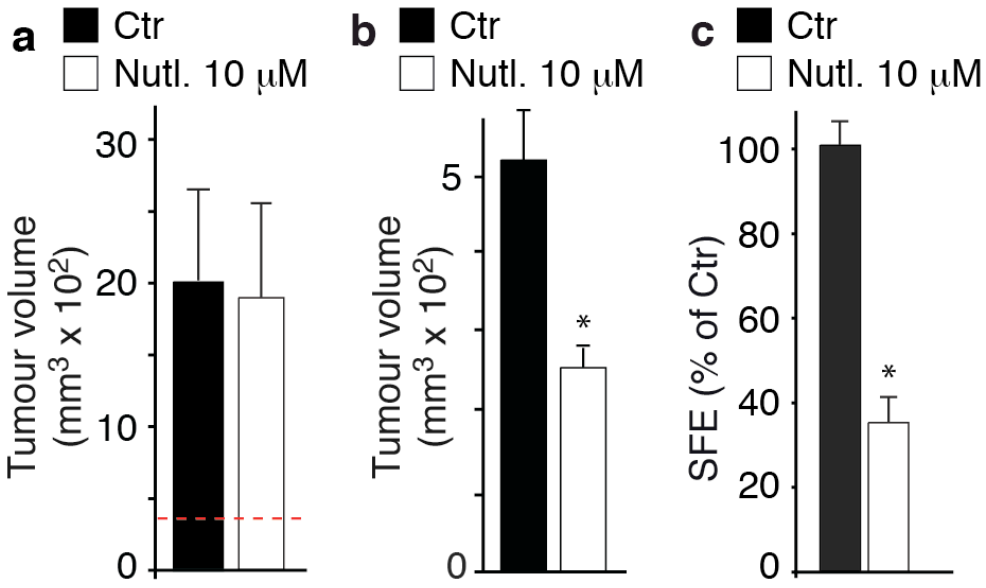

Figure 16
Effects of p53 rescue via 10 μM Nutlin-3 *in vivo* treatment on Numb KO tumors.
Numb KO (KO1) cells were injected in both breast and let the tumor mass develop.
(a) Nutlin3 (20 mg/kg) was administered intraperitoneally when the lesion was ~0.5 cm in diameter (dashed red line). The bar graph shows the difference between the tumor size reached by DMSO treated KO1 tumor (Ctrl –black column) and the Nutlin-3 treated KO1 tumor (Nutl. 10 μM –white column).
(b) MECs obtained from previous tumors were re-transplanted. The bar graph displays the difference between the second generation tumor sizes reached.
Ctrl (black column) identifies the tumor originated from MECs belonging to DMSO treated KO1.
The white column (Nutl. 10 μM) represents the tumor originated from MECs belonging to Nutlin-3 *in vivo* treated KO1 tumor.
(c) The second generation tumors were digested and SFE assay was performed on MECs obtained.

This result confirms the evidence of Nutlin-3 direct action on SCs before the first mitotic division, since only the second generation tumor size displays the effects of Nutlin-3, which by hitting directly the SCs can limit the progenitor outcome and minimizing the overall tumor growth.

To demonstrate that the difference in tumor size was not related to tumor cell proliferation rather than any increase in apoptotic rate we performed IHC investigating on KI67 and activated Caspase-3 levels.

IHC analysis confirms that Nutlin-3 had minimal effects on the bulk tumor cell proliferation or apoptosis. Staining for KI67 and activated Caspase-3 does not reveal any substantial difference independently of whether Numb-KO tumors were generated by cells pre-treated *in vitro* prior to transplantation (Fig. 17 left) or by re-implantation of cells isolated from Numb-KO tumors treated *in vivo* (Fig. 17 right).

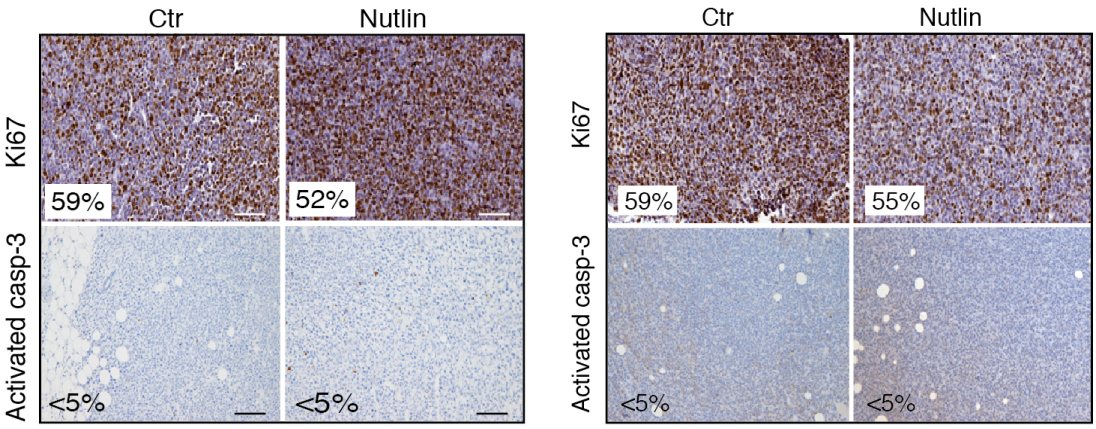

Figure 17
IHC on tumors derived from not treated Numb KO (Ctrl) and *in vivo* Nutlin-3 treated Numb KO (Nutlin). Comparison between Nutlin-3 *in vitro* treatment prior to transplantation (left) and re-implantation of cells isolated from Nutlin-3 *in vivo* treated Numb-KO tumors (right).
FFPE sections were stained for KI67 (Thermo Scientific #9106) to score the proliferation index.
Consecutive sections were stained for Activated Caspase (Cleaved Caspase 3, Asp175 Cell Signaling #9661) to quantify the number of apoptotic events.

The above results show how the loss of Numb, controlling the p53 levels and the numbers of SCs, contributes to tumorigenesis.

By the way p53 pharmacological rescue by Nutlin-3 displayed efficacy on SCs compartment in case of prior *in vitro* SCs treatment and furthermore on second generation tumor transplants (which were not further exposed to the drug).

The fact that Nutlin-3 was ineffective on first generation tumors, while being efficacious on second generation ones, would predict this drug for a SC-specific therapy aimed to tumor relapse treatment.

From mouse to human

Our results put in evidence the importance of Numb in regulating mouse SC homeostasis and the effects in terms of tumorigenesis that Numb loss brings to. According to that, we wanted to verify whether the Numb-p53 circuitry was important also for the human MSC model system.

IEO Hospital in agreement with the Molecular Medicine program guaranteed us the possibility to access to human tumor biopsies. Under strict supervision by Anatomo-Pathology Unit, and only in case of permission by patients undergoing tumor surgical removal, we were allowed to collect human tumor samples in close period to surgery and to perform both *in vitro* and *in vivo* experiments throughout xenograft in mouse model.

According to published data (Westhoff et al., 2009) one third of all breast tumors display the loss of Numb protein, an event that correlates with aggressive disease and poor prognosis. Moreover Pece et al focused their study on the correlation between Numb expression and tumor prognosis. According to The Gleason system (Gleason & Mellinger 2002) which classifies tumors on the base of their level of differentiation and grade of complexity, scoring from a G1 to a G3 class where a G1 represents a well differentiated type of tumor while a G3 is a poorly differentiated kind, Pece et al demonstrated that G3 (but also G1 tumors) resulted enriched in cancer-initiating cells. The high grade of complexity and aggressiveness of a G3

tumor could be so linked to its content in MSCs. (Pece et al., 2010). The high-grade tumors were searched, collected and reduced to MECs throughout enzymatic digestion.

We looked for tumors that, independently of their Numb status, displayed comparable exponential MSs growth and SFE (Fig. 18). Among these we finally selected MECs from two Numb-deficient (Numb-) and two Numb-proficient (Numb+) tumors that were carried for control analysis.

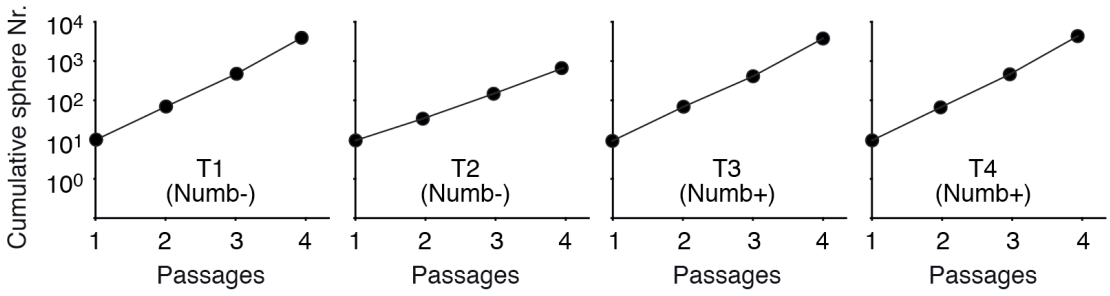

Figure 18
SFE assay on human tumor samples
Numb deficient (T1 and T2, Numb-) and Numb proficient (T3 and T4, Numb+) selected samples were tested to score *in vitro* MECs SFE on the base of the cumulative sphere number through at least 4 MS generations.

Validation of human xenografted Numb deficient model

To reproduce in NOD SCID mouse model the context displayed by human tumors and to perform *in vivo* experiments on these samples, we xenografted human MECs derived from the related tumor digestion in in NOD SCID mice. In order to verity

whether Numb levels of expression was retained even after xenograft, we performed IHC to stain Numb levels so comparing the human tumor with the mouse outgrowth.

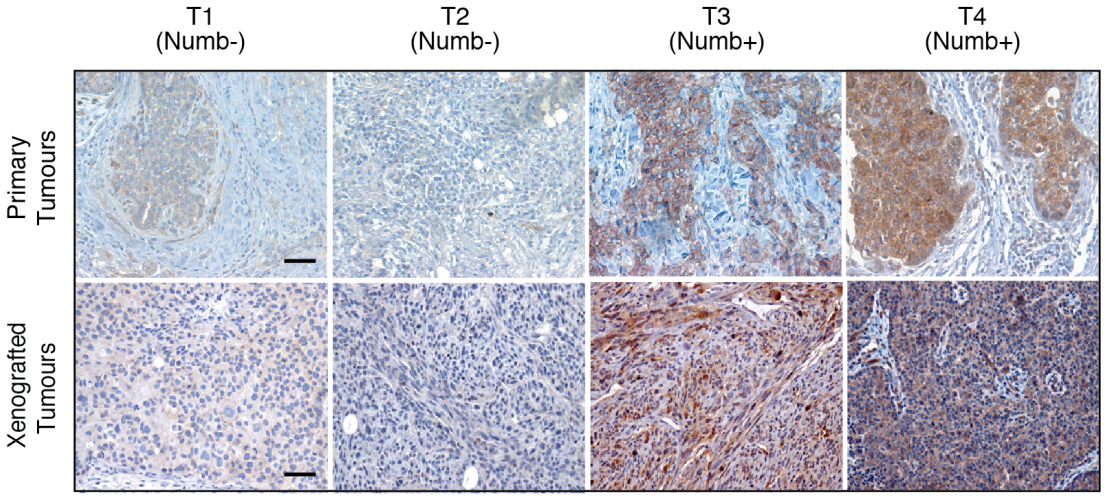

Figure 19
IHC staining for Numb levels in human tumor samples and related xenografts.
Two Numb deficient (Numb−) T1 and T2 together with two Numb proficient (Numb+) T3 and T4 were selected. Surgery biopsies were digested and the obtained MECs were xenografted in NOD SCID mice.
IHC staining compares Numb levels between patient primitive tumors and the respective xenografts. FFPE sections were stained with Ab#21

To confirm the scenario previously displayed in mouse model were the loss of Numb not only brought to destabilization in p53 homeostasis but even in mode of SC division we performed biochemical and TL analysis on xenograft derived MECs.

We investigated whether these tumors undergo an expansion of the SC compartment, as a consequence of alterations of the mode of SC division composing the same scenario seen in mouse model.

As expected, the pool of Numb- tumors displayed a decrease in p53 level compared to Numb-proficient tumors, because of MDM2 mediated ubiquitinilation and consequent degradation (Shirangi et al., 2002; Xirodimas et al., 2001 Bottger et al., 1997); p21, as p53 target gene, was found downregulated.

Moreover the *in vitro* TL analysis shows the prevalence of symmetric mode in first mitotic division, consistent with the results obtained in Numb KO MECs in mouse (Tosoni Unpublished preliminary data).

Numb restoration in Numb deficient human tumors

To test whether the continuous expansion of the SC compartment in Numb- tumors was due to the absence of Numb, we infected tumor MECs with pLVX-Numb-DsRed to rescue the expression of endogenous Numb levels. The expression of Numb-DsRed efficiently restored p53 levels as shown by Western Blot analysis and p21 level as well was restored (Fig. 20).

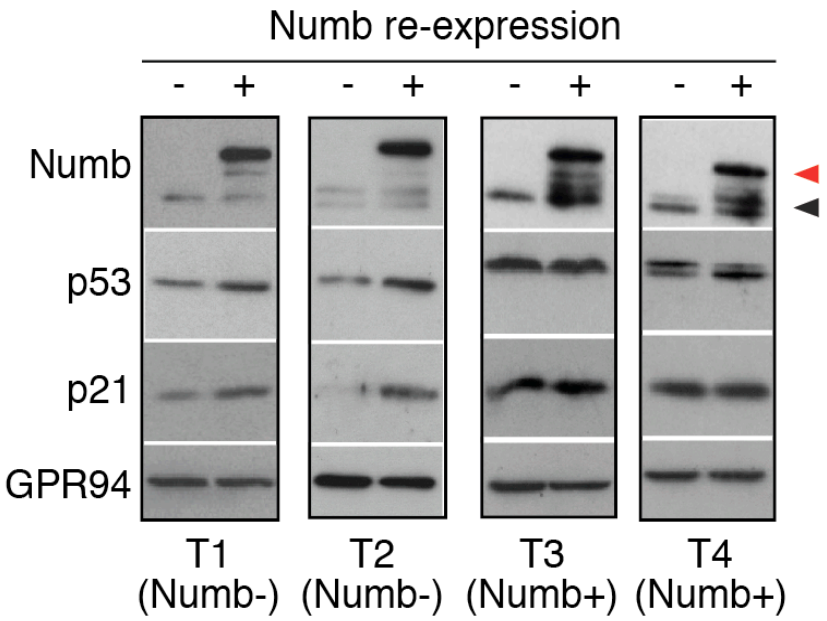

Figure 20
Immunoblot. Numb re-expression in human tumor samples
Cells obtained from digestion of human Numb deficient (Numb-) tumors (T1 and T2) were infected with pLVX puro Numb DsRed to rescue Numb levels *in vitro*. Numb proficient (Numb+) tumors (T3 and T4) were even infected and considered as control.
pLVX EV infection (-), pLVX puro Numb DsRed infection (+), endogenous Numb level (black arrow), Numb DsRed (red arrow).
Total cell lysates (30µg) from Numb- and Numb+ samples were immunoblotted with Ab#21 monoclonal antibody. Anti p53 (Cell Signaling) Anti p21 (Santa Cruz Biotechnology) were used. GPR94 was detected as protein loading control. Numb levels in Numb rescued samples are indicated by red arrow, endogenous Numb levels by black arrow.

Moreover we performed SFE assay to study the *in vitro* outcome of Numb restoration first of all to figure out possible consequences in SC compartment. The bar graph shows a ~ 2-fold decrease in SFE and mammospheres size after Numb rescue (Fig. 21) in Numb deficient tumors.

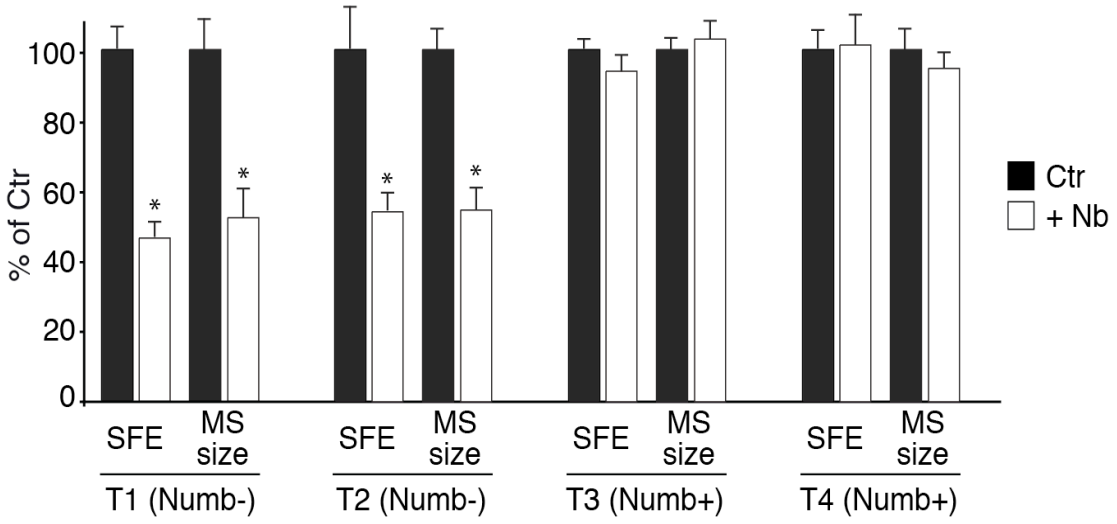

Figure 21
***in vitro* effects of Numb re-expression in human Numb deficient (T1 and T2, Numb-) and Numb proficient (T3 and T4, Numb+) samples upon pLVX Numb DsRed lentiviral infection.**
Bar graph represents Numb- and Numb+ SFE and MS size displayed *in vitro* (Ctrl -black columns).
The same parameters were considered after Numb re-expression throughout pLVX Numb DsRed lentiviral infection (+Nb -white column).

To verify whether Numb re-expression had influenced the mode of first mitotic division, which from a first investigation resulted mainly symmetric, we performed TL analysis on pLVX Numb DsRed infected human MECs. We observed a significant increase in the number of asymmetric divisions (Fig. 22) in Numb- tumor MECs reconstituted with exogenous Numb, while the Numb-DsRed expression did not affect Numb+ MECs mode of division that maintained mainly symmetric.

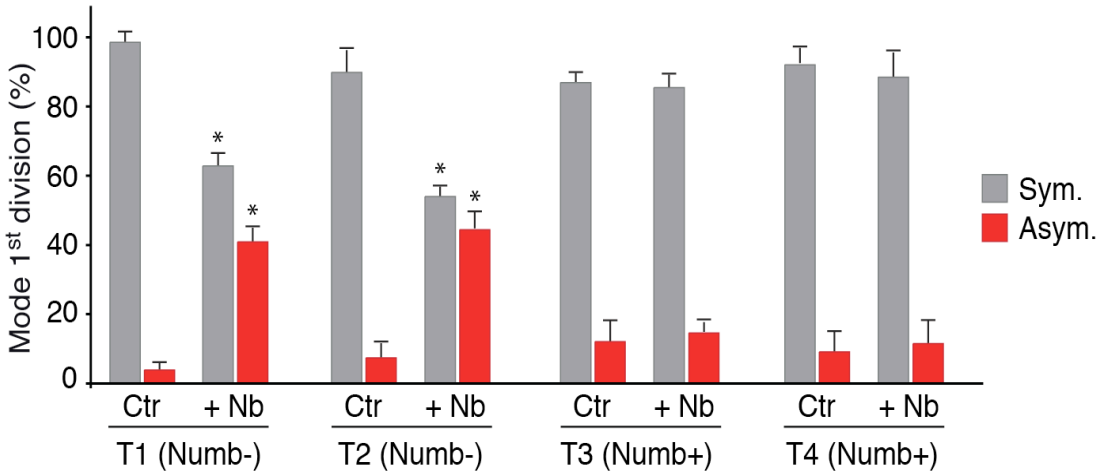

Figure 22
Time Lapse analysis: Numb re-expression *in vitro* effects in human samples
Numb deficient (Numb-) and samples were pLVX Numb DsRed infected in order to re-express Numb levels (+Nb). Numb proficient (Numb-) samples were Numb over-expressed as positive control.
pLVX-EV infection was performed on both Numb- and Numb+ as negative control (Ctr)
+/- Numb recued Numb- and Numb+ cell 1st mitotic division mode was analyzed through TL imaging.
The ratio between symmetric (grey columns) and asymmetric (red columns) events was quantified in the bar graph.

On the base of these evidences we decided to perform *in vivo* experiments in order to investigate on possible consequences of Numb reconstitution on tumor growth. Numb- tumor MECs were Numb-reconstituted by lentiviral infection and xenografted in mouse fat pad. These MECS generated tumors that were ~2-fold smaller in size compared to mock-infected controls (Fig. 23).

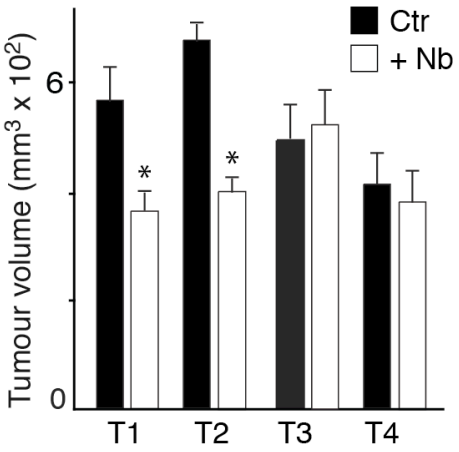

Figure 23
Numb re-expression *in vivo* effects in human tumor samples.
Numb re-expressed (+Nb, pLVX Numb DsRed infected) Numb- (T1 and T2) cells were injected in one side breast, pLVX-EV infected (Ctr) Numb- cells were injected as negative control in the other side breast and let both the tumor masses develop. Numb+ (T3 and T4) cells were equally treated and injected as positive control.
Bar graph quantifies the tumor size reached by these transplanted cells and compares the tumors originated by pLVX-EV infected cells (Ctrl) (black columns) with tumors originated by Numb re-expressed cells (+Nb) (white columns).

Numb-overexpression on MECs through lentiviral infection had on the other hand no effect on tumorigenesis and did not alter the final tumor volume in Numb proficient samples that were comparable to mock-infected controls.

To remove the possibility of increased apoptosis or decreased proliferation withstanding the decreased tumor size, we stained the tumors through IHC with KI67 and activated Caspase-3 antibodies, but no evident differences between Numb deficient tumors and Numb deficient tumors reconstituted with Numb protein were observed (Fig. 24).

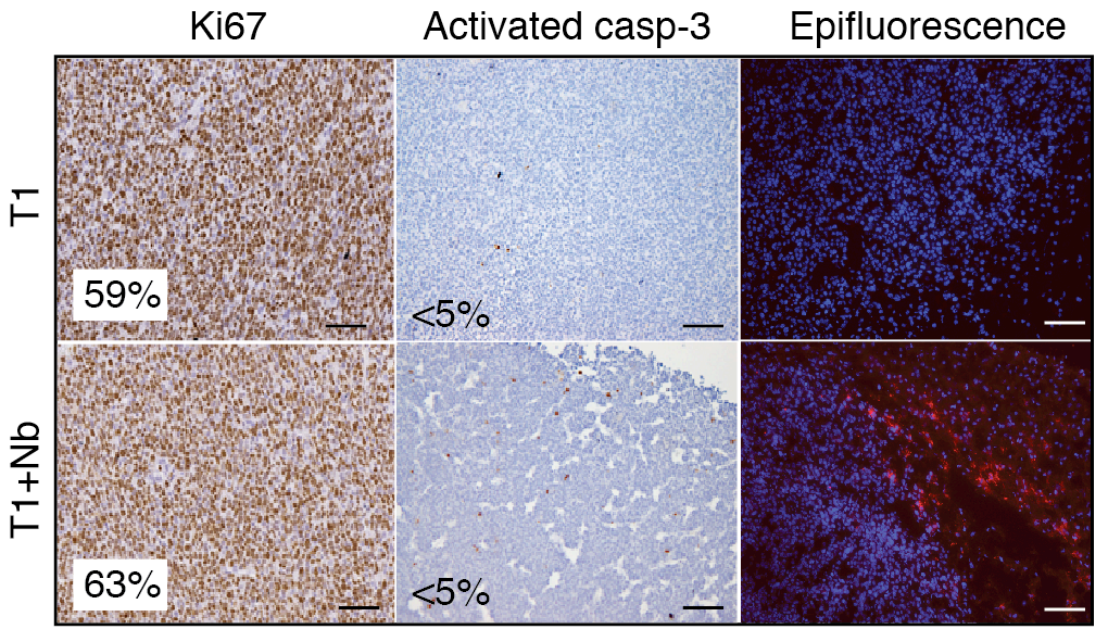

Figure 24
IHC on tumors derived from Numb deficient T1 cells, and Numb re-expressed T1 cells (T1+Nb) cells injection.
FFPE sections were stained for KI67 (Thermo Scientific #9106) to score the proliferation index.
Consecutive sections were stained for Activated Caspase (Cleaved Caspase 3, Asp175 Cell Signaling #9661) to quantify the number of apoptotic events.
OCT Frozen sections were DAPI stained and observed in red fluorescent light (560nm). Numb DsRed fluorescent fusion protein was detected.

Collectively the results argue that even in Numb- human tumors, the lack of Numb expression participates in the expansion of the SC compartment leading to tumor growth.

p53 rescue in human tumors: Nutlin-3

Once confirmed in human tumors the trend emerged in Numb KO mouse model, aware of the consequences of Numb reconstitution obtained throughout our

experimental model based on Numb DsRed lentiviral infection, as previously done with Numb KO mouse MECs, we step forward with pharmacological approach by use of Nutlin-3 in order to restore p53 levels in Numb- human MECs. Western Blot analysis confirms the previous evidence of Nutlin-3 treatment efficacy in p53 rescue in levels and activity as witnessed by p21 levels (Fig 25).

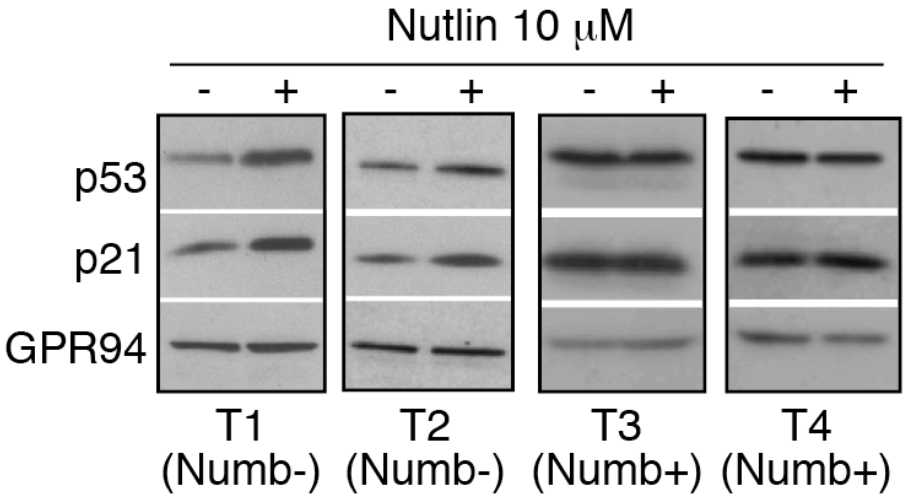

Figure 25
Immunoblot. Human tumor samples p53 rescue via Nutlin-3 *in vitro* treatment
Numb deficient (T1 and T2, Numb-) and Numb proficient (T3 and T4, Numb+) samples were *in vitro* treated with 10 μM Nutlin-3 for 24 hours (+). DMSO treatment (-) was performed on the same samples as negative control.
Total cell lysates (30μg) were immunoblotted with Anti p53 (Cell Signaling) Anti p21 (Santa Cruz Biotechnology). GPR94 was detected as a protein loading control.

Following mammosphere assay was needed to confirm Nutlin-3 treatment targeted action on SC compartment as previously emerged by the same experiment performed in Numb KO mouse model.

Upon Nutlin-3 treatment, Numb- MECs displayed a significant reduction in the number (SFE) and size of MS; above all, Nutlin-3 treatment leaded to reduction in the ability of MS to be propagated *in vitro* throughout serial passages (Fig. 26) even in that case suggesting a reduction in SCs compartment.

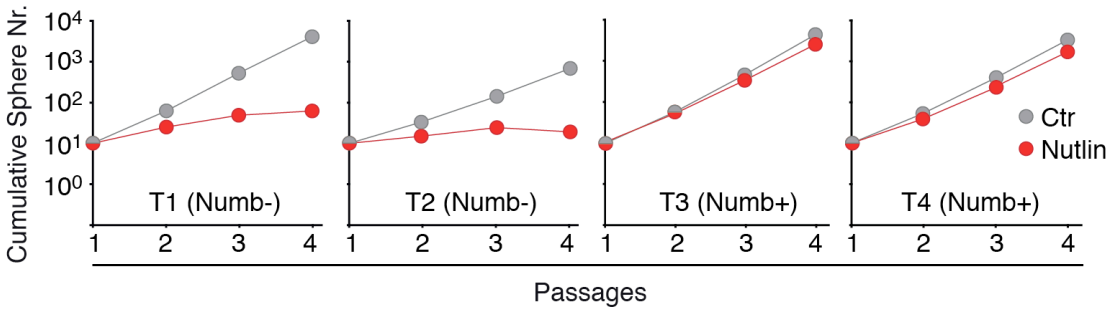

Figure 26
SFE assay performed in serial passages on human tumor samples upon *in vitro* Nutlin-3 treatment.
Numb deficient (Numb-) and Numb proficient (Numb+) selected samples were tested to score *in vitro* MECs SFE. The assay was performed for at least 4 passages. (Ctr -grey dots). The same SFE assay was performed on MECs upon *in vitro* 10 µM Nutlin-3 treatment for 24 hours. The assay was performed for at least 4 passages. (Nutlin -red dots)

TL analysis shows a switch from symmetric to asymmetric trend of division confirming a restoration of p53 activity since p53 level emerged increased in WB analysis (Tosoni Unpublished preliminary data). As control, Numb+ MECs SFE and MSs size were not affected.

in vitro vs. in vivo Nutlin-3 treatment in human tumors

Numb KO mouse cells displayed a marked susceptibility to Nutlin-3 treatment as proofed by the previous set of experiments. The major out coming evidence was that Nutlin-3 treatment did target SC compartment despite not affecting tumor growth when administrated *in vivo* in mice already developing a tumor mass.

To investigate whether Nutlin-3 moved the same mechanisms in human tumors, *in vitro*-treated Numb- MECs were xenografted in NOD SCID mouse fat pad.

The originated tumors were smaller compared to mock-treated cells and Numb+ tumors (Fig. 27).

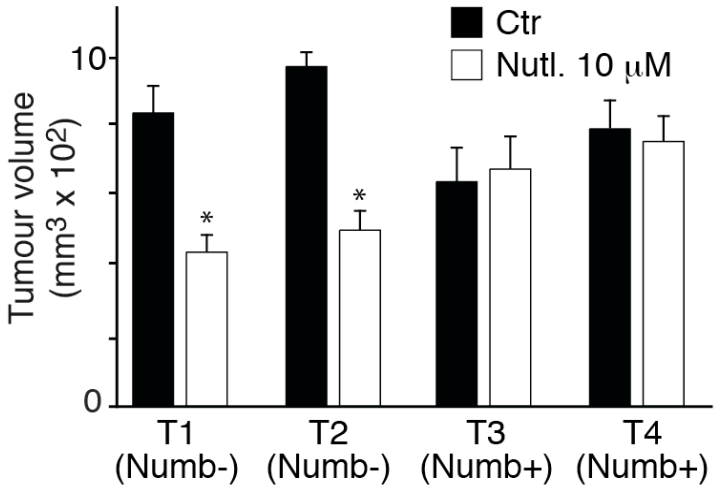

Figure 27
***in vivo* effects of p53 rescue via Nutlin-3 *in vitro* treatment on human tumor samples.**
Numb deficient (T1 and T2, Numb-) and Numb proficient (T3 and T4, Numb+) samples were *in vitro* treated with 10 μM Nutlin-3 for 24 hours (Nutl 10 μM). DMSO treatment (Ctrl) was performed on the same samples as negative control.
Nutlin-3 treated Numb- cells were xenografted in one side breast, Ctrl Numb- cells were xenografted as negative control in the other side breast and let both the tumor masses develop. Numb+ (T3 and T4) cells were equally treated and injected as positive control.
Bar graph displays the *in vivo* effects of p53 rescue quantifying the tumor size reached by xenografted cells. Here the tumors originated by Ctrl cells (black columns) together with tumors originated by p53 rescued cells (Nutl 10 μM) (white columns) are shown.

We investigated the cause of this size difference and we demonstrated that it was not due to Numb- MECs proliferation decrease or apoptotic rate increase, as demonstrated by KI67 and activated Caspase-3 IHC staining (Fig. 28).

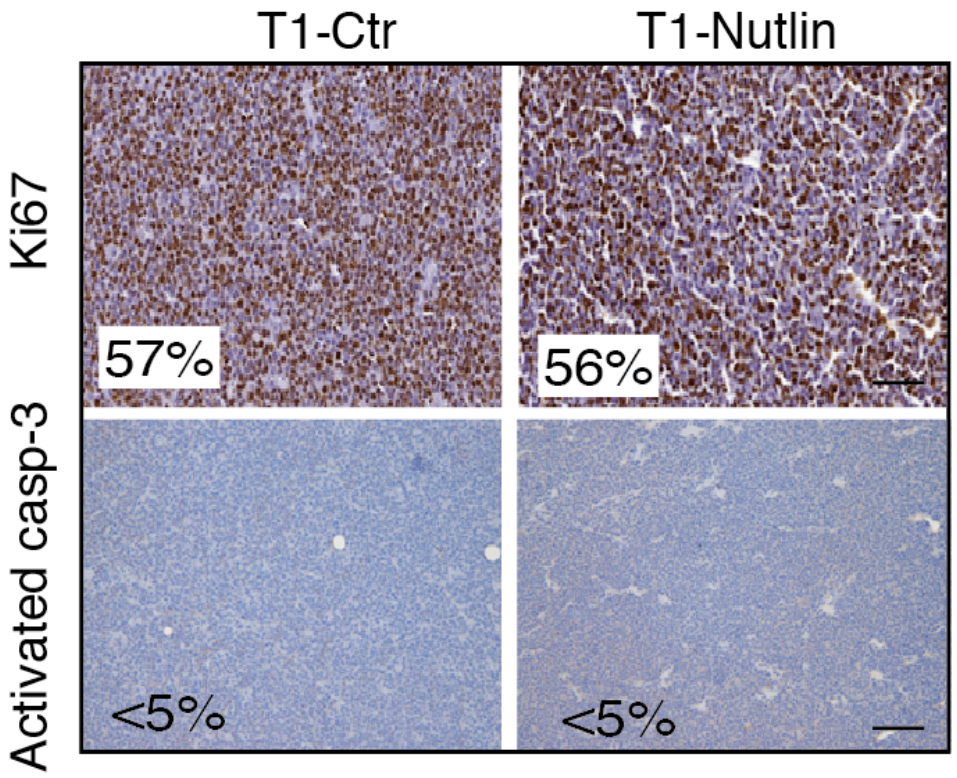

Figure 28
IHC on tumors derived from xenograft of *in vitro* Nutlin-3 treated Numb deficient T1 (T1-Nutlin) compared to DMSO treated T1 (T1-Ctr)
FFPE sections were stained for KI67 (Thermo Scientific #9106) to score the proliferation index.
Consecutive sections were stained for Activated Caspase (Cleaved Caspase 3, Asp175 Cell Signaling #9661) to quantify the number of apoptotic events.

The results obtained with Nutlin-3 *in vitro* assays drove the following experiments *in vivo*.

As previously done in Numb KO mouse model we xenografted Numb- and Numb+ human cells and once a palpable lesions had formed and reached ~0.5 cm in diameter (Fig. 29 dashed red line), Nutlin3 was administered intraperitoneally every 3 days for 12 days for a total of 4 treatments using a dose of 20 mg/kg. Tumors were let grow and interestingly *in vivo* drug treatment did not lead to a significant decrease in the final tumor size (Fig. 29).

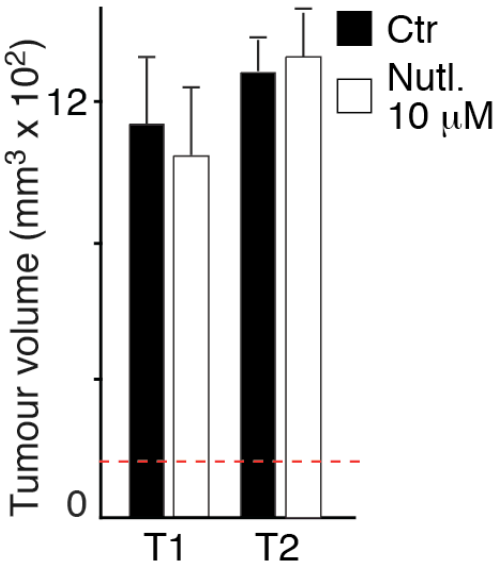

Figure 29
Effects of p53 rescue via Nutlin-3 *in vivo* treatment on human tumor samples.
Numb deficient (T1 and T2) cells were xenografted separately. Each sample cells were injected in both breasts and let the tumor mass develop up to the palpable lesion (~0.5 cm in diameter, dashed red line) when 20 mg/kg Nutlin-3 was injected intraperitoneally every 3 days for 12 days
The bar graph shows the difference between the tumor size reached by DMSO treated tumors (Ctrl -black column) and the Nutlin-3 treated tumors (Nutl. 10 μM -white column).

According to the results previously obtained on second generation Numb KO tumors that were *in vivo* treated with Nutlin-3 we explanted and reduced to MECs the human tumors undergone Nutlin-3 *in vivo* treatment. Although cells were not exposed to any further drug treatment, as happened in Nutlin-3 *in vivo* treated Numb KO tumors, human Numb- tumors MECs displayed a significant SFE and MS size decrease as emerged by *in vitro* mammosphere assay (Fig 30b) thus demonstrating SC target efficacy. Nutlin-3 *in vivo* treatment was even proofed by Western Blot analysis were Nutlin-3 treatment shows efficacy in p53 rescue both in levels and activity, as witnessed by p21 levels (Fig 30a).

Thereby we tested these Numb- tumors MECs tumorigenicity *in vivo* by xenograft assay in NOD SCID mice. Nutlin-3 *in vivo* treated MECs grew in smaller sized tumors if compared to not treated cells (Fig 30c) and again, Nutlin-3 treatment did not affect proliferation or apoptosis *in vivo* as demonstrated by KI67 and Caspase-3 activated IHC staining.

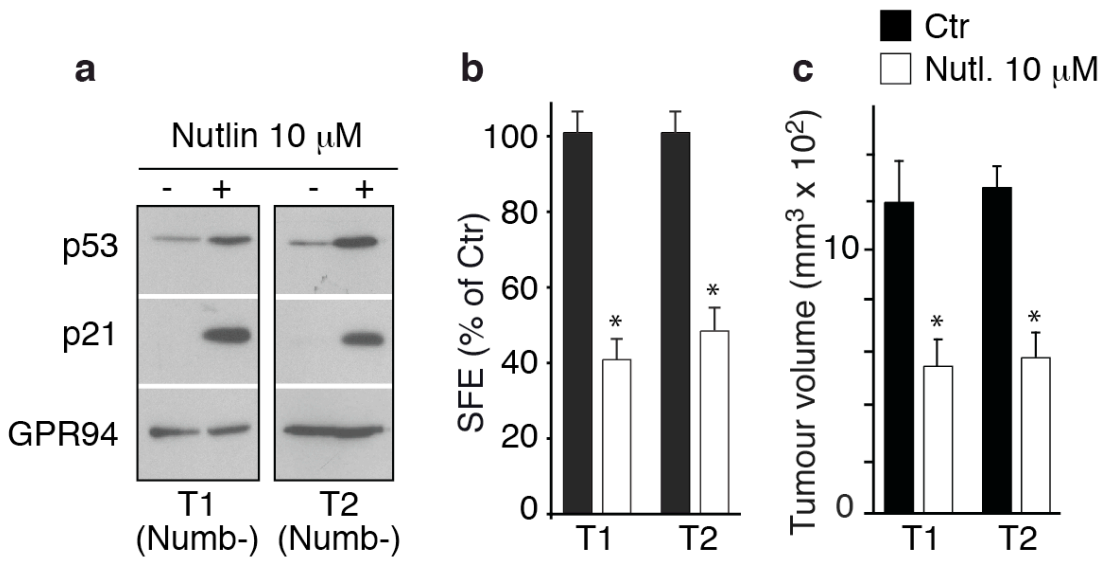

Figure 30

(a) Immunoblot. MECs obtained from Nutlin-3 *in vivo* treated Numb deficient (T1 and T2, Numb-) tumors were reduced to MECs by digestion to verify p53 rescue consequent to Nutlin-3 *in vivo* treatment (+). The immunoblot compares their p53 levels with control DMSO *in vivo* treated tumor derived MECs (-). Total cell lysates (30μg) were immunoblotted with Anti p53 (Cell Signaling) Anti p21 (Santa Cruz Biotechnology). GPR94 was detected as a protein loading control.

(b) Left: Nutlin-3 *in vivo* treated Numb deficient tumor derived MECs were xenografted and let develop the second generation tumor. Control DMSO treated tumor derived MECs were xenografted at the same time. The bar graph displays the difference between second generation tumor sizes reached by MECs belonging to DMSO treated first generation tumor (Ctrl -black column).

The white column (Nutl. 10 μM) represents the size of tumor originated from MECs belonging to Nutlin-3 *in vivo* treated first generation tumor.

(b) Right: the second generation tumors were digested and SFE assay was performed on MECs obtained.

As happened in mouse MECs, *in vivo* Nutlin-3 treatment displayed effect on SCs obtained from *in vivo* treated tumors digestion, as seen by SFE and MSs size reduction while TL analysis confirms this evidence on the base of their first mitotic division (Tosoni Unpublished preliminary data).

Interestingly the same result emerged by *in vitro* treated MECs later injected *in vivo*. Nutlin-3 appeared not efficient in *in vivo* treatment since no difference was displayed in terms of reached size between DMSO and Nutlin-3 perfused tumors. On the other hand Nutlin-3 treatment showed late effects on SFE and MS size of MECs obtained from *in vivo* treated tumors. Furthermore we could see Nutlin-3 effects when these *in vivo* treated samples where xenografted again to score their tumorigenic ability. The second generation tumor growth was impaired in Nutlin-3 previously treated sample as witnessed by their smaller size.

This evidence introduces the SC compartment as the effective aim of Nutlin-3 action. The tumor size growth is ruled by PC expansion and cannot be affected by Nutli-3 treatment. On the other hand the SFE reduction, seen in *in vitro* assays, upon Nutlin-3 treatment confirms a reduction in SC compartment even according to second generation tumor size decrease. These reduction is witness of the *in vivo* Nutlin-3 late effect on SC, of which tumorigenic phenotype is most likely reduced.

These results shows that the kinetic behavior of the SC compartment in Numb- breast cancers phenocopies the genetically-defined SC compartment of Numb-KO mice, and establish that the Numb-p53 axis plays a relevant role in human mammary tumorigenesis, via its impact on the homeostasis of the mammary SC compartment.

MATERIALS AND METHODS

Gene Knocking Out: The Cre/loxP recombination system in transgenic mice

The Cre/loxP system is useful for tissue-specific knockout of genes to investigate the in vivo effects of their loss. This technique can be used both to eliminate an endogenous gene (Knocking Out) or activate a transgene (Knocking In).

Cre is a 38 kDa recombinase protein from bacteriophage P1. This enzyme roles site specific recombination between loxP sites through both intramolecular excision or inversion. Cre can also mediate intermolecular integration of genes.

A loxP site (locus of X-ing over) consists of two 13 bp inverted repeats separated by an 8 bp asymmetric spacer region. One molecule of Cre binds per inverted repeat or two Cre molecules line up at one loxP site. The recombination occurs in the asymmetric spacer region. Those 8 bases are also responsible for the directionality of the site. Two loxP sequences in opposite orientation to each other invert the intervening piece of DNA, two sites in direct orientation dictate excision of the intervening DNA between the sites leaving one loxP site behind.

Two mouse lines are required for conditional gene deletion.

- a conventional transgenic mouse line with Cre targeted to a specific tissue or cell type; in our mouse, Cre activity is K5 promoter dependent, thereby activated in the breast and other epithelial tissues.

• a mouse strain that embodies a target gene (endogenous gene or transgene) flanked by two loxP sites in a direct orientation, the so called "floxed gene", in our experiment, Numb is double foxed in loxP-Numb-loxP.

The recombination, so the excision and consequently inactivation of the target gene, occurs only in those tissue expressing CK5 thereby performing Cre recombinase activity. Hence, the target gene remains active in all cells and tissues in which Cre is not activated (Wagner et al., 1997)

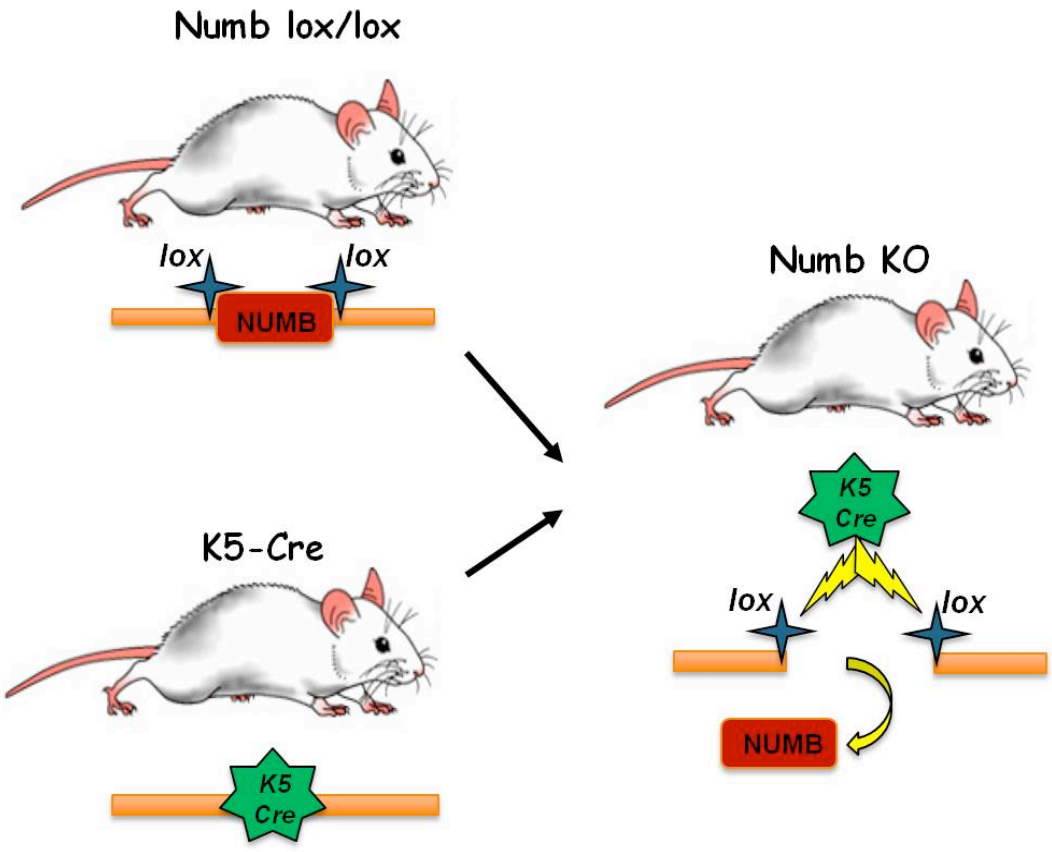

Figure 1
The Cre/loxP recombination system in transgenic mice
Mouse breeting between conventional K5-Cre transgenic mouse and double floxed Numb mouse to obtain the Numb KO mouse, lacking Numb in CK5 dependent districts.

FVB/HSD MICE

In 1966 two mouse strains, HSFS/N and HSFR/N were selected for sensitivity and resistance, respectively, to the action of Histamine after treatment with Bordetella pertussis vaccination. Later a group of mice at the eighth inbred generation of HSFS/N were found to carry the Fv-1b, allele for sensitivity to the B strain of Friend leukaemia virus. Homozygous mice were then inbred without further selection for histamine sensitivity and the final strain obtained was named FVB (Taketo et al, 1991).

This strain is slightly different from the largely used C56 strain. The microsatellite analysis indeed puts in evidence a difference of 145 markers between FVB/N and C56BL/6J strains (Neuhaus et al, 1997).

These mice have a vigorous reproductive performance with large litters, (Taketo et al, 1991) because of that, this prolific strain was chosen to explant considerable amounts of breast tissue to purify the highest number of SCs.

NOD SCID IL2 R GAMMA-CHAIN NULL

Non-obese diabetic (NOD) strain mice were developed at Shionogi Research Laboratories in Aburahi, Japan by Makino et al in 1980. This strain exhibits a susceptibility to spontaneous development of autoimmune insulin dependent diabetes mellitus (IDDM) (Kikutani H, Makino S 1992) as other autoimmune

syndromes.

NOD/SCID/ILR γ^{null} strain was generated by 8 backcross matings of C57BL/6J-γ^{null} mice and NOD/Shi-*scid* mice.

The resulting strain is a double homozygous for the severe combined immunodeficiency (SCID) mutation and interleukin-2 Receptor γ (IL-2 R γ) allelic mutation (γ^{null}). This strain was previously (Ito et al 2002) introduced as an excellent recipient mouse model for engraftment of human cells.

Human CD34+ cells transplanted into this strain, displayed a significantly higher engraftment rate in NOD/SCID/ILR γ^{null} strain than that in NOD/Shi-scid mice treated with anti-asialo GM1 antibody or in the β2-microglobulin-deficient NOD/LtSz-scid (NOD/SCID/$\beta2m^{null}$) mice.

In NOD/LtSz-scid and NOD/Shi-scid mice, in order to ameliorate engraftment efficiency for transplanted human cells, the injection of anti-NK cell antibody before transplantation was used while the γ^{null} mutation in NOD/SCID/ILR γ^{null} confers a constitutive lack in NK cell activity (Ohbo et al., 1996).

This indicate that residual NK cell activity might interfere with engraftment efficiency (Koyanagi 1997 Yoshino H 2000). Multiple immunological dysfunctions, including cytokine production capability, in addition to functional incompetence of T, B, and NK cells, may lead to the high engraftment levels of xenograft in NOD/SCID/γ^{null} mice. According to that NOD/SCID/γ^{null} display a severe reduction of interferon-γ (IFN-γ)

production from dendritic cells in the mouse spleen and even that may lead the comprehensive impairment of immunological functions (Ito et al 2002).

High engraftment rate were reported since low numbers of cells, up to 1×10^2 CD34+, could grow and differentiate in this strain underling a possible application even in multilineage cell differentiation. For this reason NOD/SCID/γ^{null} mice were considered as superior animal recipients for xenotransplantation and were especially valuable for human stem cell assay (Ito et al 2002).

Tissue collection and digestion

Five weeks old female FVB/Hsd mice are used to collect both axillary and inguinal breasts. The sample taking must be done under sterile hood and before opening the carcass the fur must be carefully disinfected.

This animal age has been chosen since from 4 to 6 weeks of life, mouse breast contain the highest number of SCs in a relatively small sized fat pad.

Tissues can be stored at 4°C in sterile saline solution or PBS until the beginning of the preparation when the sample is minced by sterile scissors into ~1−2 mm^3 pieces. Reduced tissue is immediately resuspended in 10 mL pre-warmed EDM and incubated at 37°C in a 5% CO_2 humidified incubator. The digestion mixture must be resuspended up and down with pipette several times (~5-7) every 20-30 min to aid tissue dissociation until all large fragments are digested. Groups of 5 animals for a

total number of 20 mice are used; the equivalent amount of 5 mice tissue is totally digested in 4 hours.

The digested tissue suspension is transferred in conical bottomed tubes and centrifuged at 80 × g for 10 min at room temperature. This step of differential centrifugation will allow to separate single stromal cells, mostly fibroblasts and endothelial cells which will remain in the supernatant (Eirew et al., 2008), from the epithelial portion of the mammary tissue that contains primary normal mammary epithelial cells (MECs) and SCs together with large clusters of tissue commonly referred as to “organoids”.

The supernatant is carefully removed eliminating fat residues and stromal cells; the pellet is gently resuspend in10 mL DMEM plus 2 mM L -Glutamine to yield a homogeneous suspension. The material is filtered sequentially using cell strainers (BD Falcon) of decreasing pore.

The first 100-µm cell strainer retains gross digestion residues together with fur or possible muscle and skin fragments. The so obtained flow through is sieved for first in 70-µm and than in 40-µm cell strainer. Pure organoids are retained during this step, while the last filtration with 20-µm syringe bound strainer eliminates the digestion residues such as groups of aggregated cells smaller than organoids. Pure MECs are so obtained in single cell suspension.

Blood cells are typically small sized and go through all the steps of filtration. To

remove them an ipotonic 0.2% NaCl solution can be used for 60' to induce a volume shock and to lysate red blood cells. To avoid any damage on the MECs population the physiological condition must be restored in cell suspension neutralizing the 0.2% NaCl with a 1.6% NaCl. MECs are thereby resuspended in the specific medium to allow the SCs growth, the Mammary Epithelial Stem Cell Medium (MESCM).

Notwithstanding the several adopted tricks to purify MECs a certain amount of contaminant cells remains in the MECs suspension. To remove this fraction, rather than seed cells directly on non-adherent supports in order to perform the mammosphere assay, it is useful to place MECs on non-tissue culture treated supports. This environment maintains the SCs fraction in anchorage independent conditions while permits strong adhesive cells, such as fibroblast to weakly adhere to the bottom. In a short time the bulk mammary epithelial cell population will be deprived of contaminants and the pure MECs can be delicately collected to be seeded on Poly-HEMA coated plates.

Enzyme Digestion Mixture (EDM)

EDM is obtained from a solution of DMEM (Lonza) + HAM's nutrient mixture F12 medium (Gibco) (1:1 ratio) supplemented with 1 μ g/mL insulin (Roche), 1 μ g/mL Hydrocortisone (Sigma), 100 U/mL Penicillin, 100 U/mL Streptomycin and 2 mM L-Glutamine. EDM is sterilized through a 0.2- μ m vacuum filter unit and store at 4°C

until needed. Immediately before use, 10 ng/mL EGF (Peprotech) 200 U/mL Collagenase type 1A (Sigma) and 100 U/mL Hyaluronidase (Sigma) are added. EDM should be prewarmed at 37°C in a water bath before adding to sample tissues.

Mammary Epithelial Stem Cell Medium (MESCM)

MEBM Basal Medium (Lonza) is supplemented with 100 U/mL Penicillin, 100 U/mL Streptomycin, 2 mM L -Glutamine, 5 µ g/mL Insulin, 0.5 µg/mL Hydrocortisone, 1 U/mL Heparin (Wockhardt).

The complete medium MESCM is obtained by adding 20 ng/mL EGF, 20 ng/mL FGF (Peprotech), and 2% B-27 Supplement (Gibco) immediately before use.

B-27 is a serum-free supplement typically used in research for growth and long-term viability of hippocampal neurons. The selection of its inner components makes B-27 successfully suitable even for epithelial mammary SCs research because of the absence of serum that would otherwise drive the *in vitro* SCs differentiation.

The complete medium is filter sterilized through a 0.2- µm filter prior to adding complete MESCM to cells.

Sphere culture Supports

To obtain supports suitable for cell suspension culture, low adhesion plates were prepared using Non-Tissue culture treated flat bottomed plates (Falcon). These

plates were doubly coated with the inert, chemically stable, non-toxic polymer named Poly-HEMA (2-hydroxyethylmethylmethacrylate) (Sigma).

A stock concentration (12%) Poly-HEMA solution is prepared by dissolving 25 g of Poly-HEMA crystal powder in 208 mL 95% ethanol overnight at 55°C using a rotating shaker. From this stock concentration, a 1:10 dilution in 95% ethanol is prepared to yield the Poly-HEMA working solution at a final concentration of 1.2%. Filter sterilize through a 0.2- µm vacuum. The second bottom plate coating must be applied only when the first volume of Poly-HEMA has completely dried under a sterile hood.

Isolation of primary SCs from mouse breast

This methodological approach is suitable for the isolation of pure SCs population from both mouse and human dissociated mammary gland (Pece et al., 2010; Cicalese et al., 2009).

Tosoni et al set up this strategy relying on two key defining SCs properties, namely their relative quiescence and their ability to survive in anchorage independent conditions. SCs can indeed withstand *anoikis*, an apoptotic process due to anchorage detachment (Pece et al., 2010; Cicalese et al., 2009; Dontu et al., 2003). Bulk primary mammary epithelial cells were isolated from either murine or human mammary tissues and cultivated in MESCM in absence of adhesion, condition in which, the innate shape reachable by dividing cells is the sphere, thereby the so obtained

"mammosphere".

SCs compose a small fraction of the entire dissociated bulk mammary epithelial cell population; their low division rate allows us to track them down by staining with a lipophilic dye, the PKH26 (Sigma).

PKH26 must reach a final 1:10000 ratio in the total reaction volume; PKH26 is for first pre diluted in a volume of PBS equal to the half of total reaction volume, this step avoids the cells to be stressed by pure PKH26 direct contact. Up to 10^7 cells are resuspended in an equal volume of PBS and mixed to the pre-diluted PKH26. The mix is incubated in the dark for 5' at RT, the cells are collected and seeded in culture.

PKC26 will be half-retained by the SC from the first mitotic division, while progressively diluted by the counterpart of progenitors cells (PC) undergoing several following rounds of mitosis. PKH-labelling of mammospheres was obtained using either the PKH26 (red epifluorescence) or the PKH2-GL (PKH488, green epifluorescence) dyes (Sigma), as appropriate.

To Exploit Fluorescence-activated cell sorting (FACS), which is a specialized type of flow cytometry (Herzenberg, et al., 1972), we used Vantage SE flow cytometer (Becton&Dickinson) equipped with a 488 nm laser (Enterprise Coherent) and a band-pass 575/26 nm optical filter (FL2 channel). An average sorting rate of 1,000 events per second at a sorting pressure of 20 PSI was maintained.

After 1 week of selective SC culture, single cell suspensions, from desaggregated PKH-labelled mammospheres, were sorted using a FACS assay. We were able to quantify the number of PKH^{HIGH} quiescent/not dividing SC since all the other cells (PC) have diluted the dye (thereby PKH^{LOW} and PKH^{NEG}) undergoing rounds of mitosis. FACS thereby discriminates and collects PKH^{HIGH} , by purifying SCs from the 1st generation of mammospheres we can score the starting amount of SCs in the mammary epithelial buck population.

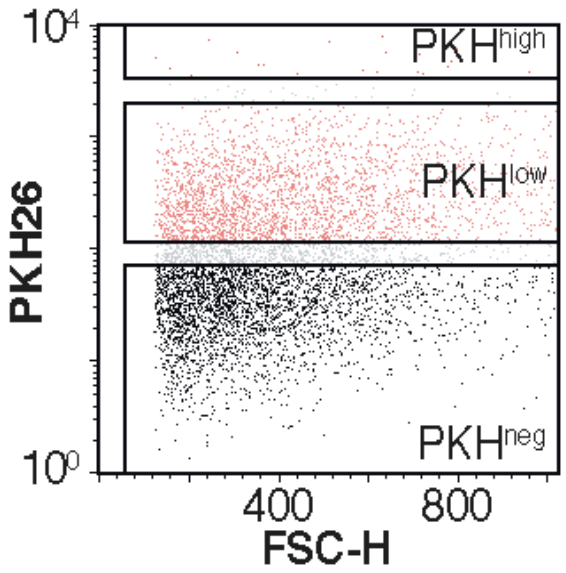

Figure 2
FACS-distribution of PKH cell subsets in WT mammospheres
Mammospheres desaggregated led to a heterogeneous distribution of stained cells. PKH^{HIGH} SC can be separated from PKH^{LOW} and PKH^{NEG} PC.

The cut off value considered to identify PKH^{HIGH} region in FACS output data was defined according to the calculated percentage of SCs in the mammospheres (Cicalese et al., 2009).

The FACS assay can be replicated for the following generations of mammospheres because of SC self renewing in order to see whether the SC compartment remains even or rather it is expanding, in our case WT PKH^{HIGH} grew in sphere until to 3rd generation while PKH^{LOW} and PKH ^{NEG} PC could not be further passaged in culture (Cicalese et al., 2009).

PKH26 can be even tracked by fluorescent light beam in the deep core of the structure obtained by the dividing PCs. This strategy is suitable not only for normal mammary SCs but also for isolation of CSCs making this technique even more essential because of the issue of breast cancer heterogeneity that would have been otherwise managed with the complex SC-specific immunophenotypical marker approach.

The mammosphere assay and SFE

According to published data (Cicalese et al., 2009) the normal SCs spawn a sphere containing ~300 cells. This structure is approximately ~100μm sized. The mammosphere assay consists in a precise retroactive study of SCs number relying on the sphere number found after a determined period of MECs culture. As previously

said, because of both the MESCM and the lack of adhesion, SCs proliferate to the detriment of MECs bulk population and the final number of sphere in suspension is indicative of the SCs number included in the early bulk population.

The SFE in an index describing this ratio; its value is obtained applying the formula:

(nr spheres counted/nr cells seeded) *100

Considering a normal SC giving a ~300 cells sized sphere, the SFE value is ~0.3%

Once counted, the spheres can be collected and mechanically disaggregating in a single cell suspension in order to count their total number to estimate the average sphere size applying the formula:

nr cells counted/nr spheres disaggregated

This assay comes useful moreover to estimate SCs self-renewing potential *in vitro*. Indeed once the SC is released from its PCs envelope that inhibited SCs mitosis, the SC can divide again skewing another sphere; that process can be repeated up to 3/4 times in a normal sample until the self-renewing extinguishment.

On the other hand, in tumor samples, as previously demonstrated (Pece et al., 2010; Cicalese et al., 2009), CSCs grow in number throughout the generations *in vitro*

giving an increase in SFE index and sphere size.

In this case the mammosphere assay gives information about the starting number of CSCs in a sample and moreover its increase though the time. To score the cumulative number of sphere throughout the generations *in vitro* the mammosphere re-plated in a serial assay.

Serial re-plating of mammospheres

For serial re-plating experiments, 5,000 (N1) cells from primary dissociated mammospheres were plated in quadruplicate onto Poly-HEMA treated plates (24 multiwell) and, after 6 days, dissociated as described and re-plated at the same density.

This procedure was repeated through several passages of dissociation/re-plating, and at each passage (i) the number of spheres (Sp) and relative dissociated cells (N) were determined. The average number of cells that compose a sphere (sphere size, S) was calculated as the ratio between (N) and (Sp).

Cumulative sphere (CS) and cell (CN) curves were respectively calculated as:

$$CS_i = CS_{i-1} \cdot (Sp_i / Sp_1)$$

$$CN_i = CN_{i-1} \cdot (N_i / N_1)$$

where CSi or CNi represent respectively the values of cumulative sphere and cell

curves at the passage i, Spi and Ni the sphere and cell numbers counted at the passage i, and Sp1 and N1 the number of plated spheres and plated cells. To note that the passages may be seen as a time unit of 6 days. Since the sphere size was constant during serial passages the value of Sp1 was calculated as the ratio between plated cell (N1=5,000) and average sphere size (S) during all passages. The cumulative curves plotted in a semi-logarithmic graph appear as straight lines, thus suggesting they resemble an exponential curve, as expected for a cell population that grow or die with a constant rate during the time. The cumulative curve may be expressed as:

$$C = C_0 \cdot GR_i$$

where C represents the value of the curve at the passage i, C0 the value of the curve at passage 0 and GR the rate by which the curve grows (if GR>1) or decreases (if GR<1). To verify the exponential correlation between the cumulative numbers and time of culture, exponential regression of the data was performed. The exponential curve was converted to a linear one, using logarithm properties:

$$C = C_0 \cdot GR_i$$

$$\log(C) = \log(C_0 \cdot GR_i)$$

$$\log(C) = \log(C_0) + \log(GR_i)$$

$$\log(C) = \log(C_0) + \log(GR) \cdot i$$

The last equation represents a linear function where log(GR) is the slope of the line and a linear regression (using the least squares method) can be performed to calculate log(GR) and then GR. (cicalese)

3D-Matrigel Assay

Cells were seeded in 4-well chamber slides (LabTek: 2000 cells/ml/well) in Matrigel (BD-Biosciences) overlay or embedding conditions as described by Lee et al., and then cultured for 15 or 20 days. The resulting outgrowths were photographed and analyzed. All measurements were made with ImageJ software.

Time Lapse (TL) Live Imaging analysis

The mammosphere assay allows estimating the overall presence of CSCs in a sample but if a deeper investigation of the dynamics at the base of this increase is needed, hence we exploited the TL analysis.

The Microscope Cage Incubator (Okolab) encloses the IX81-ZDC bright field/fluorescent microscope station (Olympus); this system has a laser-based Z-drift compensator and works as a dynamic scanner. The software plans a virtual grid above the tissue culture well and by keeping focused more fields, it can capture at different time points the cells shape recording the very first mitotic division and all the followings. The cells viability during all the record period is guaranteed by the

Cage Incubator, which maintains a microenvironment as close as possible to the culture incubator. In that manner, by analyzing the number of cells spawn from a single mitotic division it is possible to evaluate weather a symmetric rather than an asymmetric division has taken place. Furthermore overexpressing upon infections factors like Numb, by tracking Numb-DsRed, it becomes possible to study its distribution during the SCs division.

To keep the cells static during the recording, the single cell suspension is embedded in Methylcellulose-based medium (MethoCult™ Stemcell Technologies) previously reconstituted with with 10% mammosphere medium MESCM (see Mammary Epithelial Stem Cell Medium (MESCM)) containing 10-fold concentrated supplements.

Mammospheres were desaggregated to single cell suspension, resuspended in MESCM at the concentration of 5,000 cells per 30 µl and added to reconstituted methylcellulose in a 1:10 ratio. 300 µl of methylcellulose (5,000 cells) were then plated in glassed bottom wells (MatTek Corporation™) to increase imagine quality.

TL statistical analysis

The statistical analysis on TL videos was performed only on single living cells without considering the small groups or cells aggregates. The first and second mitotic divisions were considered to score the ratio between asymmetric versus symmetric

events occurred. Throughout TL analysis even MSs size and SFE were estimated and studied in relationship with the first mitotic division modality.

Transplantation experiments: *In vivo* xenograft assays

Five week-old NOD/SCID IL2R gamma-chain null female mice were used for cell transplantation.

Animals were treated with Tribromoethanol (Avertin®), a popular injectable anesthetic; witch was delivered by intra peritoneal injection. Avertin was prepared resuspending 2.5 g of 2,2,2 Tribromoethanol in 5 ml of 2-methyl-2-butanol (amylene hydrate, tertiary amyl alcohol). This step requires o/n heating to approximately 40° C and stirring. The solution was diluted in 200 ml distilled water (neutral pH), than filtered, stored at +4° C and protect from light since the material becomes toxic if it degrades.

Avertin is appropriate for short term surgical procedures, it induces anesthesia rapidly and provides good surgical analgesia for approximately one hour. Mice were injected with a size proportional volume of Avertin, (10 µl/g). (IACUC Guidelines for Use of Avertin Tribromoethanol (Avertin) in Mice)

Mice abdominal skin was excised with surgical scissors and the inguinal fat pad exposed. To evaluate the transplanted cells MRU, the breast tissue of the 4th

mammary gland, which is located in low-abdominal/inguinal area. (Figure 3. Lateral view). The fat pad was partially removed by cutting from half line on the central lymph node to lateral limit (fat pad clearance).

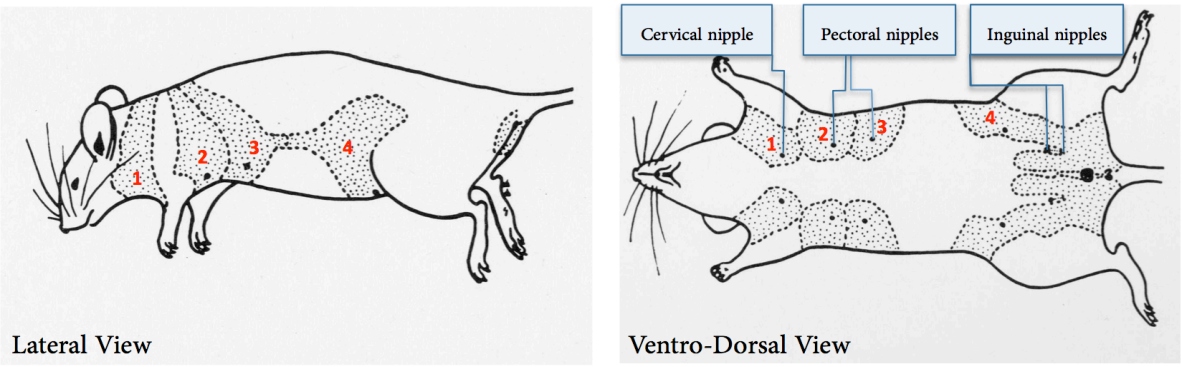

Figure 3
Diagram of Mammary Tissue
Left. Lateral view; in evidence cervical (1), thoracic (2,3) and abdominal (4) breasts.
Right. Ventro-dorsal view; distribution and contiguity of mouse breasts, in evidence the position of cervical, pectoral and inguinal nipples.
Adapted form The Virtual Mouse Necroscopy Comparative Medicine Branch

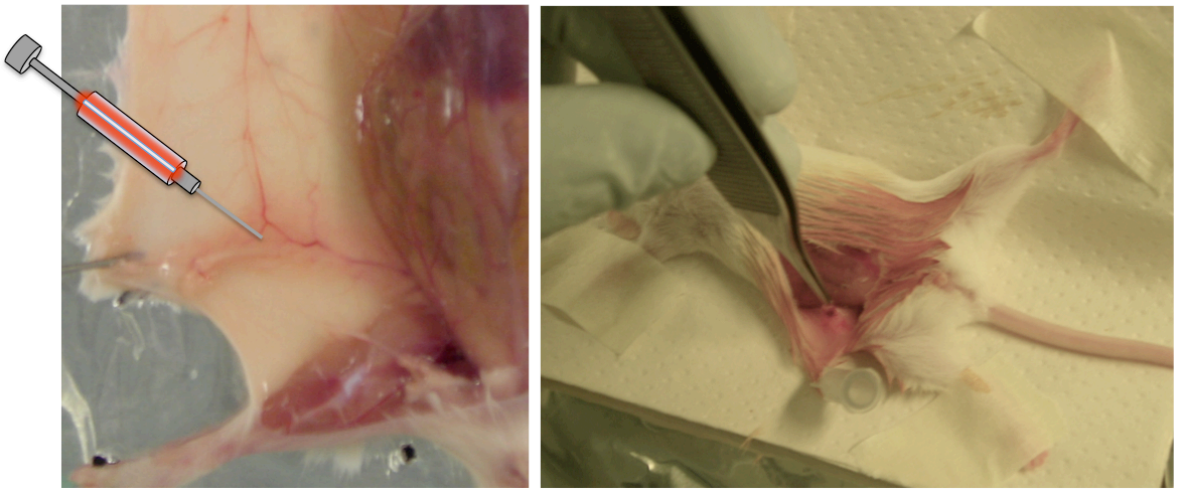

Figure 4
Macroscopic detail. 4th mammary gland undergoing transplantation
Left: site of injection. Cells are concentrated in the nipple posterior area
Right: Outcome of injection

Cells or mammospheres were were resuspended in 40 µL of a 1:1 Matrigel-PBS solution and injected with micro volume syringe (Hamilton).

Mice were monitored by hand-palpation for tumor development. Tumor growth was measured by using a vernier caliper and applying the standard formula: tumor volume = (a x b2)/2. Mice were sacrificed when tumors reached a dimension of 1.5 - 2 mm3. Tumors were explanted, weighed, and processed for formalin-fixing and paraffin embedding.

The surgical removal (clearing) of the mammary fat pad was performed as reported (DeOme et al., 1959) since in the 4th mammary gland of a 5-week old mouse the mammary epithelium is concentrated in the nipple area and has not yet grown out beyond the mammary lymph node penetrating the bulk of the fat pad. Clearing of the fat pad from the nipple to the lymph node leave the bulk of the fat pad free of epithelium and ready to receive cells throughout transplantation.

For the evaluation of outgrowths, fat pads were whole mounted (8 to 10 weeks after transplantation) and analyzed as described (DeOme et al., 1959; Sleeman et al., 2005).

Briefly, they were scored as negative for outgrowth if “no epithelial structures could be observed or if an epithelial ductal network could be seen, in which the majority of ductal branching had the same direction and had grown in from one edge of the fat pad”. They were instead scored as positive if “outgrowths could be seen to have

originated from a central region of the cleared fad pad and the directionality of the ductal branching was different in different parts of the fat pad". The exogenous epithelial reconstitution was witnessed by growing terminal ends ducts.

Statistical analysis of limiting dilution transplantation

Limiting dilution data and SC frequencies were analyzed using generalized linear models, as implemented in the limdil function of the "statmod" package (http://cran.rproject.org/web/packages/statmod/index.html) for the R computing environment (http://www.r-project.org/). The single hit Poisson model underling limiting dilution was estimated by a complementary log-log generalized linear model. A confidence interval was obtained for the SC frequency by computing two-sided 95% Wald confidence intervals. In cases of zero outgrowths, exact binomial confidence intervals (one-sided 95% Clopper- Pearson) were computed. Goodness of fit of the single-hit model was estimated by testing, using the likelihood ratio test, the null hypothesis that the angular coefficient equals to 1 in the linear model fitted with two two-parameters. The null hypothesis was not rejected ($p > 0.05$) for any dilution series (Bonnefoix et al., 1996).

Gene Knocking Down: ShRNA Interference.

In vitro NUMB KD was performed throughout ShRNA (Small hairpin RNA) Interference using lentiviral infection. Once the vector has integrated into the host cell genome, the ShRNA is transcribed in the nucleus by polymerase II and III (Zhou et al., 2005). ShRNA exportation out of the nucleus is mediated by Exportin 5 (Yi et al., 2003). Thereafter, the ShRNA is processed by Dicer (Haase et al., 2005) and cleaved in one step generating a 19-23 nt duplex SiRNA with 2 nt 3' overhangs and loaded into the RNA-induced silencing complex (RISC)(Gregory et al., 2005). While the sense strand is degraded by Ago2 (Matranga et al., 2005), which was previously recruited by Dicer itself, the antisense strand directs RISC to mRNA that has a complementary sequence. RISC represses the translation of the target mRNA, that is cleaved by Ago2 and degraded, allowing the target gene silencing. Among different PLKO Sh vector, Sh39 was chosen as most efficient in *in vitro* Numb knocking down.

Nutlin-3 treatment

Nutlin-3 (Cayman Chemical #10004372) (4-[(4S,4R)-4,5-*bis*(4-chlorophenyl))-4,5-dihydro-2-(4-methoxy-2-(1-methylethoxy)phenyl)-1H-imidazole-1-carbonyl]-2 piperazinone ($C_{30}H_{30}Cl_2N_4O_4$) was resuspended in DMSO to obtain a final 10 mM concentration. Cells were treated with a final 10μM concentration for 24 and 48 hours. Nutlin-3 treatment was performed both in cell suspension for biochemical

analysis and in Methylcellulose-based medium (MethoCult™ Stemcell Technologies) for TL experiments. For *in vivo* experiments Nutlin3 was administered intraperitoneally at the final dose of 20 mg/kg, the in vivo treatment was repeated every 3 days for 12 days for total 4 treatments. Mice were sacrificed and tumour sizes were measured. Tumors obtained were dissociated and cells were analysed by IB, to verify the efficacy of the Nutlin3 treatment and then either re-transplanted orthotopically in mice for 3 weeks

CELL LYSIS AND PROTEIN PURIFICATION

Cells were washed in PBS and lysed in RIPA lysis buffer [50 mmol/L Tris (pH 8), 120 mmol/L NaCl, 0.5% NP40, Phosphatase and protease inhibitors were added freshly to lysis and wash buffers: 20 mM Na pyrophosphate pH 7.5, 50 mM NaF, 2 mM PMSF in ethanol, 10mM Na vanadate, Protease Inhibitor Cocktail (Calbiochem). Cells were harvested directly on the plates using a cell scraper. About 300 µl of RIPA lysis buffer/10-cm plates and 50 µl RIPA buffer/for one well of a 6-well plate were used. Lysates were incubated on ice for 10 min and centrifuged at 12,000 rpm for 15 min at 4°C. The supernatant was transferred to a new Eppendorf tube and protein concentration was measured by the Bradford assay (Biorad), following manufacturer's instructions.

SDS polyacrylamide gel electrophoresis (SDS-PAGE)

Gels for resolution of proteins were made from a 30%, 29.1:1 mix of acrylamide:bisacrylamide (Sigma). As polymerization catalysts, 10% ammonium persulphate (APS) and TEMED were used.

Immunoblotting

Desired amounts of proteins were loaded onto 0.75 - 1.5 mm thick polyacrylamide gels for electrophoresis (Biorad). Proteins were transferred in western transfer tanks (Biorad) to nitrocellulose (Schleicher and Schnell) in 1 x Western Transfer buffer (diluted in 20% methanol) at 30 V overnight, or 100 V for 1 hour for small gels and at 70 V for 3 hours for large gels. Ponceau coloring was used to reveal the amount of protein transferred to the filters. Filters were blocked 1 hour (or overnight) in 5% milk or 5% BSA in TBS 0.1% Tween (TBS-T). After blocking, filters were incubated with the primary antibody, diluted in TBS-T with 5% milk or BSA, for 1 hour at room temperature, or overnight at 4°C, followed by 3 washes of 5 min each in TBS-T. Filters were then incubated with the appropriate horseradish peroxidase (HRP)-conjugated secondary antibody diluted in TBS-T with 5% milk or BSA for 30 min.

Primary antibodies

Anti Numb antibody was furnished by "Cogentech" (Consortium for Genomic Technologies), a core technology facility created by IFOM and IEO.

Anti p53 (Cell Signaling (1C12) #2524)

Anti p21 (Santa Cruz Biotechnology (F-5) #6246)

Anti-vinculin and anti tubulin home made produced, anti-e-cadherin (BD); anti n-cadherin (BD); anti GPR 94 (Enzo Life Sciences (9E10)) were also used. After the incubation with the secondary antibody, the filter was washed 3 times in TBS-T and the bound secondary antibody was revealed using the ECL (enhanced chemiluminescence) method (Amersham).

Mammary gland Whole Mount staining with Carmine Alum

Carmine Alum staining was used to study the whole mount architecture in mouse breast. Instead of the classical histological staining, which are performed on paraffin embedded 3 µm thick slides, Carmine Alum is performed directly on the fixed fat pad. This technique is exploited to get a macroscopic overview allowing for gross morphological changes appreciation.

As previously demonstrated, together with biochemical alterations, Numb loss brings to hyperplastic and pre-neoplastic phenotypes characterized by hyperbranching and enlarged primary and secondary ducts (pece 2010). To get a deeper analysis on

these features the classical histo-pathological approach together with immune histochemistry (IHC) were hence coupled with Carmine Alum staining. Carmine is a "semi-synthetic" intensely red dye used to stain glycogen, its use requires the use of a mordant, usually aluminum potassium sulfate in water and gives a nuclear stain (Dapson et al., 2007).

After the surgical remove, mouse inguinal mammary gland was stretched and flattened on a microscope slide and immediately placed in Kahle's fixing solution for a minimum of 4 hours.

Kahle's fix (500ml)- stored at RT

53 ml 37% formaldehyde

147 ml 95% EtOH

9.8 ml glacial acetic acid

290.2 ml dH2O

Once fixed, aftre 70% EtOH Wash, the mammary gland is rised in distilled water since Carmine Alum is in aqueous solution. The staining is o/n long, it is followed by a growing EtOH scale washing and a final xylene bath clears the fat pad from fat leaving an almost transparent tissue allowing the duct analysis.

Carmine Alum solution.

1g Carmine (Sigma C1022) and 2.5g aluminum potassium sulfate (Sigma A7167) were resuspended in 500ml dH2O and boiled for 20 min.

IMMUNOFLUORESCENCE

Cells were plated on glass coverslips pre-incubated with 0.5% gelatin in PBS at 37°C for 30 min. Cells were fixed in 4% paraformaldehyde (in Pipes Buffer) for 10 min, washed with PBS and permeabilized in PBS 0.1% Triton X-100 for 10 min at room temperature. To prevent non-specific binding of the antibodies, cells were incubated with PBS in the presence of 5% BSA for 30 min. The coverslips were incubated with primary antibodies diluted in PBS 0.2 % BSA. After 1 hour of incubation at room temperature, coverslips were washed 3 times with PBS. Cells were then incubated for 30 min at room temperature with the appropriate secondary antibody Cy3 (Amersham), Alexa 488-conjugated (Molecular Probes).

After three washes in PBS, coverslips were mounted in a 90% glycerol solution containing diazabicyclo-(2.2.2) octane antifade (Sigma) and examined under a wild-field immunofluorescence microscope (Leica). Images were further processed with the Adobe Photoshop software (Adobe) or with Image J to merge the images of the single channels.

IMMUNOHISTOCHEMISTRY

IHC staining was performed on both frozen and fixed tissues. After surgical explant, tissues are formalin fixed () for a size related period and paraffin embedded. Fresh tissue are frozen and covered with cryostat embedding medium (OCT).

3 μm thick samples slices are cut by microtome and incubated in xylene in order to remove paraffin.

The slices undergo antigen retrieval from formalin and paraffin through incubation in 99° C Antigen Unmasking Buffer for 40'.

Citrate: 10 mM Sodium Citrate Buffer:

To prepare 1 L add 2.94 g sodium citrate trisodium salt dihydrate to 1 L dH2O. Adjust pH to 6.0.

EDTA: 1 mM EDTA:

To prepare 1 L add 0.372 g EDTA to 1 L dH2O. Adjust pH to 8.0.

Endogenous peroxidases are quenched by 3% Hydrogen Peroxide and the slice is pre-incubated with TBST 2% normal goat serum + 2% BSA to prepare the tissue for primary antibody incubation. The antibody is diluted in the same solution and the slice incubated at RT or +4° C for an antibody affinity related period.

Secondary HRP conjugated antibodies (DAKO) were used and the DAB chromogen system (DAKO) was exploited for the secondary antibody detection.

Wash Buffer (1X TBS/0.1% Tween-20 (1X TBST) is used

Constructs and plasmids

The pLVX-puro lentiviral vector (Clontech #632164) was used to generate a construct to overexpress Numb in mammalian cells. The human isoform 71 Numb coding sequence (CDS) was taken from the vector pEGFP N1-Numb, already present in the lab (Clontech #6085-1), Numb was extracted through digestion with EcoRI and SalI. The same enzymes were used to digest an expression vector (pDsRed-Monomeric-N1 Clontech #632465) carrying DsRed coding sequence, a monomeric mutant derived from a tetrameric *Discosoma sp.* Red fluorescent protein DsRed. Numb CDS was kept in frame with DsRed ATG in order to obtain a fusion protein Numb-DsRed later retrieved with EcoRI and NotI digestion. The NotI end was reduced to a blunt end throughout 20' incubation with DNA Polymerase I, Large (Klenow) Fragment. Numb-DsRed was cloned into pLVX-puro, previously digested with EcoRI and SmaI, this last conferring a blunt end. T4 ligase was used for o/n ligation, all mentioned enzymes were New England Biolabs (NEB) products. The so obtained pLVX-Numb-DsRed was used to overexpress Numb and to rescue its physiological levels in Numb KO models *in vitro* analysis, while in TL analysis, it was exploited for Numb tracking. With this system, the expression of Numb is driven by the human cytomegalovirus immediate early promoter. pLVX contains a puromycin resistance gene under the control of the murine phosphoglycerate kinase promoter for the selection of stable transductants.

Basic cloning techniques

Agarose gel electrophoresis

DNA samples were loaded onto 0.8 - 2% agarose gels along with DNA markers. Gels were made in TAE buffer containing 0.3 µg/ml ethidium bromide and run at 80 V until the desired separation was achieved. DNA bands were visualized under a UV lamp.

Transformation of competent cells

Fresh competent cells (50 µl), Top10 (Invitrogen) for cloning and DNA preparation were thawed on ice for approximately 10 min prior to the addition of plasmid DNA. Cells were incubated with DNA on ice for 30 min and then subjected to a heat shock for 1 min at 42°C. Cells were then returned to ice for 2 min. SOC medium (300 µl) was then added and the cells were left at 37°C for 1 hour before plating them onto LB-agar plates with the appropriate antibiotic. Two plates for each reaction were used, one plated with 2/3 of the transformed bacterial cells and the other one with the rest. Plates were incubated overnight at 37°C.

Minipreps

Clones picked from individual colonies were used to inoculate 5 ml LB (containing the appropriate antibiotic) and grown overnight at 37°C. Bacteria cells were transferred to

Eppendorf tubes and pelleted for 5 min at 12,000 rpm. Minipreps were performed with the Plasmid DNA purification kit (Macherey-Nagel) following the manufacturer's instructions. The plasmids were eluted in 50 µl nuclease free H2O.

Diagnostic DNA restriction

Between 0.5 and 5 µg DNA were digested for 2 hours at 37°C with 10 – 20 units of restriction enzyme (New England Biolabs). For digestion, the volume was made up depending on the DNA volume to 20 – 50 µl with the appropriate buffer and ddH2O.

Large scale plasmid preparation

Cells containing transfected DNA were expanded into 200 ml cultures overnight. Plasmid DNA was isolated from these cells using the Maxi-prep kit (Macherey Naghel) according to the manufacturer's instructions.

Cell transfection

Transfections were performed using calcium phosphate or Lipofectamine® (Invitrogen) reagents, according to manufacturer's instructions. Lentiviral vectors lack in packaging protein genes for safety reasons, because of that a co-transfection with third generation helper vectors carrying these genes as pMDL, pREV and pVSVG are needed. For lentiviral production, 60% confluent packaging 293T cells were

transfected with calcium phosphate. Each 15 cm diameter plate was transfected with 45 µg lentiviral vector together with 15 µg of every packaging plasmid. DNA mix was added with $CaCl_2$ dropped in bubbling 2x HBS (Hepes Buffered Saline) and diluted in cells medium. Transfection was performed both o/d and o/n. Once removed the transfection medium. Virus was produced for 24 hours directly in medium of cells to be infected and used immediately after collection. The medium containing the virus was filtered through 45 µm filters, than added with fresh growth factors and hexadimethrine bromide (polybrene), a cationic polymer used to increase the efficiency of infection. In case of Lipofectamine® transfection, 80% confluent cells were used. Ninety µl of Lipofectamine® was added to DNA mix, prepared in serum-free medium using 15 µg of lentiviral vector and 5 µg each packaging vector. The mix was incubated at room temperature for 5 min and then diluted in a pare volume of serum-free medium added with 60µl of Plus Reagent provided in the kit. After additional 20 min incubation, the final mix was added to the transfection medium which was removed after 3 hours incubation. Cells were then incubated at 37°C for o/d and/or o/n 12 hours cycles. Forty-eight hours after infection, cells were split and puromycin (1 µg/ml) was added to select infected cells.

DISCUSSION

According to the Stem Cell Theory of Cancer, at the heart of the tumorigenic process, is the Stem Cell and its homeostasis. Moreover, the critical role played by genes that regulate the Stem Cell compartment controlling the SCs self-renewal potential, the number of SCs and the tumorigenic potential of SCs is of particular interest is. Among them, I studied the protein Numb and its role in the maintenance of the Stem Cell compartment with particular emphasis on the consequences of Numb loss in the pathogenesis of breast cancer either in Numb KO mouse models on in human breast tumors.

In this thesis, I have demonstrated that the cell fate determinant Numb plays a broad regulatory role in mammary gland homeostasis. At the top of the mammary hierarchy, in the MSC compartment, Numb partitions into the daughter progeny that retains the SC identity and imposes an asymmetric outcome to MSC self-renewing divisions by the liaison of p53 activity. Selective ablation of Numb or of p53 (Cicalese et al. 2009), causes the symmetric division of MSCs and a geometric expansion of the SC compartment, due to increased frequency of symmetric divisions.

Mechanistically, I showed that p53-signaling is attenuated in Numb-KO SCs. Pharmacological restoration of normal levels of p53 in Numb-null cells decreased lifespan and self-renewing divisions of cancer SCs (to an extent identical to that of the WT SCs), rescues the asymmetric replicative kinetics and reverts SC expansion and reduced tumor expansion in vivo, without affecting significantly the growth of

additional cancer cells. Thus, a Numb-p53 axis controls the homeostasis of the breast SC compartment; the subversion of the Numb-p53 axis is relevant to breast cancers. I demonstrated here that the process affected by this alteration is the mode of self-renewal of the breast cancer SC, which becomes skewed towards a symmetric pattern. Loss of Numb expression, in a mouse model, leads to immortalisation of SCs, also prone to the acquisition of a transformed phenotype. Similarly, in Numb-deficient human breast cancers, the expansion of the SC compartment can be reverted by restoration of Numb expression or of sufficient levels of p53 activity. In addition, my results indicate a gradient of alterations induced by loss of Numb in the KO model, from aberrant morphogenesis to preneoplastic lesions to various degrees of aggressiveness and tumorigenicity upon orthotopic transplantation. These observations suggest the possible selection of additional lesions to achieve a fully transformed phenotype.

My data, however, unequivocally show that the altered homeostasis of the SC compartment is necessary for tumorigenesis in Numb-deficient human breast cancers. In addition, since the effects of Numb or p53 restoration were evident only in Numb-deficient tumours, these tumours are addicted to the loss of the Numb-p53 axis, supporting the notion that the expansion of the SC compartment is selected for as an advantage-conferring event in the natural history of these tumours. As a consequence, Numb- or p53-targeted therapies should constitute SC-specific

treatments in Numb-deficient tumours. I demonstrated the proof of mechanism for such an approach in orthotopic xenografts and my work represents, to my knowledge, the first example of such anti-cancer SC targeted therapy in human solid tumours.

These data demonstrate that increased frequency of self-renewing divisions in cancer SCs is critical for tumor growth, and suggest that asymmetric division functions as a mechanism of tumor suppression in mammals. Furthermore, these findings represent the first direct evidence that the selective ablation of cancer SCs leads to reduced tumor growth, thus providing experimental support to the concept of "cancer SC-targeted therapy".

Numb asymmetric distribution at mitosis of Stem Cell

The Stem Cell Theory of Cancer point to the responsibility of SCs' number in the tumorigenic process, since the SC in normal condition divides in asymmetric mode generating two daughter cells, a SC and a progenitor cell, maintaining the starting number of SCs. When the SC mitosis does not proceed in this order, when a SC divides in symmetric mode, two identical SC are generated giving enrichment in SCs number.

Here, I have demonstrated that the asymmetric distribution of Numb during the first SC mitosis imposes an asymmetric fate on the SC progeny. Numb segregates into the daughter cell that retains the SC identity.

I obtained this evidence exploiting an *in vitro* lentiviral infection of purified mammary epithelial SCs. Bulk epithelial mammary cells were obtained through enzymatic digestion of 5 weeks old mouse mammary glands. We used PKH dye to stain the entire bulk mammary population, which upon selective culture medium, generated floating spheroid colonies identified as mammospheres. These structures are the result of SC division and their cell daughter (progenitors) proliferation. SCs underwent a single round of mitosis thereby the PKH amount has maintained higher in SC and progressively diluted in the progenitors. I purified the SCs by the use of FACS-Sorting analysis and once obtained the pure SCs, I used the lentiviral vector pLVX Numb DsRed to track Numb partition during the first SC mitosis which was microscopically monitored by Time Lapse (TL) video-microscopy Analysis.

This experiment showed that the PKH retaining cell, the true SC, was the daughter cell inheriting Numb protein.

Consequences in terms of tumorigenesis of Numb-loss of function

The presence of Numb in the SC prompted us to study the consequences of Numb loss in the Stem cell compartment. Throughout the Numb KO mouse model and even with Numb KD we obtained the selective ablation of Numb.

Throughout macroscopical (Whole mount analysis with Carmine Alum staining) and microscopical (Hematoxilin/heosin) investigations, I found that Numb KO mammary glands displayed morphological alterations, such as hyperplasia and dysplasia.

According to *in vitro* assays performed on mammary epithelial cells (MECS) obtained form Numb KO mammary glad digestion, the loss of Numb causes an increase of sphere forming efficiency (SFE) and mammosphere (MS) size in comparison with control counterpart. Moreover the Numb KO SCs display an immortal behavior compared to WT SCs.

The entire panel of *in vitro* experiments performed with Numb KO SCs was repeated with Numb KD cells with comparable results.

These results suggest that the loss of Numb causes the symmetric division of SCs and a geometric expansion of the SC compartment. In agreement with the previous studies (Colaluca et al., 2008) arguing the existence of a Numb-p53 axis controlling the homeostasis of the breast SC compartment, the loss of Numb is accompanied even by the decrease of p53 levels and activity confirmed by p21 levels as shown by Western Blot analysis.

Since SC are able to re-constitute the epithelial tissue structure, we transplanted Numb KO bulk MECs in order to quantify the SC number: MECs transplantation was performed at limiting dilution (from 10^5 to 10 cells) to score the mammary repopulating unit (MRU) index or the cancer initiating cell (CIC) number. We considered these indexes to evaluate the SC number in the starting bulk MEC population transplanted. In many cases the outgrowths obtained displayed ductal hyperplasia, severe dysplasia together with preneoplastic lesions; in a minor fraction of cases the cells originated tumors. We collected cells from these neoplastic samples (identified as KO1 and KO2) and we performed MECs transplantation at limiting dilution; the higher frequencies of MRU displayed by KO1 and KO2 argued a higher SC content in their MECs population confirming the previous hypothesis out coming the *in vitro* assays.

Rescue of Numb in Numb KO cells

On the base of the results obtained from the previous set of experiments, we decided to proceed investigating on the effects of Numb reconstitution in Numb null SC compartment throughout infection using pLVX Numb DsRed lentiviral vector.

Western Blot analysis confirms that Numb reconstitution was efficient in promoting the rescue of p53 levels and activity ensuring the efficacy of our rescue model.

SFE assay was performed on Numb reconstituted Numb KO cells which displayed a reduction both in SFE and in MS size arguing a reduction in SC compartment. This event perhaps depends on the reversion of modality of first mitotic division, from an almost predominant symmetric mode of Numb KO cells to a co-existence of both asymmetric and symmetric trends as witnessed by TL analysis.

Numb reconstituted Numb KO cells were transplanted in order to see whether the SC compartment was actually diminished, and the out came tumors were in fact smaller than tumors grown from Numb KO EV infected cells without any alteration in proliferation or apoptosis of progenitors cells.

p53 restoration by the use of Nutlin-3

The previous experiments show that Numb overexpression in Numb KO cells is sufficient to restore the p53 activity, to impose the asymmetric replicative kinetics of divisions and to revert SCs expansion.

Together with previous demonstration (Colaluca et al., 2008) that Numb sustains p53 stability and function by interfering with the ubiquitinating enzyme Mdm2, this result argues that a Numb-mediated inhibition of p53 degradation in the “stem” daughter cell is the most likely mechanism to account for the maintenance of the SC compartment. To act at the level of p53-MDM2 interaction we treated Numb KO cells with Nutlin-3. This drug because of its molecular conformation can interfere in p53-

MDM2 binding by occupying the p53 site of docking in MDM2 structure. We treated Numb KO cells with a 10μM final concentration of Nutlin-3 and the *in vitro* assay showed a reduction in SFE and MS size arguing a reduction in SC compartment. As demonstrated by TL analysis the SC number reduction was caused by a switch in the mode of first mitotic SC mitotic division, Nutlin-3 treated Numb KO cells increasing the number of asymmetric mitotic events. These cells were even transplanted to understand whether a reduction of SC compartment could lead to *in vivo* effects and interestingly the size of tumors obtained from Nutlin-3 treated Numb KO cells transplantation was smaller if compared with tumors grown from untreated cells.

Furthermore I investigated whether the results obtained from Nutlin-3 *in vitro* treatment were consistent with the *in vivo* experiments. I decided to inject (IP) Nutlin-3 in mice which were developing Numb KO palpable lesions. The pharmacological treatment did not affect the tumor growth, which is sustained by progenitor cells proliferation. To confirm whether Nutlin-3 treatment was efficient rather on SC compartment, this first generation of tumors were reduced to MECs, examined through SFE assay and transplanted again to study the Nutlin-3 treatment effects on the growth of second generation of tumors. Nutlin-3 *in vivo* treatment reduced the SFE and MS size confirming a targeted action against SC compartment, which is reduced as witnessed by the second generation tumor size. Indeed tumors grown by

MECs obtained from *in vivo* treated tumors were smaller than tumors of not treated mice.

Numb KO mouse model helped us to clarify the tumorigenic mechanisms in which SC are involved and above all we better understood the critical role of Numb and the effects of its loss in terms of p53 homeostasis and SC compartment regulation. This data were our turning point to introduce this approach of study in human contest.

From mouse to human

According to the results obtained in mouse model and aware of the evidences emerged on the role of Numb, the consequences of its loss and the further effects of its reconstitution on p53 levels and activity rather than on SC compartment, we carried the strategy pursued in mouse directly in human model system.

We screened different human tumor samples collected by IEO Anatomo-Pathology Unit. Tumor biopsies were xenografted in NOD SCID mice breast and let the tumor develop. Once the lesions were grown I compared through histological investigation (IHC) and biochemical analysis (Western Blot) whether the xenograft characteristics were representative of the human primitive counterpart. Western Blot analysis revealed that when Numb is lost in Numb defective tumors a concomitantly decrease in p53 levels and activity in seen. Thereby we sorted samples on the base of their Numb levels choosing for the next set of experiments two Numb negative and two

Numb positive samples as control. Results from *in vitro* SFE assay together with TL analysis confirmed an enrichment in SC compartment occurring in Numb negative samples as witnessed even by cumulative sphere number assay.

As done in mouse model we tried to revert this phenotype by reconstituting Numb levels using the lentiviral infection with pLVX Numb DsRed vector. Western Blot confirms the efficacy of this approach showing a reconstitution of Numb levels and a p53 rescue in levels and activity.

Later on, SFE assay displayed how Numb reconstitution was able to reduce the SFE and MS size arguing an effective action on SC compartment, then confirmed by TL analysis that reported an increase in asymmetric event in detriment of an almost total symmetric phenotype in first mitotic division after Numb reconstitution. We xenografted Numb reconstituted Numb negative cells and Numb negative cells as control in NOD SCID mice breasts and here we report a decrease in tumor volume consequent to Numb reconstitution and not to increased apoptosis or proliferation.

According to our intents in finding a cure for cancer, we performed Nutlin-3 treatment both *in vitro* and *in vivo* on previously studied human samples. Numb negative samples responded to Nutlin-3 treatment as reported by Western Blot analysis displaying p53 rescue in levels and activity. Furthermore Numb negative cells upon Nutlin-3 showed a reduced SFE as reported by cumulative sphere number in serial propagation assay arguing an effective *in vitro* Nutlin-3 action on SC

compartment. Nutlin-3 *in vitro* treated cells were even xenografted and we report a decreased growth in tumor spawned by these cells which was not dependent on increased apoptosis or proliferation as witnessed by IHC.

To investigate whether Nutlin-3 acted on SC compartment rather than on progenitors we treated *in vivo* by IP injection mice which were developing palpable Numb negative lesions and we do not report any difference in first generation tumor growth in comparison with Numb positive lesions grown as control. This evidence suggests a Nutlin-3 directed action on SC compartment, the responsible in tumorigenesis rather than the progenitor since the *in vivo* treatment was ineffective on progenitors proliferation hence tumor growth. This hypothesis was confirmed by SFE assay performed on MECs derived from Nutlin-3 *in vivo* treated: the decreased SFE is proof of Nutlin-3 action on SC compartment. We xenografted Nutlin-3 *in vivo* treated tumor derived MECs and we report a decrease in size of tumors spawned by these cells.

Taken together this last data argue an efficacy of Nutlin-3 treatment on SC compartment suggesting Nutlin-3 as a putative treatment suitable for CSC targeted therapy but at the same time not useful for arresting tumor growth since not ruled by SC compartment but by progenitors' expansion. Nutlin-3 could thereby considered as therapy for tumor relapse, event in which the SC proliferation is for sure involved.

BIBLIOGRAPHY

Abd El Rehim, D. M., Pinder, S. E., Paish, C. E., Bell, J., Blamey, R. W., Robertson, J. F., ... & Ellis, I. O. (2004). Expression of luminal and basal cytokeratins in human breast carcinoma. *The Journal of pathology*, *203*(2), 661-671.

Al-Hajj, M., Wicha, M. S., Benito-Hernandez, A., Morrison, S. J., & Clarke, M. F. (2003). Prospective identification of tumorigenic breast cancer cells. *Proceedings of the National Academy of Sciences*, *100*(7), 3983-3988.

Artavanis-Tsakonas, S., Rand, M. D., & Lake, R. J. (1999). Notch signaling: cell fate control and signal integration in development. *Science*, *284*(5415), 770-776.

Bello, B., Reichert, H., & Hirth, F. (2006). The brain tumor gene negatively regulates neural progenitor cell proliferation in the larval central brain of Drosophila. *Development*, *133*(14), 2639-2648.

Betschinger, J., & Knoblich, J. A. (2004). Dare to Be Different: Asymmetric Cell Division in< i> Drosophila</i>,< i> C. elegans</i> and Vertebrates. *Current biology*, *14*(16), R674-R685.

Betschinger, J., Mechtler, K., & Knoblich, J. A. (2006). Asymmetric Segregation of the Tumor Suppressor Brat Regulates Self-Renewal in< i> Drosophila</i> Neural Stem Cells. *Cell*, *124*(6), 1241-1253.

Bielas, J. H., Loeb, K. R., Rubin, B. P., True, L. D., & Loeb, L. A. (2006). Human cancers express a mutator phenotype. *Proceedings of the National Academy of Sciences*, *103*(48), 18238-18242.

Blaydes, J. P., Gire, V., Rowson, J. M., & Wynford-Thomas, D. (1997). Tolerance of high levels of wild-type p53 in transformed epithelial cells dependent on auto-regulation by mdm-2. *Oncogene*, *14*(15), 1859-1868.

Bonnefoix, T., Bonnefoix, P., Verdiel, P., & Sotto, J. J. (1996). Fitting limiting dilution experiments with generalized linear models results in a test of the single-hit Poisson assumption. Journal of immunological methods, 194(2), 113-119.

Böttger, A., Böttger, V., Sparks, A., Liu, W. L., Howard, S. F., & Lane, D. P. (1997). Design of a synthetic Mdm2-binding mini protein that activates the p53 response< i> in vivo</i>. *Current biology*, *7*(11), 860-869.

Boyd, L., Guo, S., Levitan, D., Stinchcomb, D. T., & Kemphues, K. J. (1996). PAR-2 is asymmetrically distributed and promotes association of P granules and PAR-1 with the cortex in C. elegans embryos. *Development*, *122*(10), 3075-3084.

Brooks, C. L., & Gu, W. (2006). p53 ubiquitination: Mdm2 and beyond. *Molecular cell*, *21*(3), 307-315.

Brown, C. J., Lain, S., Verma, C. S., Fersht, A. R., & Lane, D. P. (2009). Awakening guardian angels: drugging the p53 pathway. *Nature Reviews Cancer*, *9*(12), 862-873.

Brown, T. M., & Fee, E. (2006). Rudolf Carl Virchow: medical scientist, social reformer, role model. *American Journal of Public Health*, *96*(12), 2104.

Campbell, L. L., & Polyak, K. (2007). Breast tumor heterogeneity: cancer stem cells or clonal evolution?. *Cell Cycle*, *6*(19), 2332-2338.

Capobianco, A. J., Zagouras, P., Blaumueller, C. M., Artavanis-Tsakonas, S., & Bishop, J. M. (1997). Neoplastic transformation by truncated alleles of human NOTCH1/TAN1 and NOTCH2. *Molecular and cellular biology*, *17*(11), 6265-6273.

Cardiff, R. D., Anver, M. R., Gusterson, B. A., Hennighausen, L., Jensen, R. A., Merino, M. J., ... & Green, J. E. (2000). The mammary pathology of genetically engineered mice: the consensus report and recommendations from the Annapolis meeting. *Oncogene*, *19*(8), 968-988.

Cariati, M., & Purushotham, A. D. (2008). Stem cells and breast cancer. *Histopathology*, *52*(1), 99-107.

Carter, S., & Vousden, K. H. (2008). A role for Numb in p53 stabilization. *Genome Biol*, *9*(5), 221.

Casanova, J. E. (2007). PARtitioning numb. *EMBO reports*, *8*(3), 233-235.

Castellanos, E., Dominguez, P., & Gonzalez, C. (2008). Centrosome Dysfunction in< i> Drosophila</i> Neural Stem Cells Causes Tumors that Are Not Due to Genome Instability. *Current Biology*, *18*(16), 1209-1214.

Caussinus, E., & Gonzalez, C. (2005). Induction of tumor growth by altered stem-cell asymmetric division in Drosophila melanogaster. *Nature genetics*, *37*(10), 1125-1129.

Cayouette, M., & Raff, M. (2002). Asymmetric segregation of Numb: a mechanism for neural specification from Drosophila to mammals. *Nature neuroscience*, *5*(12), 1265-1269.

Chen, J., Wu, X., Lin, J., & Levine, A. J. (1996). mdm-2 inhibits the G1 arrest and apoptosis functions of the p53 tumor suppressor protein. *Molecular and cellular biology*, *16*(5), 2445-2452.

Chenn, A., & McConnell, S. K. (1995). Cleavage orientation and the asymmetric inheritance of Notchl immunoreactivity in mammalian neurogenesis. *Cell*, *82*(4), 631-641.

Chiou, S., et al. "Positive correlations of Oct-4 and Nanog in oral cancer stem-like cells and high-grade oral squamous cell carcinoma." *Clinical Cancer Research* 14.13 (2008): 4085-4095.

Cho, R. W., & Clarke, M. F. (2008). Recent advances in cancer stem cells. *Current opinion in genetics & development*, *18*(1), 48-53.

Cicalese, A., Bonizzi, G., Pasi, C. E., Faretta, M., Ronzoni, S., Giulini, B., ... & Pelicci, P. G. (2009). The Tumor Suppressor< i> p53</i> Regulates Polarity of Self-Renewing Divisions in Mammary Stem Cells. *Cell*, *138*(6), 1083-1095.

Clarke, M. F., and Fuller, M. "Stem cells and cancer: two faces of eve." *Cell* 124.6 (2006): 1111-1115.

Clarke, M. F., et al. "Cancer stem cells—perspectives on current status and future directions: AACR Workshop on cancer stem cells." *Cancer research* 66.19 (2006): 9339-9344.

Colaluca, I. N., Tosoni, D., Nuciforo, P., Senic-Matuglia, F., Galimberti, V., Viale, G., ... & Di Fiore, P. P. (2008). NUMB controls p53 tumour suppressor activity. *Nature*, *451*(7174), 76-80.

Conboy, I. M., & Rando, T. A. (2002). The regulation of Notch signaling controls satellite cell activation and cell fate determination in postnatal myogenesis. *Developmental cell*, *3*(3), 397-409.

Croce, C. M. (2008). Oncogenes and cancer. *New England Journal of Medicine*, *358*(5), 502-511.

Daniel, C. W., & Smith, G. H. (1999). The mammary gland: a model for development. *Journal of mammary gland biology and neoplasia*, *4*(1), 3-8.

Dapson, R. W. (2007). The history, chemistry and modes of action of carmine and related dyes. Biotechnic & Histochemistry, 82(4-5), 173-187.

DeOme, K. B., Faulkin, L. J., Bern, H. A., & Blair, P. B. (1959). Development of mammary tumors from hyperplastic alveolar nodules transplanted into gland-free mammary fat pads of female C3H mice. Cancer Research, 19(5), 515.

Dho, S. E., Trejo, J., Siderovski, D. P., & McGlade, C. J. (2006). Dynamic regulation of mammalian numb by G protein-coupled receptors and protein kinase C activation: structural determinants of numb association with the cortical membrane. *Molecular biology of the cell*, *17*(9), 4142-4155.

Dontu, G., Al Hajj, M., Abdallah, W. M., Clarke, M. F., & Wicha, M. S. (2003). Stem cells in normal breast development and breast cancer. *Cell Proliferation*, *36*(s1), 59-72.

Eirew, P., Stingl, J., Raouf, A., Turashvili, G., Aparicio, S., Emerman, J. T., & Eaves, C. J. (2008). A method for quantifying normal human mammary epithelial stem cells with in vivo regenerative ability. *Nature medicine*, *14*(12), 1384-1389.

Fakharzadeh, S. S., Rosenblum-Vos, L., Murphy, M., Hoffman, E. K., & George, D. L. (1993). Structure and organization of amplified DNA on double minutes containing the mdm2 oncogene. *Genomics*, *15*(2), 283-290.

Fearon, E. R., & Vogelstein, B. (1987). Clonal analysis of human colorectal tumors. *Science*, *238*(4824), 193-197.

Ferlay, J., et al. "Estimates of worldwide burden of cancer in 2008: GLOBOCAN 2008." *International journal of cancer* 127.12 (2010): 2893-2917.

Fidler, I. J., and Kripke M. L.. "Metastasis results from preexisting variant cells within a malignant tumor." *Science* 197.4306 (1977): 893-895.

Freedman, D. A., & Levine, A. J. (1999). Regulation of the p53 protein by the MDM2 oncoprotein—thirty-eighth GHA Clowes Memorial Award Lecture. *Cancer research*, *59*(1), 1-7.

Freeman, M. (2000). Feedback control of intercellular signalling in development. *Nature*, *408*(6810), 313-319.

Gajewska, M., Zielniok, K., & Motyl, T. (2013). Autophagy in Development and Remodelling of Mammary Gland.

Gallahan, D., Jhappan, C., Robinson, G., Hennighausen, L., Sharp, R., Kordon, E., ... & Smith, G. H. (1996). Expression of a truncated Int3 gene in developing secretory mammary epithelium specifically retards lobular differentiation resulting in tumorigenesis. *Cancer research*, *56*(8), 1775-1785.

Ganguli, G., & Wasylyk, B. (2003). p53-Independent Functions of MDM2 *Molecular cancer research*, *1*(14), 1027-1035.

Gatza, C. E., Dumble, M., Kittrell, F., Edwards, D. G., Dearth, R. K., Lee, A. V., ... & Donehower, L. A. (2008). Altered mammary gland development in the p53+/m mouse, a model of accelerated aging. *Developmental biology*, *313*(1), 130-141.

Gil, J., Stembalska, A., Pesz, K. A., & Sąsiadek, M. M. (2008). Cancer stem cells: the theory and perspectives in cancer therapy. *Journal of applied genetics*, *49*(2), 193-199.

Ginestier, C., & Wicha, M. (2007). Mammary stem cell number as a determinate of breast cancer risk. *Breast Cancer Research*, *9*(4), 109.

Gleason, D. F., & Mellinger, G. T. (2002). Prediction of prognosis for prostatic adenocarcinoma by combined histological grading and clinical staging. *The Journal of urology*, *167*(2), 953-958.

Goldstein, B., & Macara, I. G. (2007). The PAR proteins: fundamental players in animal cell polarization. *Developmental cell*, *13*(5), 609-622.

Gonzalez, C. (2007). Spindle orientation, asymmetric division and tumour suppression in Drosophila stem cells. *Nature Reviews Genetics*, *8*(6), 462-472.

Grange, C., Lanzardo, S., Cavallo, F., Camussi, G., & Bussolati, B. (2008). Sca-1 identifies the tumor-initiating cells in mammary tumors of BALB-neuT transgenic mice. *Neoplasia (New York, NY)*, *10*(12), 1433.

Gregory, R. I., Chendrimada, T. P., Cooch, N., & Shiekhattar, R. (2005). Human RISC couples microRNA biogenesis and posttranscriptional gene silencing. Cell, 123(4), 631-640.

Guo, M., Jan, L. Y., & Jan, Y. N. (1996). Control of daughter cell fates during asymmetric division: interaction of Numb and Notch. *Neuron*, *17*(1), 27-41.

Guo, S., & Kemphues, K. J. (1995). < i> par</i>-1, a gene required for establishing polarity in C. elegans embryos, encodes a putative Ser/Thr kinase that is asymmetrically distributed. *Cell*, *81*(4), 611-620.

Gupta, P. B., Chaffer C. L., and Weinberg R. A.. "Cancer stem cells: mirage or reality?." *Nature medicine* 15.9 (2009): 1010-1012.

Guzman, M. L., Rossi, R. M., Karnischky, L., Li, X., Peterson, D. R., Howard, D. S., & Jordan, C. T. (2005). The sesquiterpene lactone parthenolide induces apoptosis of human acute myelogenous leukemia stem and progenitor cells. *Blood*, *105*(11), 4163-4169.

Hanahan, D., & Weinberg, R. A. (2011). Hallmarks of cancer: the next generation. *Cell*, *144*(5), 646-674.

Harris, M. A., et al. "Cancer stem cells are enriched in the side population cells in a mouse model of glioma." *Cancer research* 68.24 (2008): 10051-10059.

Hartmann, A., Blaszyk, H., Kovach, J. S., & Sommer, S. S. (1997). The molecular epidemiology of< i> P53</i> gene mutations in human breast cancer. *Trends in Genetics*, *13*(1), 27-33.

Haase, A. D., Jaskiewicz, L., Zhang, H., Lainé, S., Sack, R., Gatignol, A., & Filipowicz, W. (2005). TRBP, a regulator of cellular PKR and HIV-1 virus expression, interacts with Dicer and functions in RNA silencing. EMBO reports, 6(10), 961-967.

Haupt, Y., Maya, R., Kazaz, A., & Oren, M. (1997). Mdm2 promotes the rapid degradation of p53. *Nature*, *387*(6630), 296-299.

Hennighausen, L., & Robinson, G. W. (2001). Signaling pathways in mammary gland development. *Developmental cell*, *1*(4), 467-475.

Hennighausen, L., & Robinson, G. W. (2005). Information networks in the mammary gland. *Nature Reviews Molecular Cell Biology*, *6*(9), 715-725.

Henrique, D., & Schweisguth, F. (2003). Cell polarity: the ups and downs of the Par6/aPKC complex. *Current opinion in genetics & development*, *13*(4), 341-350.

Herzenberg, L. A., Sweet, R. G., & Herzenberg, L. A. (1976). Fluorescence-activated cell sorting. Sci Am, 234(3), 108-117.

Horvitz, H. R., & Herskowitz, I. (1992). Mechanisms of asymmetric cell division: two Bs or not two Bs, that is the question. *Cell*, *68*(2), 237-255.

Horvitz, H. R., and Herskowitz I.. "Mechanisms of asymmetric cell division: two Bs or not two Bs, that is the question." *Cell* 68.2 (1992): 237-255.

Hovey, R. C., Mcfadden, T. B., & Akers, R. M. (1999). Regulation of mammary gland growth and morphogenesis by the mammary fat pad: a species comparison. *Journal of mammary gland biology and neoplasia*, *4*(1), 53-68.

Howard, B. A., & Gusterson, B. A. (2000). Human breast development. Journal of mammary gland biology and neoplasia, 5(2), 119-137.

Huang, Y., Yang, J., Wang, X. B., Becker, F. F., & Gascoyne, P. R. (1999). The removal of human breast cancer cells from hematopoietic CD34+ stem cells by dielectrophoretic field-flow-fractionation. *Journal of hematotherapy & stem cell research*, *8*(5), 481-490.

Innocente, S. A., Abrahamson, J. L., Cogswell, J. P., & Lee, J. M. (1999). p53 regulates a G2 checkpoint through cyclin B1. *Proceedings of the National Academy of Sciences*, *96*(5), 2147-2152.

Ito, A., Kawaguchi, Y., Lai, C. H., Kovacs, J. J., Higashimoto, Y., Appella, E., & Yao, T. P. (2002). MDM2–HDAC1-mediated deacetylation of p53 is required for its degradation. *The EMBO journal*, *21*(22), 6236-6245.

Ito, M., Hiramatsu, H., Kobayashi, K., Suzue, K., Kawahata, M., Hioki, K., ... & Nakahata, T. (2002). NOD/SCID/γ mouse: an excellent recipient mouse model for engraftment of human cells. *Blood*, *100*(9), 3175-3182.

J. Stingl, P. Eirew, I. Ricketson, M. Shackleton, F. Vaillant, D. Choi, H.I. Li, C.J. Eaves

Jan, Y. N., & Jan, L. Y. (1998). Asymmetric cell division. *Nature*, *392*(6678), 775-778.

Januschke, J., & Gonzalez, C. (2008). Drosophila asymmetric division, polarity and cancer. *Oncogene*, *27*(55), 6994-7002.

Jones, R. J., Matsui, W. H., & Smith, B. D. (2004). Cancer stem cells: are we missing the target?. *Journal of the National Cancer Institute*, *96*(8), 583-585.

Jordan, C. T., Guzman, M. L., & Noble, M. (2006). Cancer stem cells. *New England Journal of Medicine*, *355*(12), 1253-1261.

Kelly, P. N., et al. "Tumor growth need not be driven by rare cancer stem cells." *Science* 317.5836 (2007): 337-337.

Kikutani, H., & Makino, S. (1992). The murine autoimmune diabetes model: NOD and related strains. *Advances in immunology*, *51*, 285-322.

Knoblich, J. A., Jan, L. Y., & Jan, Y. N. (1997). The N terminus of the Drosophila Numb protein directs membrane association and actin-dependent asymmetric localization. *Proceedings of the National Academy of Sciences*, *94*(24), 13005-13010.

Komaki, K., Sano, N., & Tangoku, A. (2006). Problems in histological grading of malignancy and its clinical significance in patients with operable breast cancer. *Breast Cancer*, *13*(3), 249-253.

Koyanagi, Y., Tanaka, Y., Kira, J. I., Ito, M., Hioki, K., Misawa, N., ... & Yamamoto, N. (1997). Primary human immunodeficiency virus type 1 viremia and central nervous system invasion in a novel hu-PBL-immunodeficient mouse strain. *Journal of virology*, *71*(3), 2417-2424.

Kubbutat, M. H., Jones, S. N., & Vousden, K. H. (1997). Regulation of p53 stability by Mdm2. *Nature*, *387*(6630), 299-303.

Kussie, P. H., Gorina, S., Marechal, V., Elenbaas, B., Moreau, J., Levine, A. J., & Pavletich, N. P. (1996). Structure of the MDM2 oncoprotein bound to the p53 tumor suppressor transactivation domain. *Science*, *274*(5289), 948-953.

Lane, D. P. (1992). p53, guardian of the genome. *Nature*, *358*, 15-16.

Lanzkron, S. M., Collector, M. I., & Sharkis, S. J. (1999). Homing of Long-Term and Short-Term Engrafting Cells In Vivoa. *Annals of the New York Academy of Sciences*, *872*(1), 48-56.

Lapidot, T., Sirard, C., Vormoor, J., Murdoch, B., Hoang, T., Caceres-Cortes, J., ... & Dick, J. E. (1994). A cell initiating human acute myeloid leukaemia after transplantation into SCID mice.

Lechler, T., & Fuchs, E. (2005). Asymmetric cell divisions promote stratification and differentiation of mammalian skin. *Nature*, *437*(7056), 275-280.

Lee, C. Y., Andersen, R. O., Cabernard, C., Manning, L., Tran, K. D., Lanskey, M. J., ... & Doe, C. Q. (2006). Drosophila Aurora-A kinase inhibits neuroblast self-renewal by regulating aPKC/Numb cortical polarity and spindle orientation. *Genes & development*, *20*(24), 3464-3474.

Levine, A. J. (1997). p53, the cellular gatekeeper for growth and division. *cell*, *88*(3), 323-331.

Levine, A. J., Chang, A., Dittmer, D., Notterman, D. A., Silver, A., Thorn, K., ... & Wu, M. (1994). The p53 tumor suppressor gene. *The Journal of laboratory and clinical medicine*, *123*(6), 817.

Li, L., & Xie, T. (2005). Stem cell niche: structure and function. *Annu. Rev. Cell Dev. Biol.*, *21*, 605-631.

Li, M., Chen, D., Shiloh, A., Luo, J., Nikolaev, A. Y., Qin, J., & Gu, W. (2002). Deubiquitination of p53 by HAUSP is an important pathway for p53 stabilization. *Nature*, *416*(6881), 648-653.

Li, S. C., Zwahlen, C., Vincent, S. J., McGlade, C. J., Kay, L. E., Pawson, T., & Forman-Kay, J. D. (1998). Structure of a Numb PTB domain–peptide complex suggests a basis for diverse binding specificity. *Nature Structural & Molecular Biology*, *5*(12), 1075-1083.

Lin, J., Chen, J., Elenbaas, B., & Levine, A. J. (1994). Several hydrophobic amino acids in the p53 amino-terminal domain are required for transcriptional activation, binding to mdm-2 and the adenovirus 5 E1B 55-kD protein. *Genes & development*, *8*(10), 1235-1246.

Macara, I. G. (2004). Par proteins: partners in polarization. *Current biology*, *14*(4), R160-R162.

Matranga, C., Tomari, Y., Shin, C., Bartel, D. P., & Zamore, P. D. (2005). Passenger-strand cleavage facilitates assembly of siRNA into Ago2-containing RNAi enzyme complexes. Cell, 123(4), 607-620.

McGill, M. A., & McGlade, C. J. (2003). Mammalian numb proteins promote Notch1 receptor ubiquitination and degradation of the Notch1 intracellular domain. *Journal of Biological Chemistry*, *278*(25), 23196-23203.

Medina, D., & Warner, M. R. (1976). Mammary tumorigenesis in chemical carcinogen-treated mice. IV. Induction of mammary ductal hyperplasias. Journal of the National Cancer Institute, 57(2), 331-337.

Medina, D. (1996). The mammary gland: a unique organ for the study of development and tumorigenesis. *Journal of mammary gland biology and neoplasia*, *1*(1), 5-19.

Meletis, K., Wirta, V., Hede, S. M., Nistér, M., Lundeberg, J., & Frisén, J. (2006). p53 suppresses the self-renewal of adult neural stem cells. *Development*, *133*(2), 363-369.

Momand, J., Zambetti, G. P., Olson, D. C., George, D., & Levine, A. J. (1992). The< i> mdm-2</i> oncogene product forms a complex with the p53 protein and inhibits p53-mediated transactivation. *Cell*, *69*(7), 1237-1245.

Morrison, S. J., and Kimble J.. "Asymmetric and symmetric stem-cell divisions in development and cancer." *Nature* 441.7097 (2006): 1068-1074.

Mumm, J. S., & Kopan, R. (2000). Notch signaling: from the outside in. *Developmental biology*, *228*(2), 151-165. Nature, 439 (2006), pp. 993–997

Nalepa, G., Rolfe, M., & Harper, J. W. (2006). Drug discovery in the ubiquitin–proteasome system. Nature Reviews Drug Discovery, 5(7), 596-613.

Neuhaus, I. M., Sommardahl, C. S., Johnson, D. K., & Beier, D. R. (1997). Microsatellite DNA variants between the FVB/N and C3HeB/FeJLe and C57BL/6J mouse strains. *Mammalian genome*, *8*(7), 506-509.

Neumüller, R. A., & Knoblich, J. A. (2009). Dividing cellular asymmetry: asymmetric cell division and its implications for stem cells and cancer. *Genes & development*, *23*(23), 2675-2699.

Nowell, P. C. (1976). The clonal evolution of tumor cell populations. *Science*, *194*(4260), 23-28.

Nowell, P.C. "Mechanisms of tumor progression." *Cancer Res* 46.5 (1986): 2203-2207.

Ohbo, K., Suda, T., Hashiyama, M., Mantani, A., Ikebe, M., Miyakawa, K., ... & Sugamura, K. (1996). Modulation of hematopoiesis in mice with a truncated mutant of the interleukin-2 receptor gamma chain. Blood, 87(3), 956-967.

Ohno, S. (2001). Intercellular junctions and cellular polarity: the PAR–aPKC complex, a conserved core cassette playing fundamental roles in cell polarity. *Current opinion in cell biology*, *13*(5), 641-648.

Pece, S., Serresi, M., Santolini, E., Capra, M., Hulleman, E., Galimberti, V., ... & Di Fiore, P. P. (2004). Loss of negative regulation by Numb over Notch is relevant to human breast carcinogenesis. *The Journal of cell biology*, *167*(2), 215-221.

Pece, S., Tosoni, D., Confalonieri, S., Mazzarol, G., Vecchi, M., Ronzoni, S., ... & Di Fiore, P. P. (2010). Biological and molecular heterogeneity of breast cancers correlates with their cancer stem cell content. Cell, 140(1), 62-73.

Petersen, O. W., & Polyak, K. (2010). Stem cells in the human breast. Cold Spring Harbor perspectives in biology, 2(5).

Pharoah, P. D. P., Day, N. E., & Caldas, C. (1999). Somatic mutations in the p53 gene and prognosis in breast cancer: a meta-analysis. *British journal of cancer*, *80*(12), 1968.

Piccirillo, S. G. M., Reynolds, B. A., Zanetti, N., Lamorte, G., Binda, E., Broggi, G., ... & Vescovi, A. L. (2006). Bone morphogenetic proteins inhibit the tumorigenic potential of human brain tumour-initiating cells. *Nature*, *444*(7120), 761-765.

Piltti, K., Kerosuo, L., Hakanen, J., Eriksson, M., Angers-Loustau, A., Leppä, S., ... & Wartiovaara, K. (2006). E6/E7 oncogenes increase and tumor suppressors decrease the proportion of self-renewing neural progenitor cells. *Oncogene*, *25*(35), 4880-4889.

Quintana, E., et al. "Efficient tumour formation by single human melanoma cells." *Nature* 456.7222 (2008): 593-598.

Rambhatla, L., Ram-Mohan, S., Cheng, J. J., & Sherley, J. L. (2005). Immortal DNA Strand Cosegregation Requires p53/IMPDH–Dependent Asymmetric Self-renewal Associated with Adult Stem Cells. *Cancer research*, *65*(8), 3155-3161.

Ramírez, A., Bravo, A., Jorcano, J. L., & Vidal, M. (1994). Sequences 5′ of the bovine keratin 5 gene direct tissue-and cell-type-specific expression of a< i> lacZ</i> gene in the adult and during development. *Differentiation*, *58*(1), 53-64.

Reya, T., et al. "Stem cells, cancer, and cancer stem cells." *nature* 414.6859 (2001): 105-111.
Reynolds, B. A., & Weiss, S. (1996). Clonal and population analyses demonstrate that an EGF-responsive mammalian embryonic CNS precursor is a stem cell. *Developmental biology*, *175*(1), 1-13.

Rhyu, M. S., Jan, L. Y., & Jan, Y. N. (1994). Asymmetric distribution of numb protein during division of the sensory organ precursor cell confers distinct fates to daughter cells. *Cell*, *76*(3), 477-491.

Robbins, J. O. A. N., Blondel, B. J., Gallahan, D., & Callahan, R. (1992). Mouse mammary tumor gene int-3: a member of the notch gene family transforms mammary epithelial cells. *Journal of virology*, *66*(4), 2594-2599.

Santisteban, M., et al. "Immune-induced epithelial to mesenchymal transition in vivo generates breast cancer stem cells." *Cancer research* 69.7 (2009): 2887-2895.

Shen, Q., Zhong, W., Jan, Y. N., & Temple, S. (2002). Asymmetric Numb distribution is critical for asymmetric cell division of mouse cerebral cortical stem cells and neuroblasts. *Development*, *129*(20), 4843-4853.

Shinin, V., Gayraud-Morel, B., Gomès, D., & Tajbakhsh, S. (2006). Asymmetric division and cosegregation of template DNA strands in adult muscle satellite cells. *Nature cell biology*, *8*(7), 677-682.

Shipitsin, M., & Polyak, K. (2008). The cancer stem cell hypothesis: in search of definitions, markers, and relevance. *Laboratory Investigation*, *88*(5), 459-463.

Shirangi, T. R., Zaika, A., & Moll, U. M. (2002). Nuclear degradation of p53 occurs during down-regulation of the p53 response after DNA damage. *The FASEB Journal*, *16*(3), 420-422.

Singh, A., and Settleman J.. "EMT, cancer stem cells and drug resistance: an emerging axis of evil in the war on cancer." *Oncogene* 29.34 (2010): 4741-4751.

Sleeman, K. E., Kendrick, H., Ashworth, A., Isacke, C. M., & Smalley, M. J. (2005). CD24 staining of mouse mammary gland cells defines luminal epithelial, myoepithelial/basal and non-epithelial cells. Breast Cancer Research, 8(1), R7.

Smalley, M., & Ashworth, A. (2003). Stem cells and breast cancer: a field in transit. *Nature Reviews Cancer*, *3*(11), 832-844.

Smith, C. A., Lau, K. M., Rahmani, Z., Dho, S. E., Brothers, G., She, Y. M., ... & McGlade, C. J. (2007). aPKC-mediated phosphorylation regulates asymmetric membrane localization of the cell fate determinant Numb. *The EMBO journal*, *26*(2), 468-480.

Stingl, J., & Caldas, C. (2007). Molecular heterogeneity of breast carcinomas and the cancer stem cell hypothesis. *Nature Reviews Cancer*, *7*(10), 791-799.

Stingl, J., Eaves, C. J., Kuusk, U. and Emerman, J. T. (1998), Phenotypic and functional characterization in vitro of a multipotent epithelial cell present in the normal adult human breast. Differentiation, 63: 201–213. doi: 10.1111/j.1432-0436.1998.00201.x

Stingl, J., Eirew, P., Ricketson, I., Shackleton, M., Vaillant, F., Choi, D., ... & Eaves, C. J. (2006). Purification and unique properties of mammary epithelial stem cells. *Nature*, *439*(7079), 993-997.

Suzuki, A., & Ohno, S. (2006). The PAR-aPKC system: lessons in polarity. *Journal of cell science*, *119*(6), 979-987.

Tai, M. H., Chang, C. C., Olson, L. K., & Trosko, J. E. (2005). Oct4 expression in adult human stem cells: evidence in support of the stem cell theory of carcinogenesis. Carcinogenesis, 26(2), 495-502.

Taketo, M., Schroeder, A. C., Mobraaten, L. E., Gunning, K. B., Hanten, G., Fox, R. R., ... & Hansen, C. T. (1991). FVB/N: an inbred mouse strain preferable for transgenic analyses. *Proceedings of the National Academy of Sciences*, *88*(6), 2065-2069.

Tan, B. T., Park, C. Y., Ailles, L. E., & Weissman, I. L. (2006). The cancer stem cell hypothesis: a work in progress. *Laboratory investigation*, *86*(12), 1203-1207.

Tavassoli, F. A., & Schnitt, S. J. (1999). *Pathology of the Breast* (2nd ed., pp. 329-332). Stamford, CT: Appleton & Lange.

Taketo, M., Schroeder, A. C., Mobraaten, L. E., Gunning, K. B., Hanten, G., Fox, R. R., ... & Hansen, C. T. (1991). FVB/N: an inbred mouse strain preferable for transgenic analyses. Proceedings of the National Academy of Sciences, 88(6), 2065-2069.

Tovar, C., Rosinski, J., Filipovic, Z., Higgins, B., Kolinsky, K., Hilton, H., ... & Vassilev, L. T. (2006). Small-molecule MDM2 antagonists reveal aberrant p53 signaling in cancer: implications for therapy. *Proceedings of the National Academy of Sciences of the United States of America*, *103*(6), 1888-1893.

Uemura, T., Shepherd, S., Ackerman, L., Jan, L. Y., & Jan, Y. N. (1989). < i> numb</i>, a gene required in determination of cell fate during sensory organ formation in Drosophila embryos. *Cell*, *58*(2), 349-360.

Vaillant, F., Asselin-Labat, M. L., Shackleton, M., Forrest, N. C., Lindeman, G. J., & Visvader, J. E. (2008). The mammary progenitor marker CD61/β3 integrin identifies cancer stem cells in mouse models of mammary tumorigenesis. *Cancer Research*, *68*(19), 7711-7717.

Vassilev, L. T. (2007). MDM2 inhibitors for cancer therapy. *Trends in molecular medicine*, *13*(1), 23-31.

Verdi, J. M., Schmandt, R., Bashirullah, A., Jacob, S., Salvino, R., Craig, C. G., ... & McGlade, C. J. (1996). Mammalian NUMB is an evolutionarily conserved signaling adapter protein that specifies cell fate. *Current Biology*, *6*(9), 1134-1145.

Visvader, J. E. (2011). Cells of origin in cancer. *Nature*, *469*(7330), 314-322.

Visvader, J. E., & Lindeman, G. J. (2008). Cancer stem cells in solid tumours: accumulating evidence and unresolved questions. *Nature Reviews Cancer*, *8*(10), 755-768.

Vogelstein, B., Lane, D., & Levine, A. J. (2000). Surfing the p53 network. *Nature*, *408*(6810), 307-310.

Wagner, K. U., Wall, R. J., St-Onge, L., Gruss, P., Wynshaw-Boris, A., Garrett, L., ... & Hennighausen, L. (1997). Cre-mediated gene deletion in the mammary gland. Nucleic acids research, 25(21), 4323-4330.

Wang, H., Ouyang, Y., Somers, W. G., Chia, W., & Lu, B. (2007). Polo inhibits progenitor self-renewal and regulates Numb asymmetry by phosphorylating Pon. *Nature*, *449*(7158), 96-100.

Wang, X., Taplick, J., Geva, N., & Oren, M. (2004). Inhibition of p53 degradation by Mdm2 acetylation. *FEBS letters*, *561*(1), 195-201.

Wang, Y., Krushel, L. A., & Edelman, G. M. (1996). Targeted DNA recombination in vivo using an adenovirus carrying the cre recombinase gene. *Proceedings of the National Academy of Sciences*, *93*(9), 3932-3936.

Wang, Z., Sandiford, S., Wu, C., & Li, S. S. C. (2009). Numb regulates cell–cell adhesion and polarity in response to tyrosine kinase signalling. *The EMBO journal*, *28*(16), 2360-2373.

Weiss, S., Dunne, C., Hewson, J., Wohl, C., Wheatley, M., Peterson, A. C., & Reynolds, B. A. (1996). Multipotent CNS stem cells are present in the adult mammalian spinal cord and ventricular neuroaxis. *The Journal of neuroscience*, *16*(23), 7599-7609.

Westhoff, B., Colaluca, I. N., D'Ario, G., Donzelli, M., Tosoni, D., Volorio, S., ... & Di Fiore, P. P. (2009). Alterations of the Notch pathway in lung cancer. *Proceedings of the National Academy of Sciences*, *106*(52), 22293-22298

Williams, J. M., & Daniel, C. W. (1983). Mammary ductal elongation: differentiation of myoepithelium and basal lamina during branching morphogenesis. *Developmental biology*, *97*(2), 274-290.

Wilson, A., Ardiet, D. L., Saner, C., Vilain, N., Beermann, F., Aguet, M., ... & Zilian, O. (2007). Normal hemopoiesis and lymphopoiesis in the combined absence of numb and numblike. *The Journal of Immunology*, *178*(11), 6746-6751.

Wirtz-Peitz, F., Nishimura, T., & Knoblich, J. A. (2008). Linking cell cycle to asymmetric division: Aurora-A phosphorylates the Par complex to regulate Numb localization. *Cell*, *135*(1), 161-173.

Wu, X., Bayle, J. H., Olson, D., & Levine, A. J. (1993). The p53-mdm-2 autoregulatory feedback loop. *Genes & development*, *7*(7a), 1126-1132.

Xirodimas, D. P., Stephen, C. W., & Lane, D. P. (2001). Cocompartmentalization of p53 and Mdm2 is a major determinant for Mdm2-mediated degradation of p53. *Experimental cell research*, *270*(1), 66-77.

Yi, R., Qin, Y., Macara, I. G., & Cullen, B. R. (2003). Exportin-5 mediates the nuclear export of pre-microRNAs and short hairpin RNAs. Genes & development, 17(24), 3011-3016.

Yilmaz, Ö. H., Valdez, R., Theisen, B. K., Guo, W., Ferguson, D. O., Wu, H., & Morrison, S. J. (2006). Pten dependence distinguishes haematopoietic stem cells from leukaemia-initiating cells. *Nature*, *441*(7092), 475-482.

Yoshino, H., Ueda, T., Kawahata, M., Kobayashi, K., Ebihara, Y., Manabe, A., ... & Tsuji, K. (2000). Natural killer cell depletion by anti-asialo GM1 antiserum treatment enhances human hematopoietic stem cell engraftment in NOD/Shi-scid mice. *Bone marrow transplantation*, *26*(11), 1211-1216.

Zhang, M., and Rosen J. M.. "Stem cells in the etiology and treatment of cancer." *Current opinion in genetics & development* 16.1 (2006): 60-64.

Zhou, H., Xia, X. G., & Xu, Z. (2005). An RNA polymerase II construct synthesizes short-hairpin RNA with a quantitative indicator and mediates highly efficient RNAi. Nucleic acids research, 33(6), e62-e62.

Zilian, O., Saner, C., Hagedorn, L., Lee, H. Y., Säuberli, E., Suter, U., ... & Aguet, M. (2001). Multiple roles of mouse Numb in tuning developmental cell fates. *Current Biology*, *11*(7), 494-501.